論文 / 著書情報
Article / Book Information

題目(和文)	
Title(English)	Coal fly ash application as water retention material and porous composite adsorbent
著者(和文)	宋萌珠
Author(English)	Song Mengzhu
出典(和文)	学位:博士(工学), 学位授与機関:東京工業大学, 報告番号:甲第11347号, 授与年月日:2019年12月31日, 学位の種別:課程博士, 審査員:高橋 史武,日野出 洋文,中﨑 清彦,江頭 竜一,時松 宏治
Citation(English)	Degree:Doctor (Engineering), Conferring organization: Tokyo Institute of Technology, Report number:甲第11347号, Conferred date:2019/12/31, Degree Type:Course doctor, Examiner:,,,,
学位種別(和文)	博士論文
Type(English)	Doctoral Thesis

Doctoral Dissertation

Coal fly ash application as water retention material and porous composite adsorbent

Mengzhu Song

Advisor: Associate Professor Fumitake Takahashi

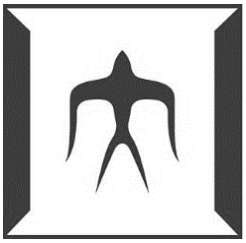

Global Engineering for Development Environment and Society,

Department of Transdisciplinary Science and Engineering

School of Environment and Society

Tokyo Institute of Technology

December 2019

Table of Contents

Chapter 1
Introduction

1.1 Introduction

1.1.1 Coal fly ash

Fly ash (FA) is one of the by-products from the coal combustion process of thermal power plants. The coal combustion process and by-products generation usually shown as follows (see Figure 1-1). Most of the pulverized coal is burned off in the combustion boiler, and approximately 10-30% of the original coal remains as noncombustible by-products (Temuujin, 2013). The composition of unburned ashes and their characteristics depend on the design of the furnace, combustion method and conditions, collector setup, and coal quality. Fly ash and bottom ash contribution from the total ash varies in ranges of 65–95 and 5–35 %, respectively (Jayaranjan et al., 2014). Bottom ash usually is a dark grey, granular, porous, predominantly sand-sized aggregate material that falls to the boiler bottom. Fly ash is light and fine particles, which can be captured by a series of collection devices from the exhausting gases (Abdulhameed et al., 2012).

1.1.2 Physical characterization of FA

Fly ash particles are generally spherical, powdery, and glassy, either solid or hollow, except for carbonaceous material in fly ash is composed of angular particles (Ayanda et al., 2012). The particle size ranges from 0.5 μm to 300 μm, with 65–90% of the particles with a diameter of less than 10μm. In general, fly ash has a low bulk density (1.01–1.43 g/cm3). Particle densities for non-magnetic and magnetic particles are 2.7 and 3.4 g/cm3, respectively (Black, 2016; Basu,

2009). The specific gravity of fly ash usually around 2.0 but can vary to a large extent (1.6 to 3.0) (Bhatia, 2017). Its specific surface area ranges from 170 to 1000 m^2/kg (Ahmaruzzaman, 2010). FA has low hydraulic conductivity, while the moisture retention ranges from 6.1% at 15 bar to 13.4% at 1/3 bar (Basu, et al., 2009; Natusch, 1974). The color of FA depends on the amount of unburned carbon. The lower the carbon content, the lighter the FA color, which can vary from tan to gray to black. Lignite or sub-bituminous coal fly ashes are usually light tan to buff in color, indicating relatively low amounts of carbon and the presence of some lime or calcium (Ayanda et al., 2012).

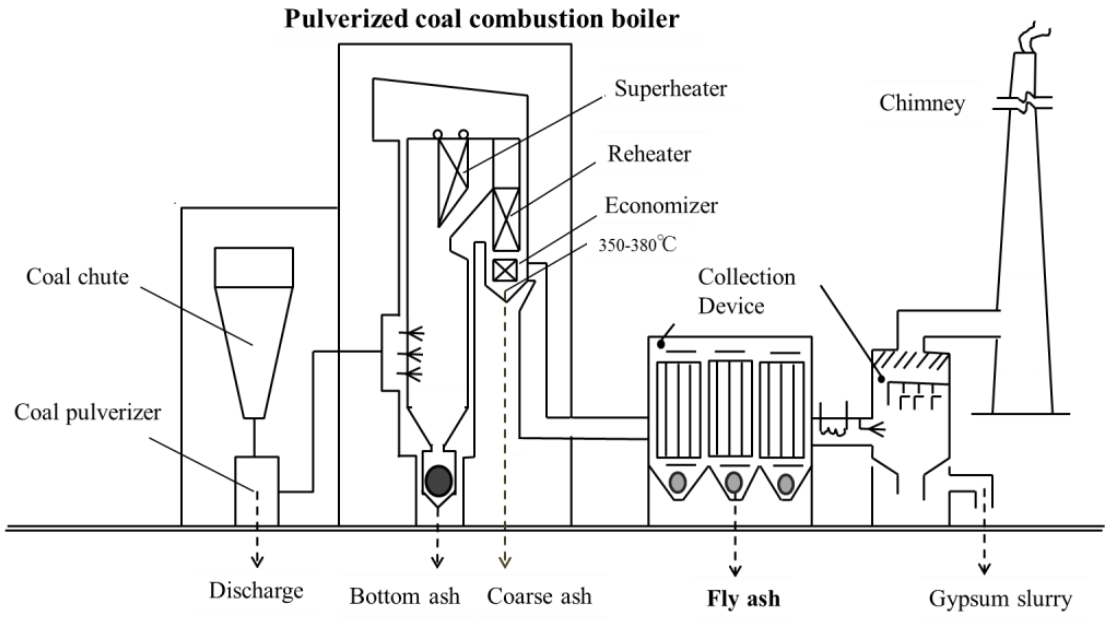

Figure 1-1. The collection of by- products from coal combustion (Chen, 2003; Yao, 2013)

1.1.3 Chemical characterization of FA

The chemical properties of FA mainly depend on the type of coal used. FA consists of composites of alkaline metallic oxides and nonmetal oxides, such as Al_2O_3, Fe_2O_3, K2O, MgO, Na_2O, CaO, and SO_3, P_2O_5, SiO_2 (Lieberman et al., 2015). In general, FA from the high-rank bituminous and anthracite coals contains higher Al_2O_3, SiO_2, and lower MgO, CaO, SO_3 compared to the lignite and sub-bituminous coals. The major chemical compositions are the basis for evaluating the suitability of FA as cement replacement material. According to the American Society for Testing and Material (ASTM), FA is divided into three classes: C, F, and N (see Table 1-1) (Yao, 2013). Class F ash generally contains less than 10% of CaO, while Class C ash typically contains CaO over 10% up to 40%. SiO_2, Al_2O_3, and Fe_2O_3 contribute to 50-70% of the total component for Class C ash and more than 70% for Class F ash, respectively (Vassilev, 2006). When coal fly ash is initially mixed with water, the initial pH of leachate may be strongly acidic (pH 4) or alkaline (pH12). However geochemical buffering reactions can subsequently narrow the pH range because the leachate of acidic fly ash may be neutralized by the dissolution of calcium and magnesium oxides, and alkaline fly ash leachate tends to absorb carbon dioxide. Eventually, the pH range is close to 7 to 9 (Roy et al., 2011). The pH of the leaching solution is the key factor that affects the mobility of trace elements in FA. There are many kinds of heavy metals and toxic elements in FA, such as Cr, Cu, Se, As, Cd, Sr, Hg, Pb, etc. The amount of these trace elements in FA varies in different regions. The leachability of these elements is closely related to the associated phase and the leaching conditions. (Davison, 1974; Jankowski, 2006; Neupane, 2012).

Table 1-1. Composition and chemical requirements of FA classes as ASTM standards

	Class		
	F	C	N
Silicon dioxide (SiO_2) plus aluminum oxide (Al_2O_3) plus iron oxide (Fe_2O_3), (min, %)	70.0	50.0	70.0
Sulfur trioxide (SO_3), (max, %)	5.0	5.0	4.0
Moisture content, (max, %)	3.0	3.0	3.0
Loss on ignition, (max, %)	6.0	6.0	10.0

1.2 Utilization and recycling of fly ash

Coal provides 30% of global primary energy needs and generates over 41.1% of the world's electricity. Global demand for coal used in power generation is predicted to rise over time (IEA, 2010; IEA, 2013; WCA, 2015). The annual FA generation in global is estimated to be about 750 million Mg (Blissett and Rowson, 2012). FA recycle still a significant social challenge referred to massive FA generation as described above. In worldwide, the FA recycle ratio varied widely in different countries. For example, more than 112 million Mg of coal FA is produced every year in India, and the utilization of FA is only around 38 %. In China, FA utilization increased from 20% to 67%, although the annual FA generation was estimated to be 500 million Mg. The current average FA recycles ratio in global is expected to be less than 50 %(Ahmaruzzaman, 2010; Tang, 2013; Yao, 2013; Dwivedi, 2014). It is clear that vast amounts of FA are disposed and accumulated in landfill sites or dumps. Untreated FA causes severe social and environmental problems due to its occupation of a large area for disposal and adverse ecological impacts (Carlson, 1993; Prasad, 1996; Hansen, 2002). Therefore, there is a constant need for developing new recycling methods for FA.

Currently, FA is commonly used as a cement replacement material in the construction industry. It reduces the production costs of concrete due to the lower price of fly ash compared

to cement. Considering the physical and chemical properties of FA, different types of building materials can be made. FA is typically added to structural concrete at 15-35 wt.% of the cement and can be up to 70 wt% in the pavement, walls, and parking lots and 80 wt.% in autoclaved aerated concrete (Dilmore and Neufeld, 2001; Harveer, 2014). The use of fly ash in concrete is very beneficial to keep the environment clean and healthy. However, the recycle ratio of FA as an ingredient in cement and other construction materials is relatively low. FA utilization is gaining vast importance in the scientific owing to its contamination in the atmosphere, posing a severe threat to the environment. Its disposal is a great challenge faced by the environmentalists and techniques to use it effectively is a concern worldwide. For waste minimization, alternative uses of FA as a value-added product are needed.

1.2.1 FA uses and application in soil water amendment

According to the physical and chemical properties of FA, there have been many studies that report FA utilization as soil amendment (Page, 1979; Yao, 2015), to improve soil properties (Kalra, 1998; Ram, 2014), such as soil texture (Campell, 1983; Lu, 2014; Adriano, 2001; Pathan, 2003), soil moisture (Campell, 1983; Ghodrati, 1995; Gangloff, 2000; Adriano, 2001; Pathan, 2001; Pathan, 2003) and soil pH (Matsi, 1999). For example, FA can be beneficially utilized as a mine soil amendment to provide an array of plant available macro-nutrients (Ca, Mg, K and S) and micro-nutrients (B, Fe, Mn, Cu, Zn, etc.) along with improved water holding capacity and aggregation (Daniels, 2002). Lime and FA amendment were utilized to aid the revegetation of acidic coal soil (Taylor, 1988). FA has excellent potentials in agriculture due to its efficacy to modify soil performance and crop production (Tolle, 1982; Basu, 2009; Jala, 2006). Many essential elements contained in FA can be used for planting, such as P, K, Ca, Mg Zn, Fe, Cu, Mn, and B etc. The trace elements in FA might be used to replace trace elements in soil (Jala,

2006). FA could change the bulk density of sandy soil and alter the soil micro-porosity, whereas hydraulic conductivity decreased (Campell, 1983). FA was primarily fine sand and silt-sized particles. Adding and mixing FA into sandy soils could permanently alter soil texture because sandy soils are predominantly comprised of coarse sand-sized particles. If soil mixed with FA at a proper ratio, it can improve soil texture and thus soil moisture content (Campell, 1983; Ghodrati, 1995; Gangloff, 2000; Adriano, 2001; Pathan, 2001; Pathan, 2003). For example, FA has been shown to increase available water for plants in sandy soil (Gangloff, 2000; Pathan, 2001). Besides, when the FA surface was modified by apatite synthesis, the FA amendment suppressed evaporation and increased water retention in FA-amended soils even at 40 ºC (Lin, 2015). In general, the FA amendment is reported to be capable to increase soil moisture (Campell, 1983; Ghodrati, 1995; Gangloff, 2000; Adriano, 2001; Pathan, 2001; Pathan, 2003) while there are also several reports about the negative impact of FA on the soil. For example, the application of FA as soil ameliorant would possibly cause an undesirable change in soil pH, increase soil salinity, elevated concentration of trace elements to toxic levels and cause nutrient imbalance (Kumpiene, 2010). These problems, however, are usually associated with excess or inappropriate FA applications (Shaheen, 2014). Although the use of FA as a soil amendment has been wildly studied, the technology for application has not been implemented in full scale. Therefore, more researches should be conducted in this potential application area.

1.2.2 FA uses and application in polymer composites and absorbent

Functional polymers are promising candidates in the fabrication of FA-based composite. Many researchers tried to study the effectiveness of fly ash as fillers in polymer composite materials. There are many reports about the effects of polymer modified fly ash on mechanical and thermal properties, such as tensile strength, friction and sliding characteristics (Chauhan,

2010; Deepthi, 2010; Gu, 2007; Gupta, 2001). From the above research works, it was noticed that fly ash as the filler has both positive as well as the negative effect on composite properties. The polymer modification on the surface of FA particles has a significant impact on the mechanical properties of the FA-composite.

On the other hand, it is recognized that fly ash is a promising adsorbent for the removal of various pollutants, such as NOx, SOx, organic compounds, and mercury in air, and cations, anions, dyes and other organic matters in waters. Researches on utilizing fly ash as a low-cost adsorbent for various adsorption processes for the removal of pollutants have been conducted in the past decades (Tsuchiai, 1995; Ahmaruzzaman, 2009). However, there were very few research works that examined the properties of polymer-modified fly ash as water-retentive and absorbent material. It will be ideal to utilize FA as an eco-friendly product if they make it as a value-added polymer composite.

1.3 Desertification

Desertification is the degradation of land due to the loss of soil nutrients and moisture, vegetation reduction, salinization, and accelerated wind and water erosion. Land deterioration and following desertification is a severe problem in arid areas. Severe land degradation is now affecting 168 countries across the world, threatening regions like western China, northern Africa, the Middle East, middle Australia, and America (UNCCD, 2016). Approximately 12 million ha of the earth surface areas are turning into a new dessert each year (UNEP, 2006). About two billion people depend on ecosystems in dryland areas, which are vulnerable to desertification (UN, 2016). The dry lands could be easily affected by desertification and turn into semi-arid regions. According to rough estimates, about 10-20 percent of the susceptible drylands are considered to have already undergone land degradation (MEA, 2005). Damage of soil and

reduce water availability are significant impacts from desertification (Li, 2006). In the areas that are suffering from desertification, the fine particles (clay and silt) of the soil are reducing at a high rate. Tiny soil particles are carried high into the air by the wind, then larger-sized soil particles are dislodged by the wind and roll along the soil surface. The stable surface aggregates of soil are broken down by the abrasion that results from windblown particles, which further increases the soil erosion. Consequently, the process of soil erosion leads to a loss of water-holding capacity of the soil, making the effects of desertification amplified. Therefore, to keep and increase soil productivity with limited water resources, water holding agents for the land is desirable.

1.4 Purpose of this study

This study aims to utilize FA as a water-retentive material to increase the water retention capacity of soil in arid and semi-arid areas. In some arid regions such as northern China, for example, coal-fired power plants are the dominant power sources, and thus vast amounts of FA are generated. Therefore, if FA can be recycled as water amending material, it will give a promising solution for both FA management and desertification at the same time.

Although many works on FA uses in soil amendment have been conducted, there are still various uncertainties about the effects of the FA amendment on soil water retention. Besides, the diverse experimental methodologies on measuring soil water retention lead to different data analysis. Conventional methods for soil water moisture measurement are under water-saturated conditions which are controlled by gravity or pressure. However, water saturation of soil is a limited situation in arid areas, and temperature-driven evaporation is the main pathway of soil moisture loss. In this study, a new method was tested to evaluate evaporation mitigation capacity (EMC) in soil under unsaturated condition by simple drying experiment. The EMC

measurement will be elaborated in the next chapter.

As described above, FA used as water retention material to improve soil condition is attractive in the arid area. Also, functional polymers are promising candidates in the fabrication of FA-based composites because of their high chemical stability, good compressive strength, and high durability. If FA can be recycled as water retention and absorbent materials, it would provide potential applications of FA in the agriculture and industry field.

Reference

1. Abdulhameed, U.A., Khairul S.B. (2012). Potential use of Malaysian thermal power plants coal bottom ash in construction. International Journal of Sustainable Construction Engineering & Technology. Vol 3, Issue 2.
2. Adriano, D. C., Weber, J. T.: Influence of fly ash on soil physical properties and turfgrass establishment. J. Environ. Qual. 30(2), 596-601 (2001)
3. Ahmaruzzaman, M. (2009). Role of Fly Ash in the Removal of Organic Pollutants from Wastewater. Energy Fuels. 2331494-1511
4. Ahmaruzzaman, M. (2010). A review on the utilization of fly ash. Progress in Energy and Combustion Science. 36 327–363
5. Ayanda S.O., Olalekan S.F., et al. (2012). Characterization of fly ash generated from Matla power station in Mpumalanga, South Africa. E-Journal of Chemistry. 9(4), 1788-1795
6. Basu, M., Pande, M., Bhadoria, P. B. S., Mahapatra, S. C.: Potential fly-ash utilization in agriculture: A global review. Prog. Nat. Sci. 19(10), 1173-1186 (2009)
7. Basu, Manisha., Manish, Pandea., et al. (2009). Potential fly-ash utilization in agriculture: A global review. Progress in Natural Science, Volume 19, Issue 10, Pages 1173-1186.
8. Bhatia, A. (2017). Utilization of coal fly ash in concrete industry to protect the environment. International Journal of Research in Engineering and Applied Sciences (IJREAS). 7(1), 46-56.
9. Black, L. (2016). Low clinker cement as a sustainable construction material. Sustainability of Construction Materials (Second Edition), Woodhead Publishing Series in Civil and Structural Engineering, Pages 415-457.
10. Blissett,R.S., Rowson, N.A., (2012). A review of the multi-component utilization of coal fly ash. Fuel. 97, 1-23.

11. Campbell, D. J., Fox, W. E., Aitken, R. L., Bell, L. C.: Physical characterization of sands
12. Carlson, C. L., Adriano, D. C. Environmental Impacts of Coal Combustion Residues. J. Environ. Qual. 22(2), 227-247 (1993).
13. Chauhan S. R., Kumar A., Singh I., Kumar and P. (2010). Effect of fly ash content on friction and dry sliding behavior of glass fiber reinforced polymer composites - A Taguchi approach. Minerals & Materials Characterization & Engineering. 9(4), 365-387.
14. Chen, T.P. Crystallization of glass ceramic prepaered from bottom ash and magnesium carbonate. Master Dissertation, Cheng Kung University, Taiwan, 2003.
15. Daniels, W. L., Barry, S., Kathryn, H., Carl, Z.: The Potential for Beneficial Reuse of Coal Fly Ash in Southwest Virginia Mining Environments, Virginia Cooperative Extension, publication 460-134 (2002)
16. Davison, L. Richard., Natusch, F. S. David., et al. (1974). Trace elements in fly ash. Dependence of concentration on particle size. Environ. Sci. Technol. 19748131107-1113.
17. Deepthi M. V., Sharma M., Sailaja R. R. N., et al. (2010). Mechanical and thermal characteristics of high density polyethylene-fly ash cenosphere composites", Materials and Design. 2051–2060.
18. Dilmore, R.M., Neufeld, R,D. (2001). Autoclaved aerated concrete produced with low-NOx burner/selective catalytic reduction fly ash. J. Energy Eng. 127, 37-50.
19. Dwivedi, A., Jain, M. K.: Fly ash–waste management and overview: A Review. Recent Research in Science and Technology, 6(1): 30-35 (2014)
20. Gangloff, W. J., Ghodrati, M., Sims, J. T., Vasilas, B. L.: Impact of fly ash amendment and incorporation method on hydraulic properties of a sandy soil. Water, Air Soil Poll. 119(1-4), 2331-245 (2000)
21. Ghodrati, M., Sims, J. T., Vasilas, B. L.: Evaluation of Fly-ash as a Soil Amendment for the

Atlantic Coastal-plain.1. Soil Hydraulic-properties and Elemental Leaching. Water, Air Soil Poll. 81(3-4), 349-361 (1995)

22. Gu J., Wu G. and Zhang Q. (2007). Effect of porosity on damping properties of modified epoxy composites filled with fly ash, Scripta Materialia. 57: 529–532.
23. Gupta N., Brar B. S., and Woldesenbet E. (2001). Effect of filler addition on the compressive and impact properties of glass fiber reinforced epoxy. Bulletins of Material Science. 24(2): 219-223.
24. Hansen, Y., Notten, P. J. & Petrie, J. G. The environmental impact of ash management in coal-based power generation. Appl. Geochem. 17(8), 1131-1141 (2002).
25. Harveer, Laura. (2014) Concrete mix design with fly ash and superplasticizer, International Journal of Multidisciplinary Research and Development 2014; 1(1): 107-110
26. International Energy Agency (IEA) (2010) Power Generation from Coal: Measuring and Reporting Efficiency Performance and CO2 Emissions, Coal Industry Advisory Board (CIAB) http://www.iea.org/ciab/papers/power_generation_from_coal.pdf (Accessed on 1st June. 2019).
27. International Energy Agency (IEA) (2013) Medium-Term Coal Market Report 2013 http://www.iea.org/publications/freepublications/publication/MTcoalMR2013_free.pdf (Accessed on 1st June. 2019).
28. Jala, S., Goyal, D. Fly ash as a soil ameliorant for improving crop production - a review. Bioresour. Technol. 97, 1136-1147 (2006)
29. Jankowski, Jerzy., Ward, Colin., et al. (2006). Mobility of trace elements from selected Australian fly ashes and its potential impact on aquatic ecosystems. Fuel. 85(2):243-256.
30. Jayaranjan, M. L. D., van Hullebusch, E. D., Annachhatre. A. P. (2014). Reuse options for coal fired power plant bottom ash and fly ash. Rev. Environ. Sci. Biotechnol. 13(4),

467-486

31. Kalra, N, Jain, M. C., Joshi, H. C., Choudhary, R., Harit, R. C., Vatsa, B. K., Sharma, S. K., Kumar V.: Fly ash as a soil conditioner and fertilizer. Bioresour. Technol. 64, 163-167 (1998).
32. Kumpiene, J.: Trace element immobilization in soil using amendments, Trace Element in Soils, Edited by Peter S. Hooda, 2010 Blackwell Publishing, Ltd, (2010)
33. Lieberman R.N., Green U., et al. (2015). Coal fly ash as a potential fixation reagent for radioactive wastes, Fuel,153:437-444.
34. Lin, S. L., Takahashi, F.: Raw and Treated Coal Fly Ash Amendment Aiming for Water Holding Capacity Adjustment of Natural Soils. J. Residuals Sci. Technol. 12(2), 73-84 (2015)
35. Lu, S. G., Sun, F. F., Zong, Y. T.: Effect of rice husk biochar and coal fly ash on some physical properties of expansive clayey soil (Vertisol). Catena. 114, 37–44 (2014)
36. Matsi, T., Keramidas, V. Z.: Flyash application on two acid soils and its effect on soil salinity, pH, B, P and on ryegrass growth and composition. Environ Pollut, 104, 107–112 (1999)
37. Natusch, DFS., Wallace, JR. (1974). Urban aerosol toxicity: the influence of particle size. Science. 186:695.
38. Neupane, Ghanashyam., Donahoe, Rona. (2012). Leachability of elements in alkaline and acidic coal fly ash samples during batch and column leaching tests. Fuel. 104:758-770.
39. Page, A. L., Elseewi, A. A., Straughan, I. R.: Physical and chemical properties of fly ash from coal-fired power plants with special reference to environmental impacts, Residue Rev, 71, 83–120 (1979)
40. Pathan, S. M., Aylmore, L. A. G., Colmer, T. D.: Fly ash amendment of sandy soil to

improve water and nutrient use efficiency in turf culture, International Turfgrass Society Research Journal, 9, 33-39 (2001)

41. Pathan, S. M., Aylmore, L. A., Colmer, T. D.: Properties of several fly ash materials in relation to use as soil amendments. J Environ Qual. 32(2), 687-93 (2003)
42. Prasad, B., Banerjee, N. N., Dhar, B.B. Environmental assessment of coal ash disposal: A review. J. Sci. Ind. Res. India. 55(10), 772-780 (1996).
43. Ram, L. C., Masto, R.E.: Fly ash for soil amelioration: A review on the influence of ash blending with inorganic and organic amendments. Earth-Sci. Rev. 128, 52-74 (2014)
44. Roy, W.R., Berger, P.M. (2011). Geochemical controls of coal fly ash lechate pH. Coal Combustion and Gasification Products. 3,63-66.
45. Shaheen, S. M., Hooda, P. S., Tsadilas, C. D.: Opportunities and challenges in the use of coal fly ash for soil improvements - A review. J. Environ. Manage. 145, 249-267 (2014)
46. Tang, Z.H., Ma, S.H., Ding, J.: Current status and prospect of fly ash utilization in China. 2013 World of Coal Ash (WOCA) Conference, 037, Lexington, KY, April 22-25 (2013)
47. Taylor, E. M., Schumann, G. E.: Fly ash and lime amendment of acidic coal soil to aid revegetation, J Environ Qual, 17 , pp. 120–124 (1988)
48. Temuujin, Jadambaa. (2013). Characterization and utilization of coal combustion by-products in Mongolia. In book: Fly Ash: Sources, Applications and Potential Environmental Impacts, Publisher: Nova Publishers (ISBN: 978-1-62948-044-2), pp.165-180.
49. Tolle, D. A., Arthur, M. F., Pomeroy, S. E.: Fly ash use for agriculture and land reclamation: a critical literature review and identification of additional research needs. RP-1224-5. Columbus. Ohio: Battelle Columbus Laboratories (1982)
50. Tsuchiai, Hiroaki., Ishizuka, Tomohiro., et al. (1995). Highly Active Absorbent for SO2

Removal Prepared from Coal Fly Ash. Ind. Eng. Chem. Res. 3441404-1411

51. Vassilev, S. V., Vassilev, C. G. (2006). A new approach for the classification of coal fly ashes based on their origin, composition, properties, and behavior. Fuel. 86, 1490-1512.
52. World Coal Association (WCA) (2015) Coal Facts 2015. https://www.worldcoal.org/file_validate.php?file=Coal%20Facts%202015.pdf (Accessed on 1st June. 2019).
53. Yao, Z. T., Ji, X. S., Sarker, P. K., Tang, J. H., Ge, L. Q., Xi, M. S., Xi, Y. Q. (2015): A comprehensive review on the applications of coal fly ash. Earth-Sci. Rev. 141, 105-121
54. Yao, Zhitong. (2013). Generation, characterization and extracting of silicon and aluminum from coal fly ash. In book: Fly Ash: Sources, Applications and Potential Environmental Impacts, Publisher: Nova Publishers (ISBN: 978-1-62948-044-2), pp.3-58.

Chapter 2

Evaporation mitigation capacity of soil/sand mixed with/without raw fly ash

2.1 Background

2.1.1 Soil water and soil water holding capacity

There are three main types of soil water: gravitational water, capillary water, and hygroscopic water (Parker, 1922). Gravitational water is free to drain downwards through the soil. Capillary water is available for plants. It stays around the soil particles in the capillary zone by surface forces (Figure 2-1). Gravity cannot remove it from the soil particles, but it can evaporate quickly at atmospheric temperatures. Hygroscopic water cannot be separated from the soil unless it is heated. It remains tightly on the surface of soil particles that plants cannot absorb it.

The definition of water holding capacity (WHC) is the total amount of water that a soil can hold under positive suction pressure. The WHC is an essential characteristic of soil. Land with a larger WHC was less leaching losses of nutrients and is well-suitable for plant growth.

2.1.2 Factors have influence on soil water retention capacity

Several characteristics can have influences on the soil WHC (Figure 2-2), such as soil texture and structure, porosity, particle size and the soil organic matter content (Gupta et al., 1979; Hollis et al., 1977; Jong et al., 1983). Soil structure refers to the arrangement of soil particles into stable units called aggregates, which can be loose and friable. Soil porosity depends on both soil texture and structure. Soil porosity refers to the space between soil

particles, which consist of different amounts of water or air. Soil texture refers to the composition of the soil in terms of particle size distribution. It determines the rate at which water drains through saturated soil. The amount of hygroscopic water varies inversely with the size of soil particles. The smaller the particle, the higher amount of hygroscopic water it adsorbs. In general, clay soils have a more excellent water holding capacity than sandy soils. Soil organic matter content also influences the water holding capacity due to the affinity of organic matter to water.

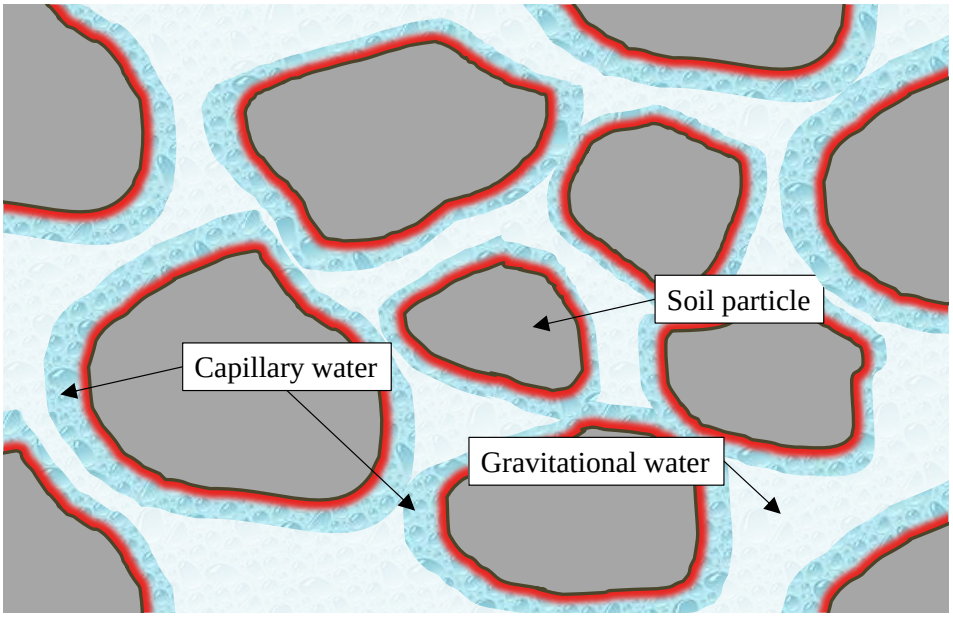

Figure 2-1. Types of soil water that can be absorbed by plants (Lin, 2018).

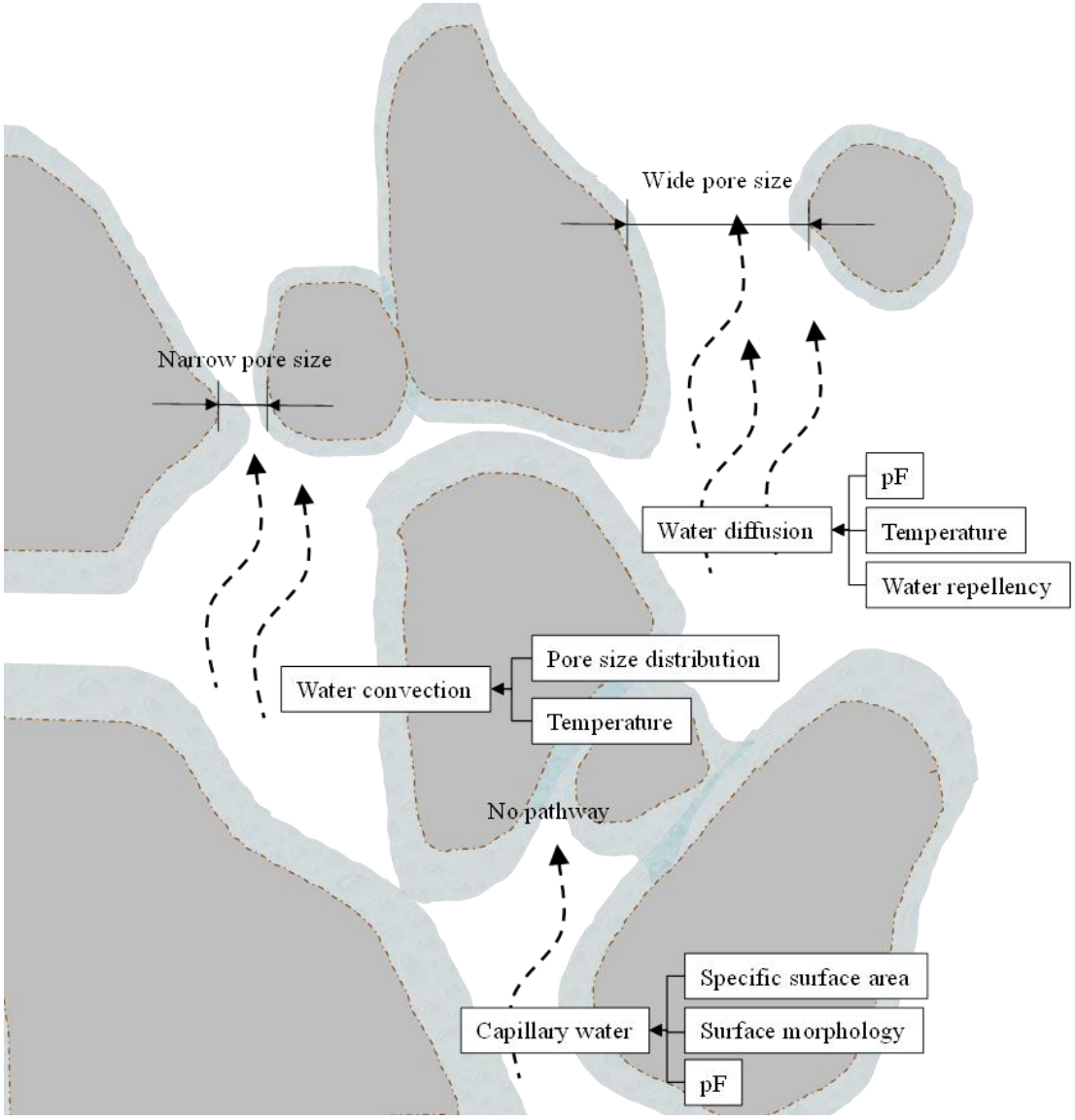

Figure 2-2 Factors that affect soil water holding capacity (Lin, 2018)

2.1.3 Conventional measurements on soil water holding capacity

Many lab-scale methods have been developed to determine soil WHC. For example, in the European maximum water holding capacity method (Figure 2-3), the soil sample is saturated with water in a cylinder placed on a permeable membrane. The excess water is drawn away by gravity into the porous layer. When the equilibrium in this system is reached, WHC can be calculated according to the weight of the water held in the sample versus the sample dry weight. The typical measurements on soil water holding capacity are usually under saturated conditions and controlled by gravity or pressure.

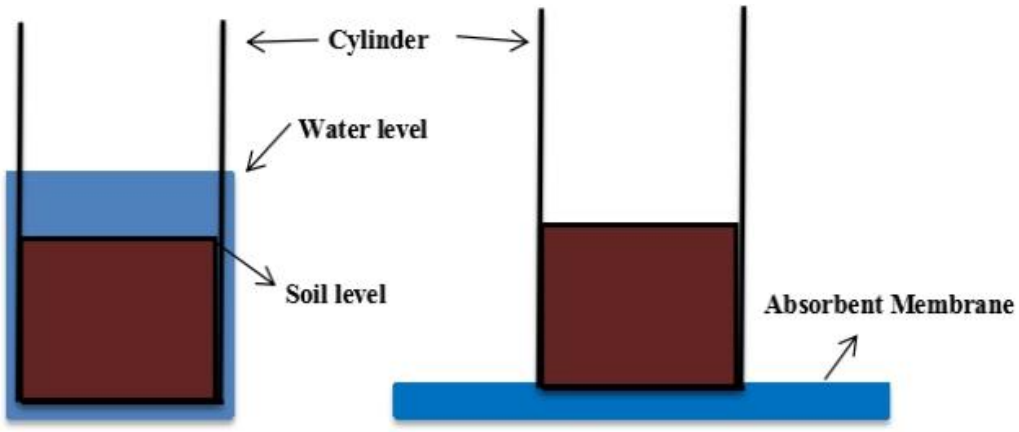

Figure 2-3. "European" maximum water holding capacity method

However, in arid/semi-arid areas, the major pathway of water loss from the soil system is natural evaporation when evapotranspiration by grasses and plants is excluded. Even after rainfall, only soil surface layer will be saturated and lower layer will be still unsaturated. Excluding initial runoff and evapotranspiration of plants, temperature-driven evaporation is a main pathway of soil moisture loss in arid areas. However, conventional measurements on soil water holding capacity usually exclude temperature-driven evaporation. This study aims to simulate water loss via temperature-driven evaporation, not pressure-driven evaporation like WHC measurement. In addition applications of FA as a water holding material in real

arid/semi-arid areas are limited. There is a large gap between the effective increase of WHC by the FA amendment and real FA applications as a water holding material in arid/semi-arid areas. Therefore, in this study, a new method was used on measuring the evaporation mitigation capacity (EMC). It represented water loss mitigation capacity against physical evaporation, which was measured by drying experiments (Lin, 2015).

2.2 Experimental materials & methods

2.2.1 Coal fly ash (FA), soils and sands properties

FA utilized in this study was taken from one coal-fired power plant in Japan. The elemental content of tested FA, analyzed by Energy Dispersive X-Ray Fluorescence spectrometer, is shown in Table 2-1. According to the elemental content, FA tested in this study is classified into Class F. The particle size of tested FA is less than 150 μm. Microscopic surface conditions of FA particles were observed by scanning electron microscope (SEM; JSM-6610LA, JEOL Co.), which is shown in Figure 2-4. It can be noticed that the fly ash sample consists of dominantly regular spherical particles ranging fine silt size (0.5 to 15 μm) in diameter (see Figure 2-5).

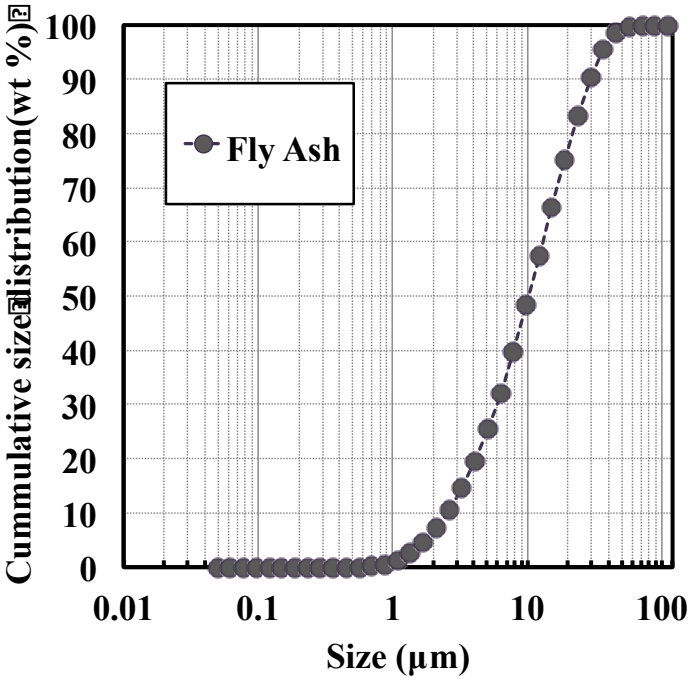

Figure 2-5. Cumulative size distribution of fly ash (Unit: wt %)

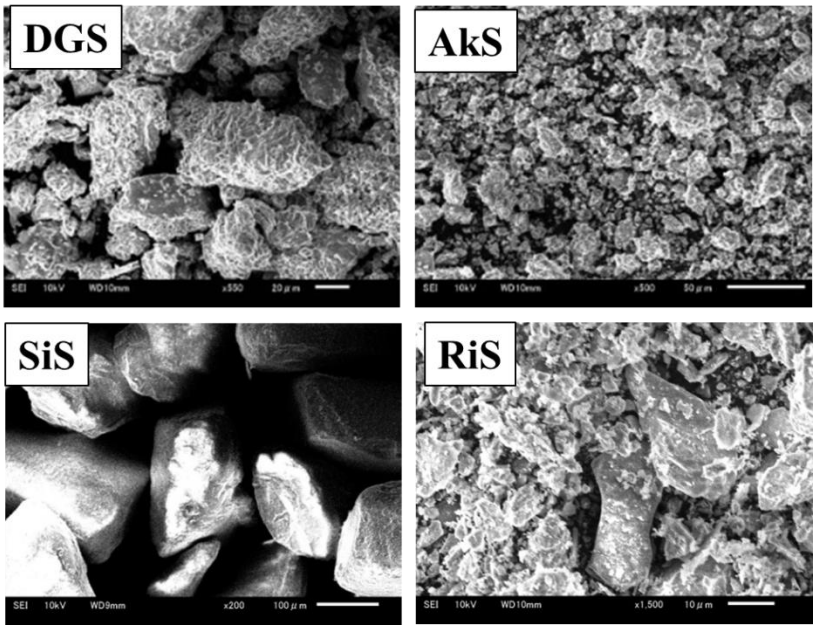

Figure 2-6. Surface morphology of Surface morphology of DGS, AkS, SiS and RiS.

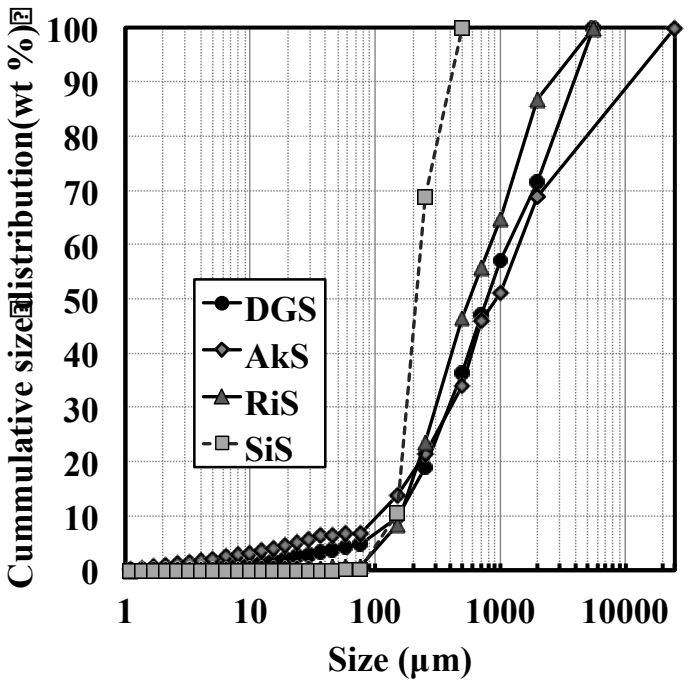

Figure. 2-7. Cumulative size distribution of tested soils and sands (Unit: wt %)

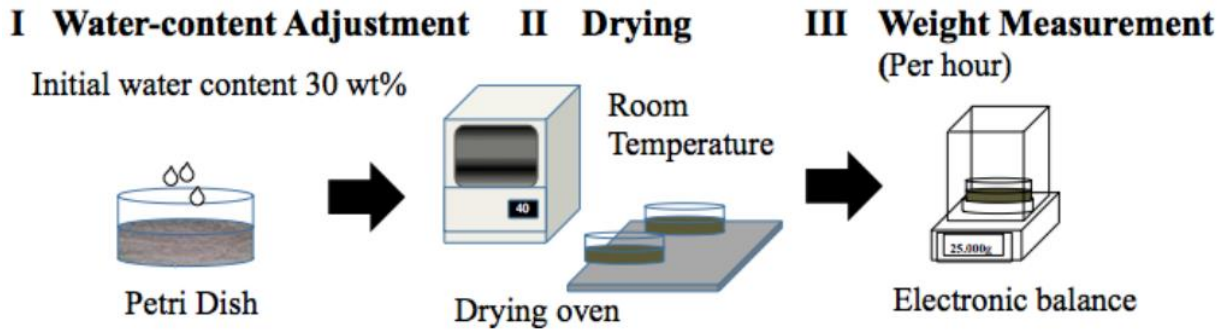

Figure 2-8. Procedure of the drying experiment on measuring EMC

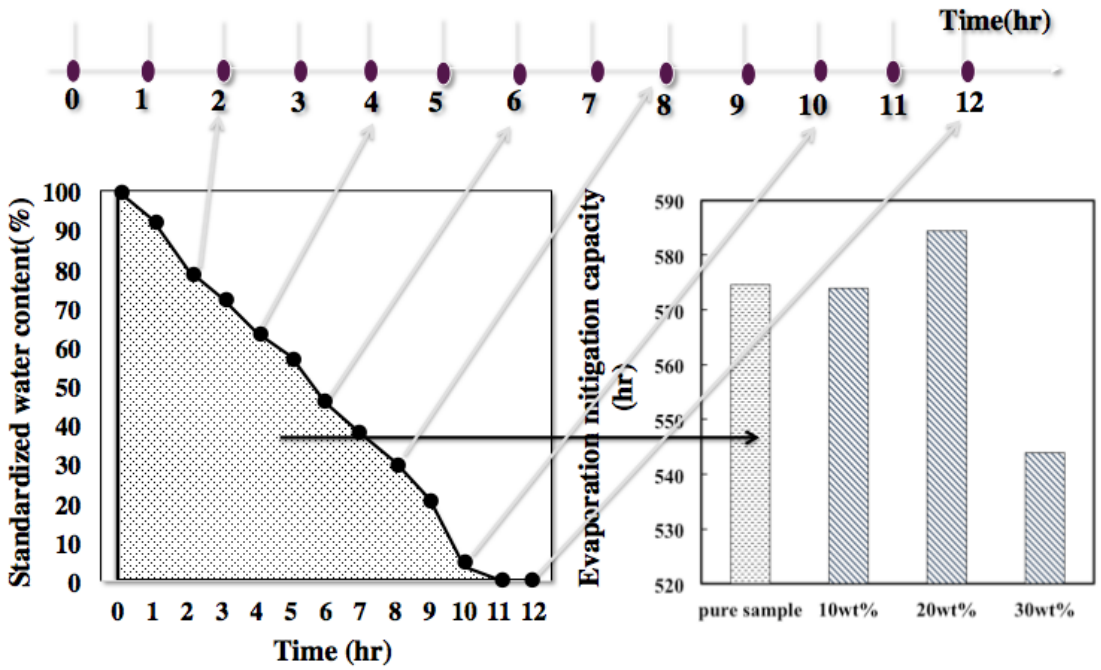

Figure 2-9. Concept of evaporation mitigation capacity (EMC) measured in this study

In this study, two kinds of gardening soils (akatama soil (AkS) and decomposed granite soil (DGS)) and two kinds of sands (river sand (RiS) and silica sand (SiS)) were used. The surface morphology of these soils and sands are shown in Figure 2-6. According to the soil classification category (World Reference Base for Soil Resources, 2014), decomposed granite soil is classified into Technosols. Akatama soil, river sand and silica sand are artificial soil and sands. The main content of akatama soil is classified into Volcanogeneous Regosols. The main composition of silica sand is SiO_2. Cumulative sieving size distributions of soils and sands measured by sequential sieving are illustrated in Figure 2-7. Based on soil grain size classification of American Association of State Highway and Transportation officials (AASHTO) (ASTM D3282-09), the initial percentage of clay, silt, sand, gravel of DGS are 0.22 %, 4.45 %, 67.1 %, and 28.3 %, respectively. Those of AkS are 0.89 %, 5.70 %, 62.3 %, and 31.1 %, respectively. Therefore, both soil samples are categorized as sand. RiS consists of

0.07 % of clay, 0.59 % of silt, 86.0 % of sand, and 13.3 % of gravel. Those of SiS are 0 %, 0.18 %, 99.8 %, and 0 %, respectively. According to sieving size distribution, the coefficients of Uniformity (ASTM D2487) were calculated to be 7.8 for DGS, 13.5 for AkS, 1.6 for SiS, and 5.3 for RiS, respectively. Coefficients of Gradation (ASTM D2487) are 0.91 for DGS, 1.1 for AkS, 0.98 for SiS, and 0.75 for RiS, respectively.

2.2.2 Soil/sand particles sieving

In order to investigate the effect of FA amendment on soil/sand EMC and its dependency on soil/sand sieving size, soil and sand samples were sieved into different size ranges; smaller than 75 μm, 75-150 μm, 150-250 μm, 250-500 μm, 500-710 μm, 710 μm-1 mm, 1-2 mm, and larger than 2 mm. In the case of DGS and RiS, the largest sieving size is 5.6 mm. The largest sieving size of AkS is 25 mm. The sieving size fraction <75 μm of RiS samples was not used in this study. SiS had only three sieving size ranges; 75-150 μm, 150-250 μm, and 250-500 μm.

2.2.3 Water holding capacity (WHC) measurement

The definition of WHC is the total amount of water that a soil can hold under certain suction pressure. In this research, 20 g of the soil/sand samples were saturated with water in a funnel. The excess water was discharged by gravity until the system reached to the equilibrium. The WHC was calculated according to the percentage of the remaining water in the sample to the sample dry weight.

2.2.4 EMC measurement

The measurement procedure is shown as Figure 2-8. Drying experiments were conducted at room temperature (around 20 ºC) and at 40 ºC in an incubator, respectively. In order to simulate water content of soil/sand in arid/semi-arid areas just after rainfall, the initial water

content was adjusted as 30 wt%. 7.5 g of distilled water was added to 17.5 g of pure soil/sand samples (DGS, AkS, RiS and SiS) or FA-mixed samples. The mass of the samples was monitored for 12 hours at one-hour-intervals to determine evaporation mitigation capacity (EMC). In order to reduce the impact of errors in initial water content adjustment, water content monitored at each drying time was standardized using the initial moisture weight (30 wt%) when water content curve was drawn. It sets 100 % at the beginning of drying experiment. 50 % means that half amount of water remained in the sample (15 wt% water content) and 0 % means complete drying. In this method, EMC was defined as the areas under EMC curve (see Figure 2-9). It should be noted that EMC measured by this method means water evaporation resistance rather than retainable water in soil structure at certain suction pressure. When soil/sand can hold a higher amount of water and keep water for longer time, EMC score will increase correspondingly. This study aimed to investigate the effect of the FA amendment on the EMC of soil/sand with different size ranges. Therefore, soil/sand samples were sieved and then used for EMC measurement as well as non-sieved one. FA was mixed with the different sieving size fractions of the soils and sands. FA mixing ratios were 10, 20, and 30 wt %. EMC of soils and sands with/without the FA amendment were measured by drying experiments. They were repeated three times to check experimental errors. One-sided Welch's t-test was used to identify statistically significant differences of EMC in the different sieving size fractions of the FA-amended/non-amended samples. The significance level of Welch's t-test was 5%.

2.2.5 Organic compound measurement by loss on ignition

The weight ratios of organic matter in the different sieving size fractions of soils and sands were measured. The amount of organic matter of the soils and sands was determined by the weight loss after thermal decomposition at 440 ºC in a muffle furnace overnight. Before thermal

decomposition, all samples were dried to make moisture weight negligible. The weight ratio of organic matter was calculated by the weight of organic matter divided by the initial weight of the sample. The measurements were repeated three times to check experimental errors owing to sample heterogeneity.

2.3. Results and Discussion

2.3.1 WHC of the different sieving size fractions and effect of FA amendment on WHC

The WHC measurement results show that there is a consistent trend between the WHC and the soil/sand sieving size (see Figure 2-10). WHCs are higher in smaller soil/sand sieving size fractions than those of the larger sieving size fractions. In general, soil/sand WHC is controlled primarily by the soil texture. Small size fractions have a larger specific surface area and lower hydraulic conductivity. Therefore the WHCs are higher, and the measurement results agree with the expectation. On the other hand, the FA amendment gave a limited effect on WHCs, although it increased silt size fractions greatly in terms of size distribution. Increases of WHC by FA amendment were usually regarded as significant by the t-test at 5 % significance level for 30 wt% amendment cases. However, they were always less than 9% increase for any sieving size and soil/sand types. Experimental results show that the effect of the FA amendment on WHC of tested samples is much smaller than the sieving size effect. Limited impact of the FA amendment on WHC is different from previous researches, which reported the high impact of the FA amendment to increase WHC (Campbell et al., 1983; Adridno et al., 2001; Gangloff et al., 2000; Pathan et al., 2001). Because this study tested sieved samples with minimal range of size distribution, the size distribution of pores (or voids) in the sample would also be limited. The diversity of pore size is limited. The FA amendment might work ineffectively to produce intergranular capillary zones for water retention. This hypothesized explanation might be

partially supported by Simpson (Simpson, 2014). Using Ottawa 50/70 sand with limited particle size range (0.1-2 mm, the coefficient of Uniformity = 1.07), Simpson reported a negligible increase of the intergranular void ratio of Ottawa sand until clay addition to around 20 wt%. The spherical void ratio of the sand also shows negligible increase until 30 wt% clay addition when they are mixed densely, which was estimated by thermal conductivity measurement. Tracy et al. quantified water distribution in soil pores using X-ray Computed Tomography (CT) coupled with image-based modeling (Tracy et al., 2015). This technique might be useful for further study to explain the limited effect of the FA amendment (and silt/clay addition) on WHC of samples with limited sieving size distribution.

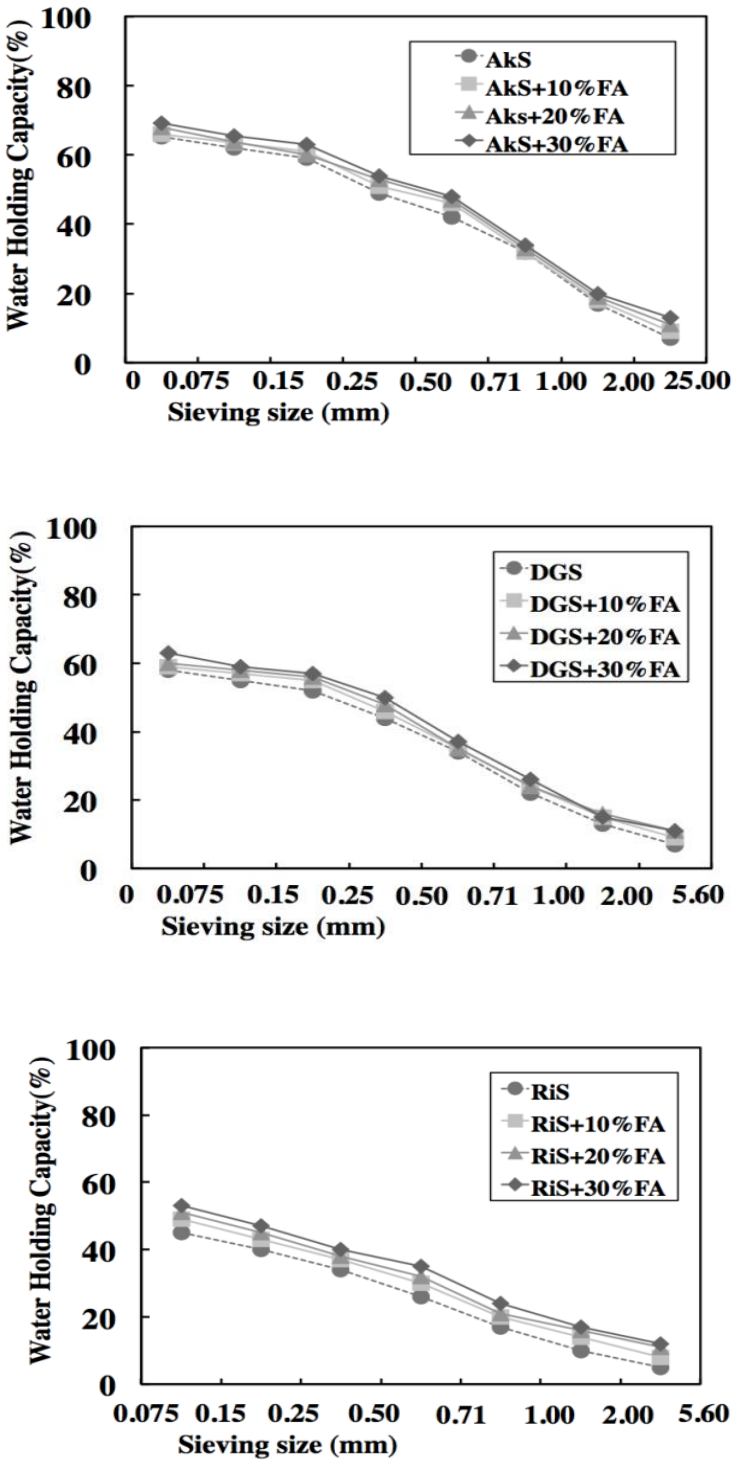

Figure 2-10. WHC of soil/sand of the different sieving size fractions and different amounts of FA added

2.3.2 EMC of the different sieving size fractions

EMC of soil/sand samples (DGS, AkS, RiS, and SiS) are shown in Figure 2-19 and 2-20. To make EMC comparison easier, EMC of soil/sand samples at each sieving size was standardized. They are divided by the weighted average of EMC based on sieving size distribution. They are shown in Figure 2-21 for natural temperature (around 20 ºC) and in Figure 2-22 for 40 °C, respectively. There was a non-linear relationship between the EMC and the soil/sand sieving size. The highest or lowest EMC appeared in a specific range of sieving sizes, and it differentiated with soil/sand type and temperature. In the cases of DGS at room temperature, EMCs at the sieving size fraction of both 150-250 μm and 250-500 μm are approximately equal to the maximum.

On the other hand, DGS with the sieving size fraction of 250-500 μm and 1-2 mm almost have the same EMC with the maximum at 40 °C. EMC of DGS for the 75-150 μm sieving size fraction was found to be the highest at room temperature but the second lowest at 40 °C. EMC of AkS also shows temperature dependency. At room temperature, AkS has the second highest EMC for the 150-250 μm fraction. However, the same sieving size fraction has the second lowest EMC at 40 °C. Such sieving size and temperature dependencies were also found for RiS at the sieving size fraction of 75-150 μm. RiS with 75-150 μm sieving size fraction has lower EMC than the average at room temperature but has the second highest EMC at 40 °C. The similar variations are also found for SiS though it has only three sieving size fractions. At natural temperature, the highest and lowest EMC s of SiS are located at the sieving size fraction of 250-500 μm and 150-250 μm, respectively. In contrast, the highest EMC of SiS at 40 °C is found at the sieving size fraction of 75-150 μm.

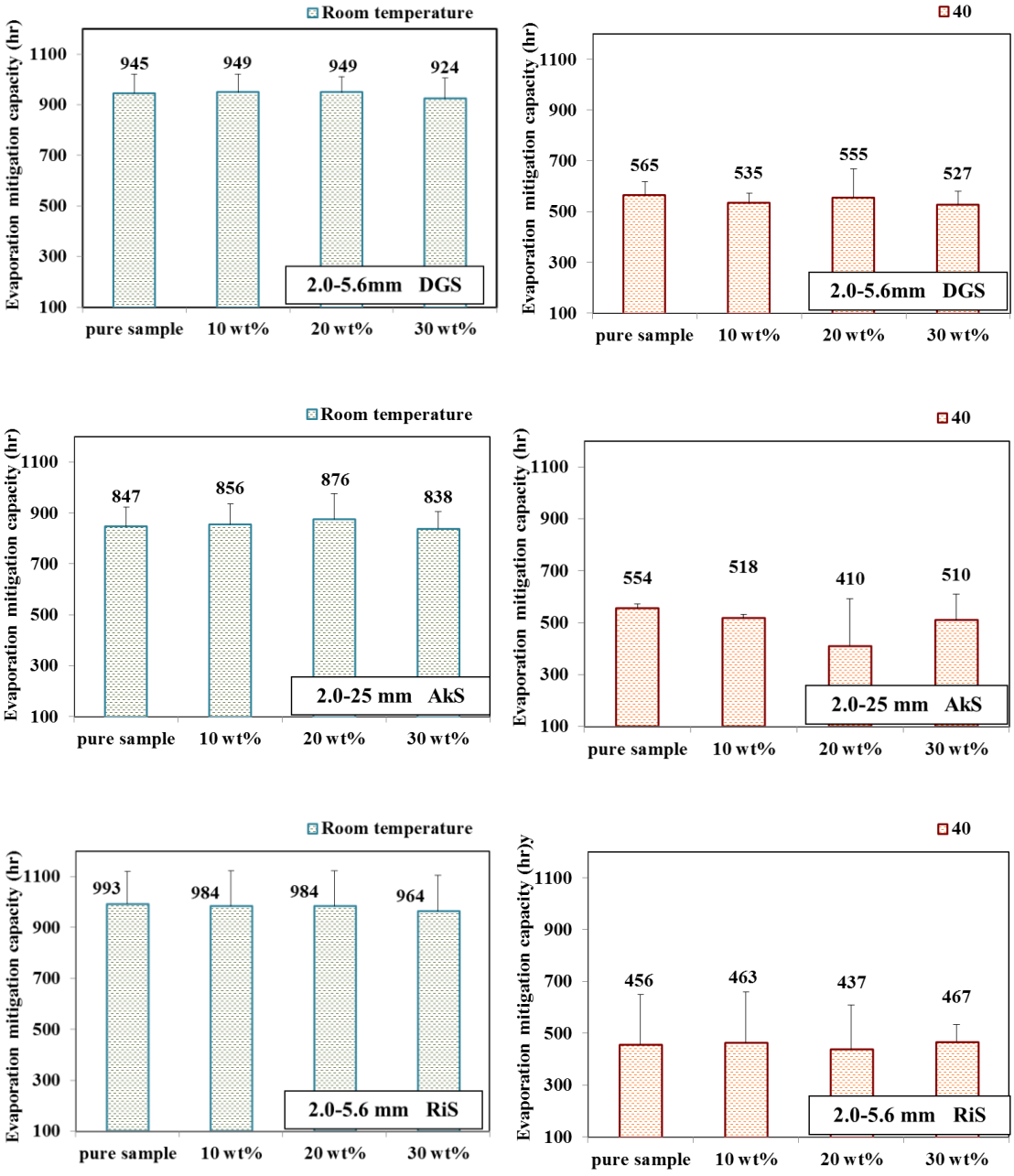

Figure 2-11. EMC of raw FA-amended soil/sand in the size range > 2mm at room temperature and 40 ºC.

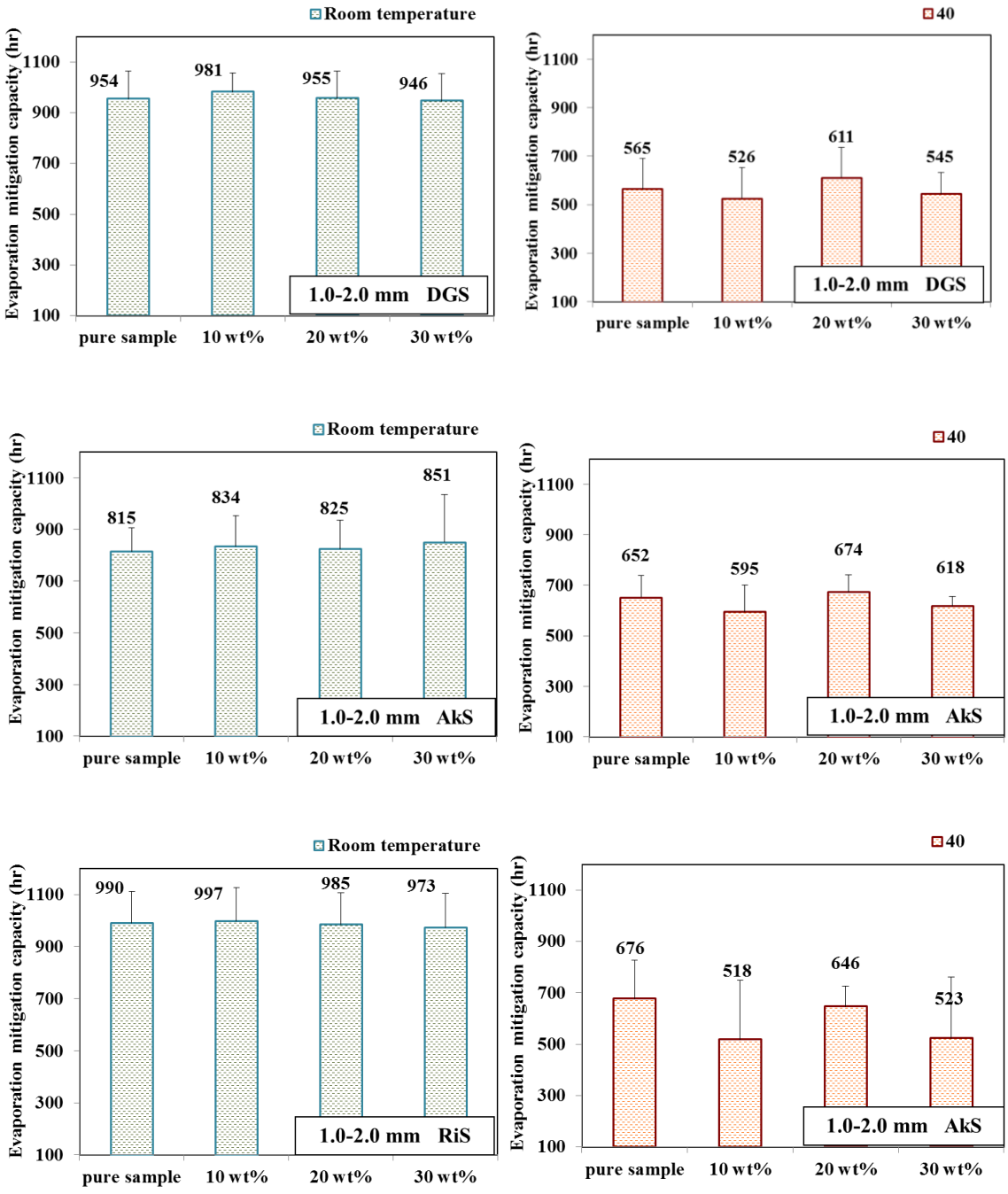

Figure 2-12. EMC of raw FA-amended soil/sand in the size range 1-2 mm at room temperature and 40 ºC.

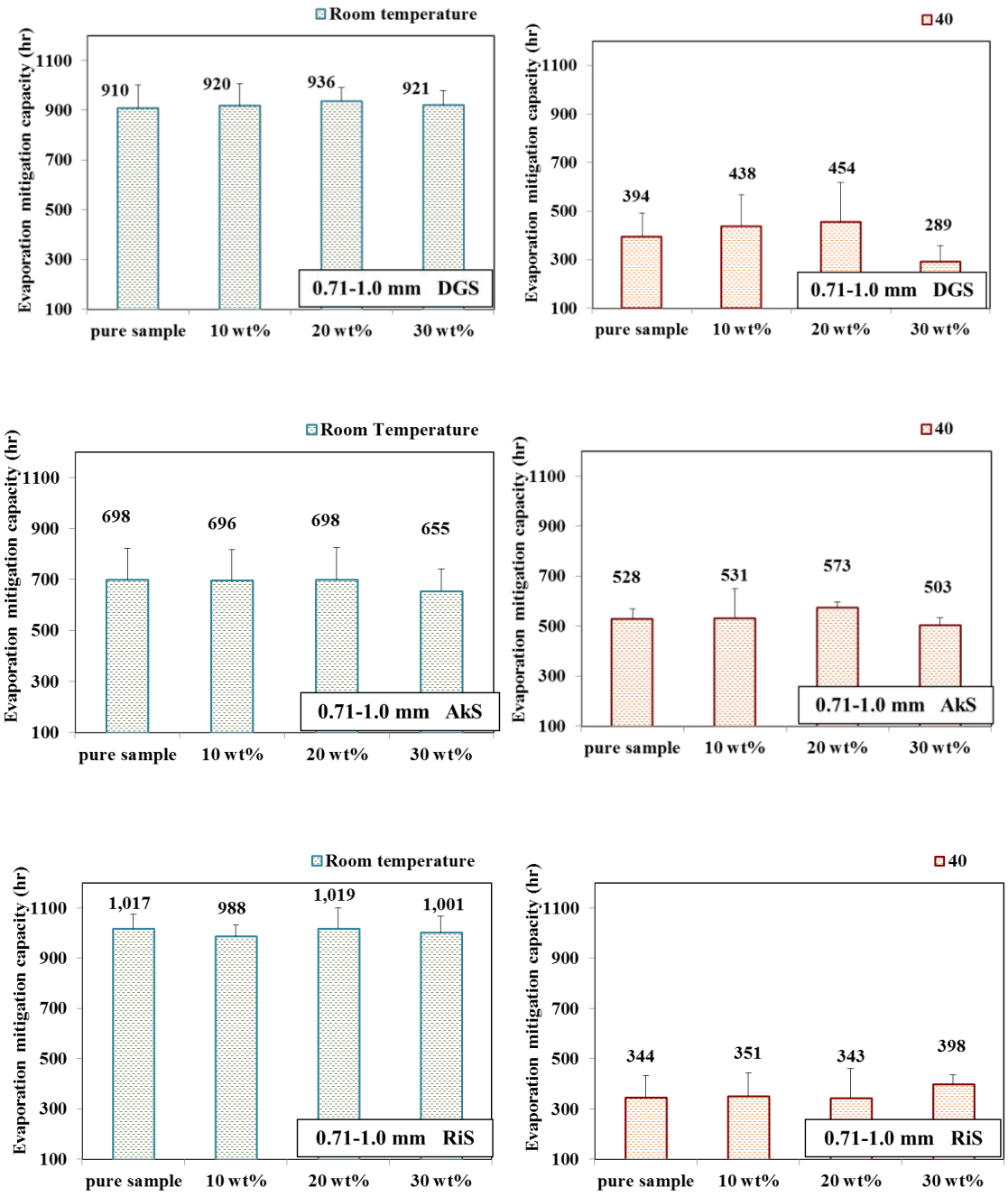

Figure 2-13. EMC of raw FA-amended soil/sand in the size range 0.71-1 mm at room temperature and 40 ºC.

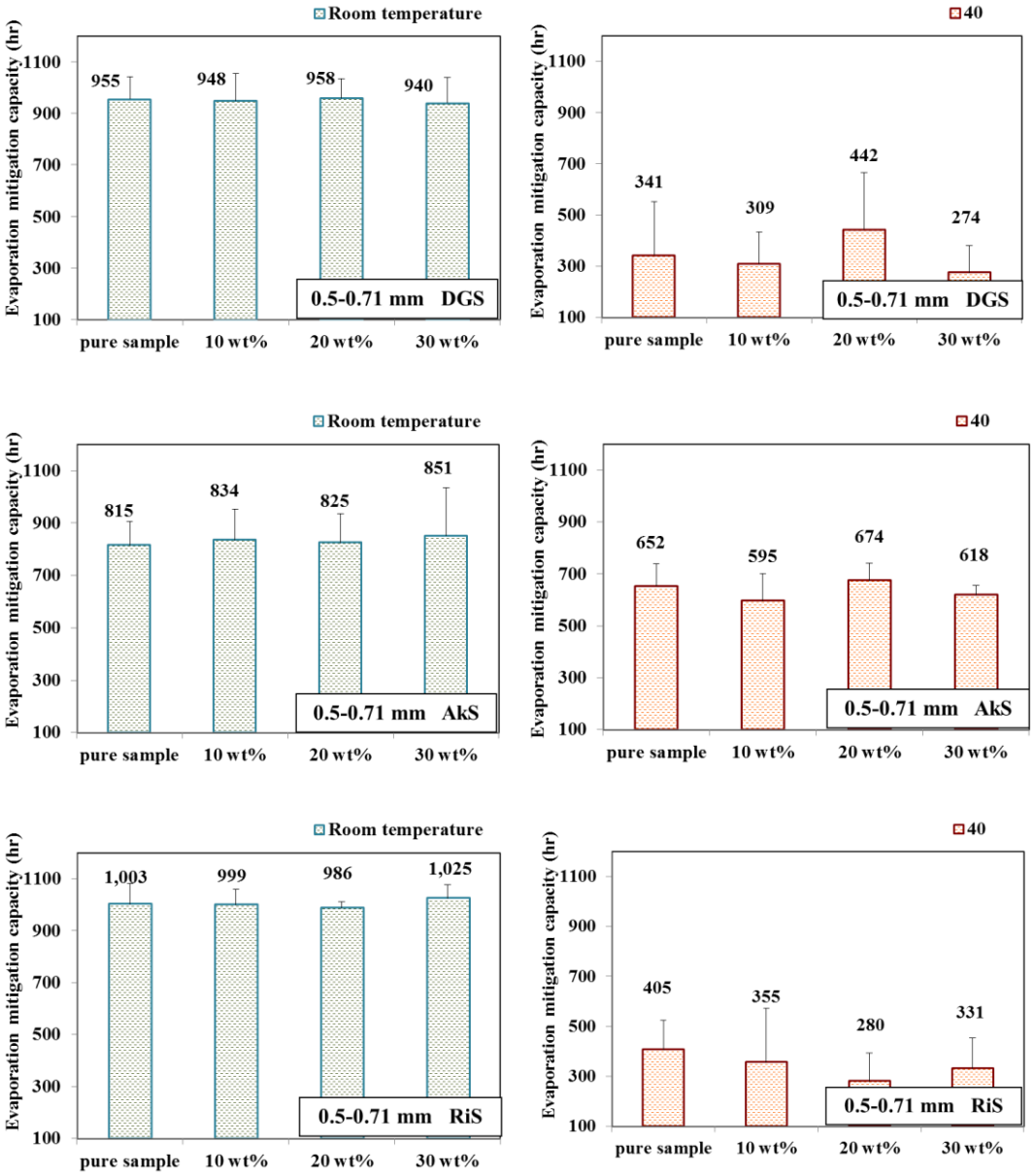

Figure 2-14. EMC of raw FA-amended soil/sand in the size range 0.5-0.71 mm at room temperature and 40 ºC.

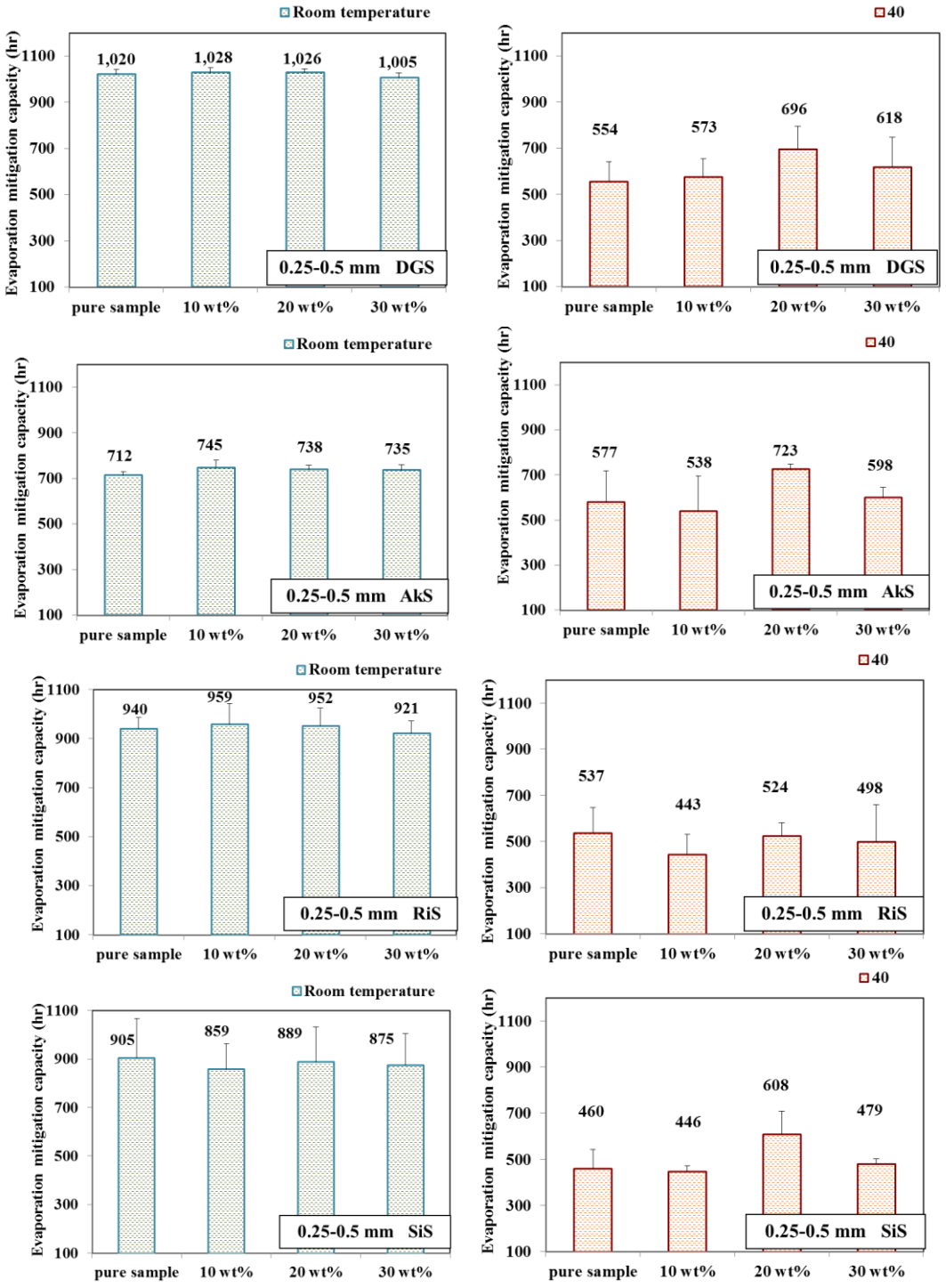

Figure 2-15. EMC of raw FA-amended soil/sand in the size range 0.25-0.5 mm at room temperature and 40 ºC.

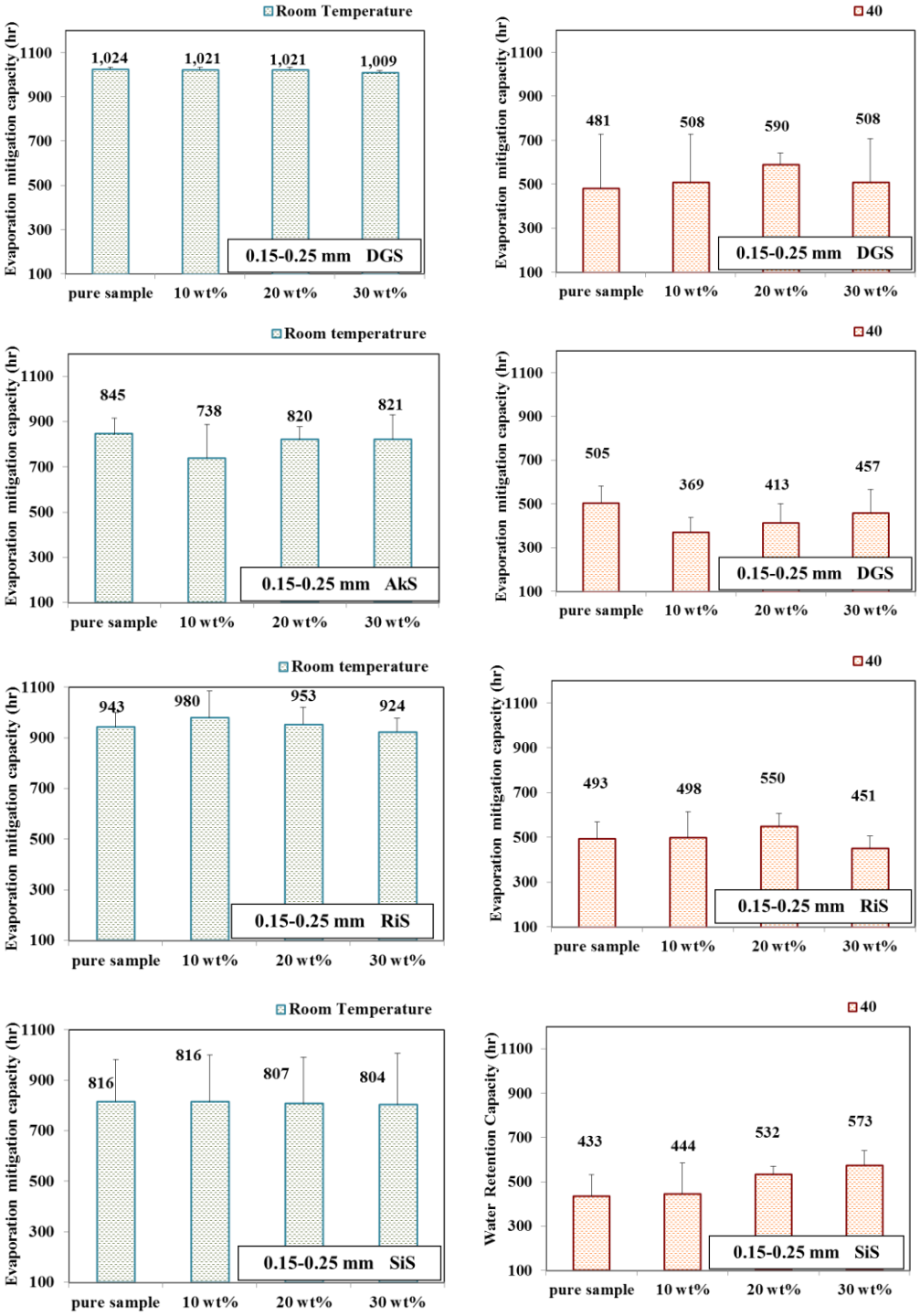

Figure 2-16 EMC of raw FA-amended soil/sand in the size range 0.15-0.25 mm at room temperature and 40 ºC.

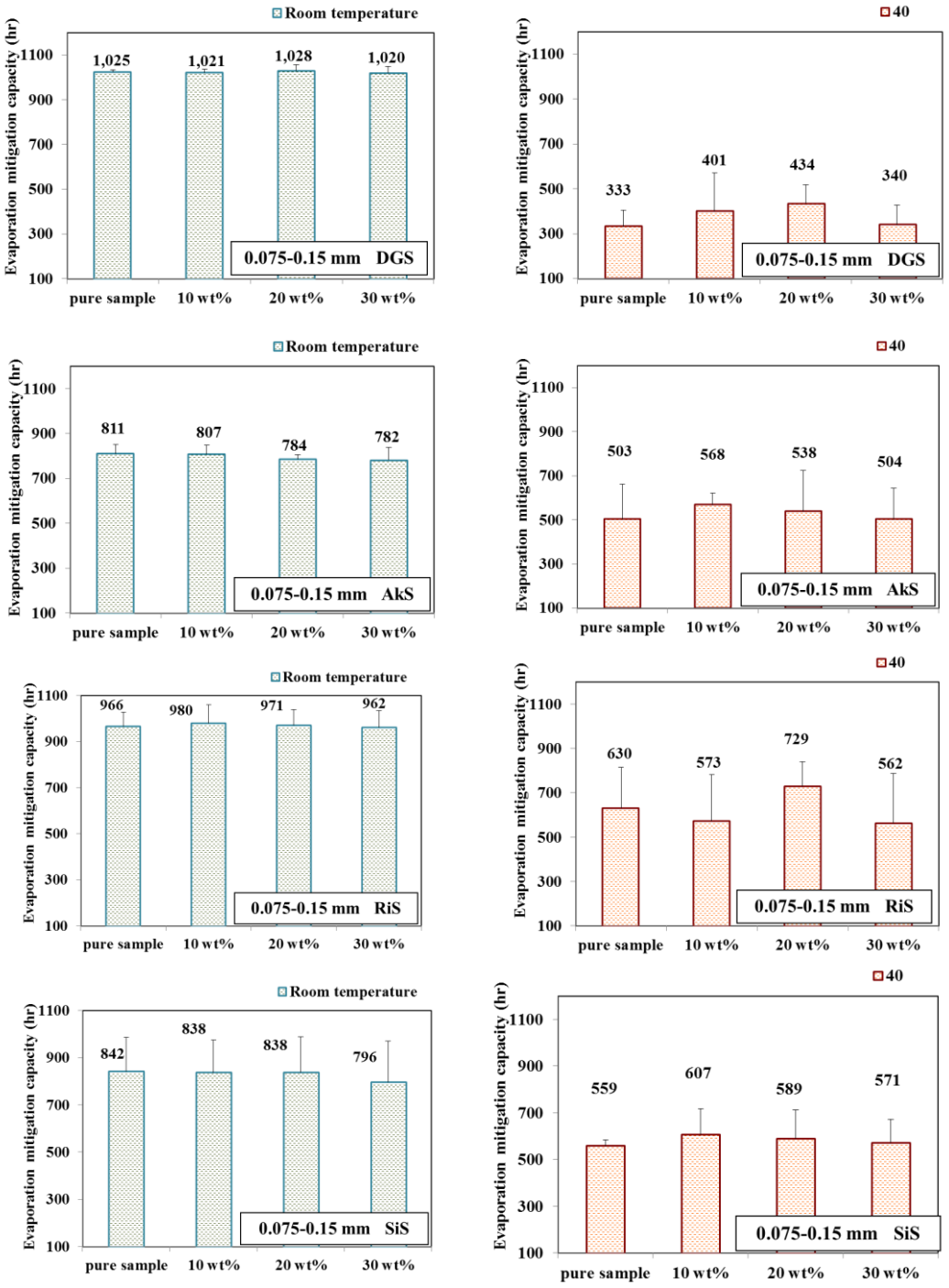

Figure 2-17. EMC of raw FA-amended soil/sand in the size range 0.075-0.15 mm at room temperature and 40 ºC.

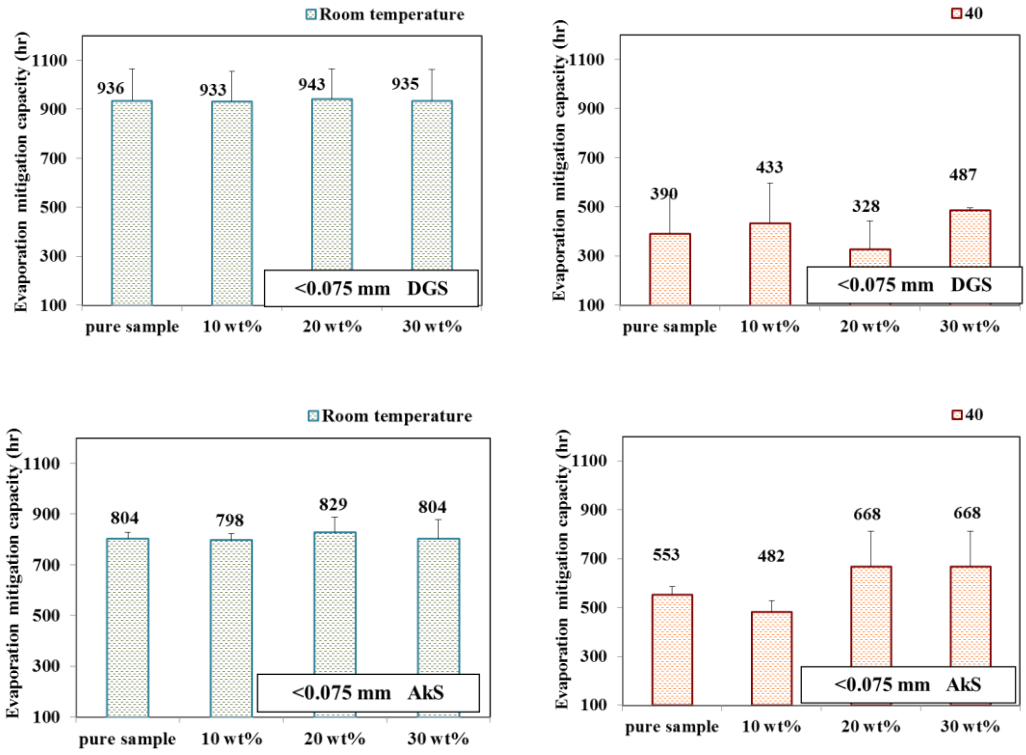

Figure 2-18. EMC of raw FA-amended soil/sand in the size range <0.075 mm at room temperature and 40 ºC.

Table 2-4. Relative changes of EMC of raw-FA amended soil/sand in the size range >2 mm

Size>2mm	Relative change of EMC (%)					
Temperature	Room Temperature			40 ºC		
FA ratio	10 wt%	20 wt%	30 wt%	10 wt%	20 wt%	30 wt%
DGS	+0.361	+0.361	-2.27	-5.38	-1.80	-6.76
AS	+1.02	+3.37	-1.05	-12.9	+7.45	-13.1
RS	-0.893	-0.955	-2.924	+1.45	-4.25	+2.28

Table 2-5. Relative changes of EMC of raw-FA amended soil/sand in the size range of 1-2 mm

Size 1-2mm	Relative change of EMC (%)					
Temperature	Room Temperature			40 ºC		
FA ratio	10 wt%	20 wt%	30 wt%	10 wt%	20 wt%	30 wt%
DGS	+2.89	+0.170	-0.839	-7.07	+8.13	-3.65
AS	+2.26	+1.25	+4.35	-8.77	+3.29	-5.25
RS	+0.673	-0.525	-1.77	-23.4	-4.45	-22.7

Table 2-6. Relative changes of EMC of raw-FA amended soil/sand in the size range of 710 µm-1 mm

710µm-1 mm	Relative change of EMC (%)					
Temperature	Room Temperature			40 ºC		
FA ratio	10 wt%	20 wt%	30 wt%	10 wt%	20 wt%	30 wt%
DGS	+1.11	+2.95	+1.23	+11.1	+15.2	-26.68
AS	-0.330	+0.0184	-6.27	+0.632	+8.66	-4.76
RS	-2.91	+0.122	-1.57	+2.13	-0.239	+15.8

Table 2-7. Relative changes of EMC of raw-FA amended soil/sand in the size range of 500 µm-710 µm

500-710 µm	Relative change of EMC (%)					
Temperature	Room Temperature			40 ºC		
FA ratio	10 wt%	20 wt%	30 wt%	10 wt%	20 wt%	30 wt%
DGS	-0.653	+0.373	-1.54	-9.51	29.6	-19.6
AS	+0.0842	+4.10	+1.41	-3.60	-4.35	-7.86
RS	-0.37	-1.65	+2.20	-12.3	-30.9	-18.4

Table 2-8. Relative changes of EMC of raw-FA amended soil/sand in the size range of 250 µm-500 µm

250-500 µm	Relative change of EMC (%)					
Temperature	Room Temperature			40 ºC		
FA ratio	10 wt%	20 wt%	30 wt%	10 wt%	20 wt%	30 wt%
DGS	+0.811	+0.673	-1.22	+3.54	+25.7	+11.6
AS	+4.65	+3.77	+3.30	-6.76	+25.4	+3.71
RS	+1.99	+1.26	-1.99	-17.5	-2.40	-7.12
SS	-5.07	-1.81	-3.37	-2.96	+32.3	+4.31

Table 2-9. Relative changes of EMC of raw-FA amended soil/sand in the size range of 150 µm-250 µm

150-250 µm	Relative change of EMC (%)					
Temperature	Room Temperature			40 ºC		
FA ratio	10 wt%	20 wt%	30 wt%	10 wt%	20 wt%	30 wt%
DGS	-0.269	-0.265	-1.44	+5.58	+22.6	5.58
AS	-12.7	-2.87	-2.76	-26.8	-18.2	-9.36
RS	+3.93	+1.07	-2.07	+0.985	+11.4	-8.59
SS	-0.0251	-1.02	-1.50	+2.46	+22.9	+32.5

Table 2-10. Relative changes of EMC of raw-FA amended soil/sand in the size range of 75 µm-150 µm

75-150 µm	Relative change of EMC (%)					
Temperature	Room Temperature			40 ºC		
FA ratio	10 wt%	20 wt%	30 wt%	10 wt%	20 wt%	30 wt%
DGS	-0.319	+0.364	-0.474	+20.4	+30.6	+2.31
AS	-0.386	-3.22	-3.58	+13.1	+7.13	+0.218
RS	+1.46	0.512	-0.419	-9.10	+15.7	-10.8
SS	-0.584	-0.590	-5.52	+8.62	+5.44	+2.28

Table 2-11. Relative changes of EMC of raw-FA amended soil/sand in the size range of < 75 μm

<75 μm	Relative change of EMC (%)					
Temperature	Room Temperature			40 ºC		
FA ratio	10 wt%	20 wt%	30 wt%	10 wt%	20 wt%	30 wt%
DGS	-0.299	+0.768	-0.0498	+10.9	-16.0	+24.7
AS	-0.658	+3.15	+0.0286	-12.8	+20.8	+20.8

Table 2-12 The weight ratio of organic matter content in each particle size fraction of soil/sand

Particle size range (mm)	>2mm	1-2 mm	0.71-1 mm	0.5-0.71 mm	0.25-0.5 mm	0.15-0.25mm	0.075-0.15mm	<0.075 mm
Average Weight Ratio of Organic Matter content (wt %)								
DGS	1.268	1.866	1.449	3.194	4.410	4.209	6.994	11.08
AkS	20.99	20.68	21.92	18.19	18.94	19.64	22.38	20.80
RiS	0.7369	1.102	0.8350	0.9365	1.121	1.088	1.236	-
SiS	-	-	-	-	0.6279	0.8552	2.730	-

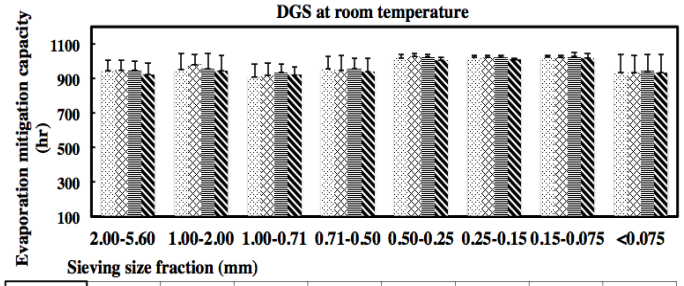

FA 0 wt%	945	954	910	955	1020	1024	1025	936
FA 10 wt%	949	981	920	948	1028	1021	1021	933
FA 20 wt%	949	955	936	958	1026	1021	1028	943
FA 30 wt%	924	946	921	940	1005	1009	1020	935

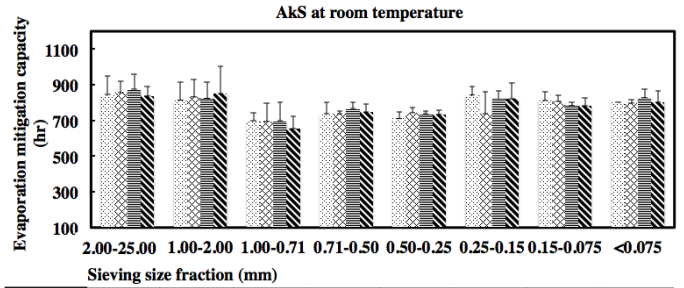

FA 0 wt%	847	815	698	738	712	845	811	804
FA 10 wt%	856	834	696	738	745	738	807	798
FA 20 wt%	876	825	698	768	738	820	784	829
FA 30 wt%	838	851	655	748	735	821	782	804

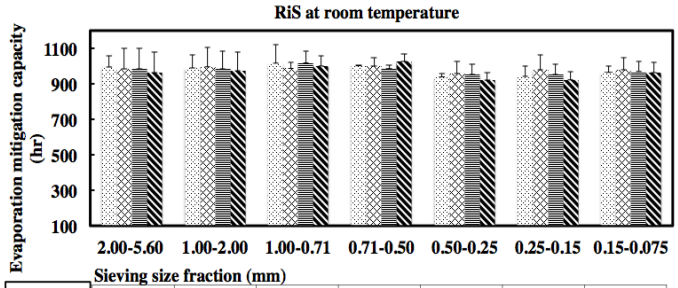

FA 0 wt%	993	990	1017	1003	940	943	966
FA 10 wt%	984	997	988	999	959	980	980
FA 20 wt%	984	985	1019	986	952	953	971
FA 30 wt %	964	973	1001	1025	921	924	962

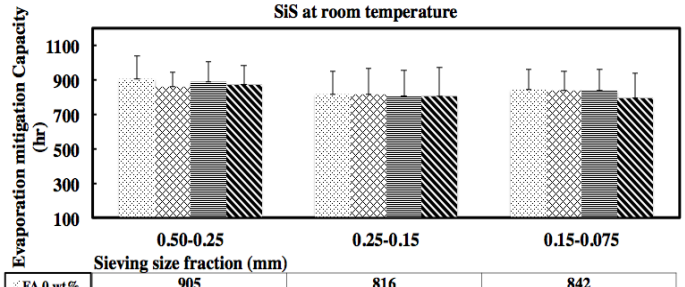

FA 0 wt%	905	816	842
FA 10 wt%	859	816	838
FA 20 wt%	889	807	838
FA 30 wt%	875	804	796

Figure 2-19. EMC of soil/sand of the different sieving size fractions and different amounts of FA added at about 20°C."

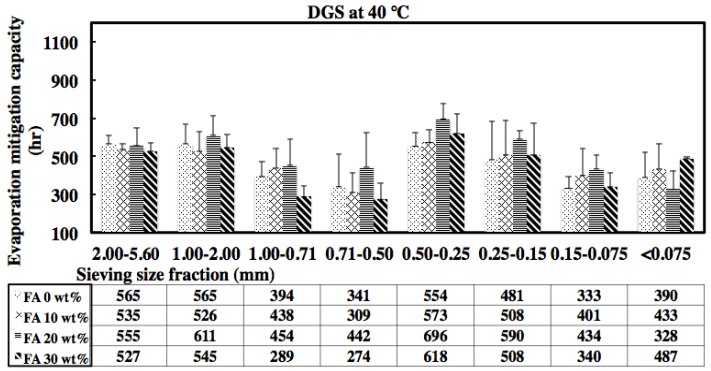

FA 0 wt%	565	565	394	341	554	481	333	390
FA 10 wt%	535	526	438	309	573	508	401	433
FA 20 wt%	555	611	454	442	696	590	434	328
FA 30 wt%	527	545	289	274	618	508	340	487

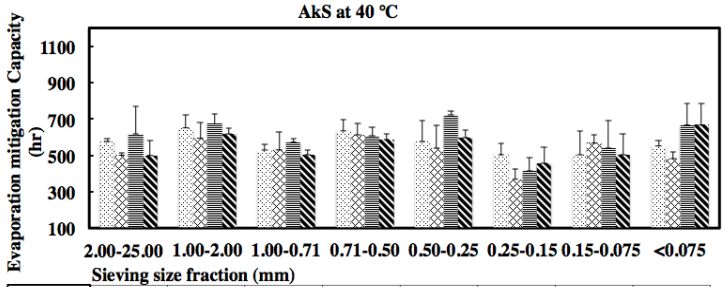

FA 0 wt%	576	652	528	635	577	505	503	553
FA 10%	501	595	531	612	538	369	568	482
FA 20%	619	674	573	608	723	413	538	668
FA 30%	500	618	503	585	598	457	504	668

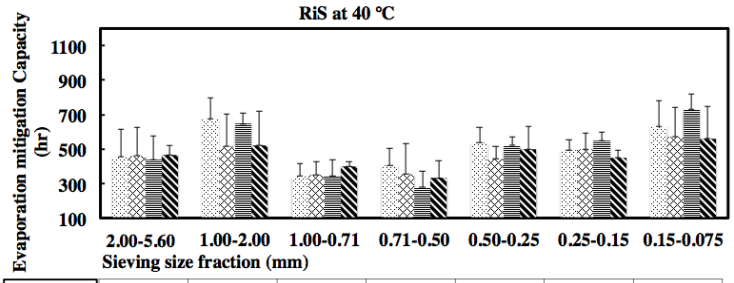

FA 0 wt%	456	676	344	405	537	493	630
FA 10 wt%	463	518	351	355	443	498	573
FA 20 wt %	437	646	343	280	524	550	729
FA 30 wt %	467	523	398	331	498	451	562

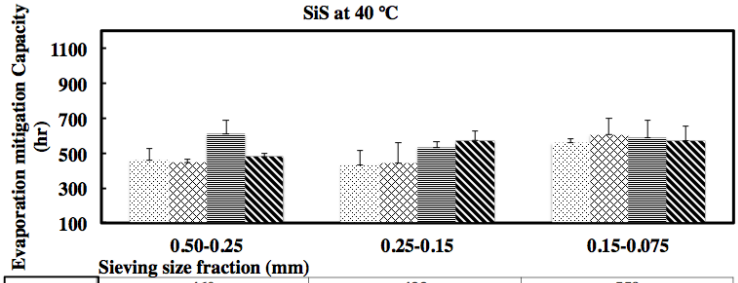

FA 0 wt%	460	433	559
FA 10 wt%	446	444	607
FA 20 wt%	608	532	589
FA 30 wt%	479	573	571

Figure 2-20: EMC of soil/sand of the different sieving size fractions and different amounts of FA added at 40 °C

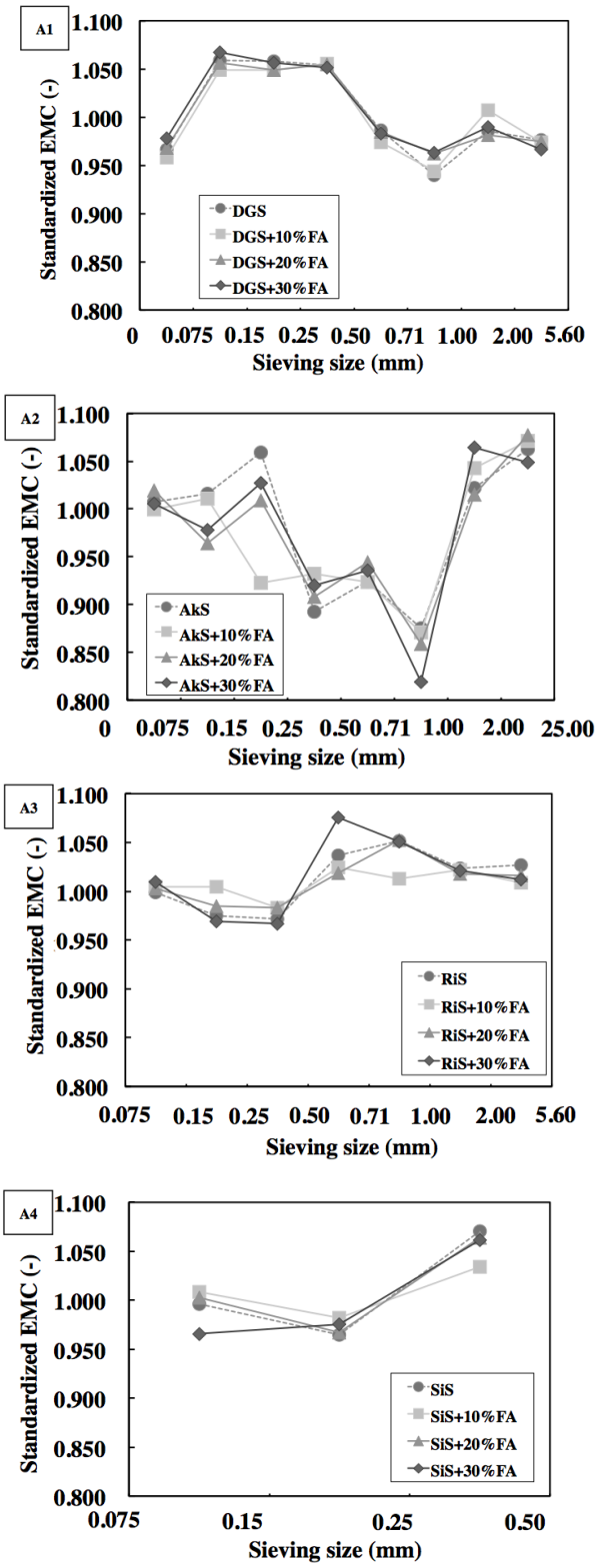

Figure 2-21. Soil/sand EMC of different particle size fractions relative to weighted average EMC over the full particle size range at about 20°C ([A1] DGS, [A2] AkS, [A3] RiS, [A4] SiS)

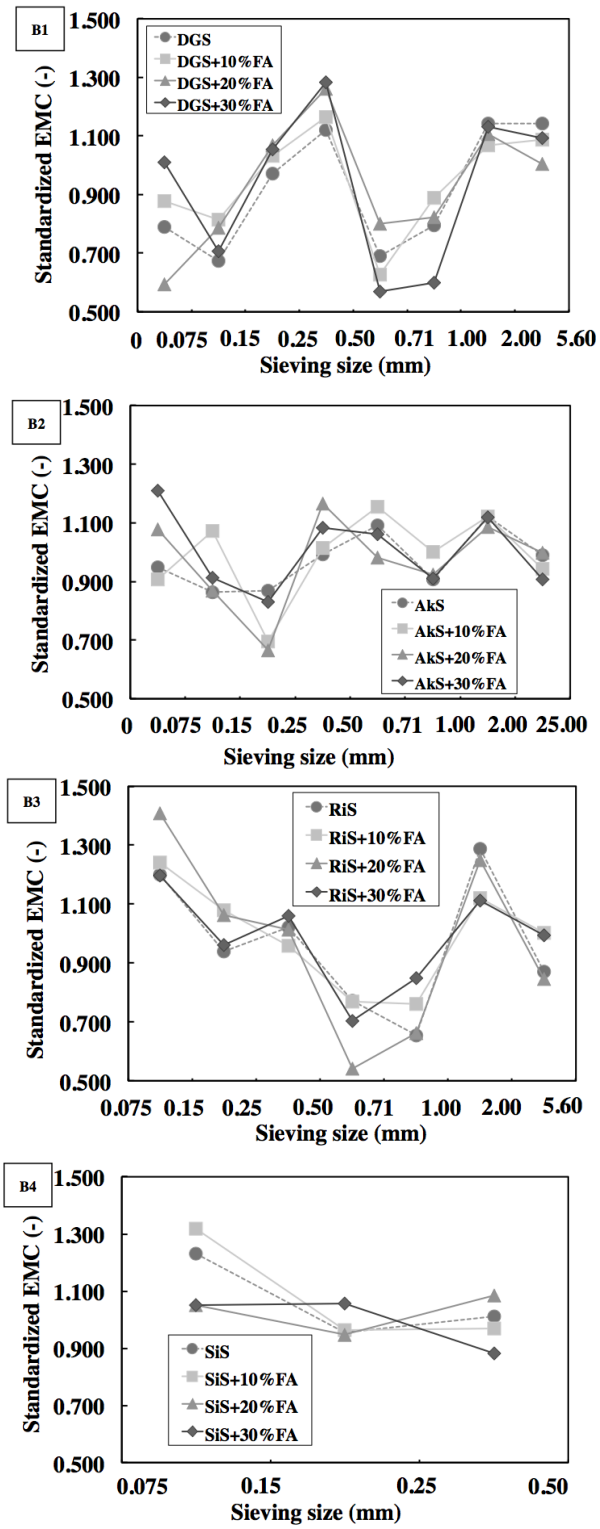

Figure 2-22. Soil/sand EMC of different particle size fractions relative to weighted average EMC over the full particle size range at 40°C ([B1] DGS, [B2] AkS, [B3] RiS, [B4] SiS)

Table 2-2. Results of Walsh´s t-test to reveal statistically significant differences of EMC between the pure soil and the soil amended with different amounts of FA for the different particle size fractions at about 20°C. The statistically significant differences are marked in grey. The P-level to reject was 0.05

Natural Condition	Size Range							
	>2mm	1-2 mm	0.71-1 mm	0.5-0.71 mm	0.25-0.5 mm	0.15-0.25 mm	0.075-0.15 mm	<0.075 mm
DGS+10 wt% FA	0.081	0.171	0.113	0.303	0.083	0.255	0.240	0.344
DGS+20 wt% FA	0.354	0.232	0.229	0.376	0.305	0.235	0.397	0.117
DGS+30 wt% FA	0.019	0.052	0.364	0.072	0.159	0.005	0.385	0.262
AkS+10 wt% FA	0.129	0.195	0.381	0.477	0.199	0.241	0.243	0.362
AkS+20 wt% FA	0.106	0.233	0.491	0.180	0.176	0.056	0.075	0.172
AkS+30 wt% FA	0.228	0.298	0.102	0.391	0.067	40.211	0.123	0.497

Table 2-3 Results of Walsh´s t-test to reveal statistically significant differences of EMC between the pure soil and the soil amended with different amounts of FA for the different particle size fractions at 40°C. The statistically significant differences are marked in grey. The P-level to reject was 0.05

40 °C	Size Range							
	>2mm	1-2 mm	0.71-1 mm	0.5-0.71 mm	0.25-0.5 mm	0.15-0.25 mm	0.075-0.15 mm	<0.075 mm
DGS+10 wt% FA	0.212	0.051	0.477	0.325	0.221	0.006	0.180	0.068
DGS+20 wt% FA	0.405	0.255	0.104	0.149	0.132	0.088	0.176	0.174
DGS+30 wt% FA	0.042	0.261	0.023	0.162	0.393	0.336	0.251	0.192
AkS+10 wt% FA	0.030	0.149	0.297	0.106	0.265	0.180	0.242	0.135
AkS+20 wt% FA	0.348	0.409	0.190	0.101	0.225	0.176	0.131	0.154
AlS+30 wt% FA	0.161	0.267	0.192	0.163	0.311	0.251	0.464	0.051

The differences between EMC among tested sieving size fractions might be explained partially by experimental errors. However, EMC differences among sieving size fractions are regarded as statistically significant by Welch's t-test at 5% significance level. For example, AkS has the second lowest EMC at the sieving size fraction of 250-500 μm. When this EMC was compared to the higher EMCs of other sieving size fractions, these differences are regarded as statistically significant by Welch's t-test. In the case of DGS at 40 °C, statistically significant differences are found between the lower EMC at the sieving size fraction of 500-710 μm and the higher EMC at the sieving size fraction of 250-500 μm. In the case of RiS at 40 °C, statistically significant differences appear between the lowest EMC at the sieving size fraction of 500 μm-1 mm and the highest EMC at the sieving size fraction of 75-150 mm. SiS also has significant differences between the lower EMC and higher EMC at both room temperature and 40 °C. These results are summarized as follows. EMC of pure soils/sands was found to be dependent on the sieving size fraction, though the correlation between sieving size and EMC is non-linear. In addition, EMC also depends on temperature. Optimum size range for the highest EMC shifts to smaller or larger sieving size fraction when drying temperature changes.

2.3.3 The impact of raw FA mixing ratio on EMC

Relative changes of EMC of soil/sand were calculated based on the EMC of non-amended soil/sand. The results are shown in Table 2-11-2-20, to analyze the performance of the raw-FA amendment on EMC of soil/sand in the same size fraction in detail. The positive value means EMC of soil/sand was increased when mixing with FA, and a negative value means EMC decreased when mixing with FA.

Generally, in the soil samples, when the FA ratio was 30 wt%, the EMCs were decreased, or the performance of the FA amendment was not positive. For example, in the sieving size range

of 710 μm-1 mm at 40 ºC, when the FA mixing ratio was 20 wt %, the EMC of DGS was increased by15.2%. While the FA mixing ratio was 30 wt%, the EMC of DGS in the same sieving size range was decreased by 26.68%. In the case of AkS at 40 ºC, in the sieving size range > 2mm, when the FA mixing ratio was 20 wt %, the EMC was increased by 7.45%, but when the FA mixing ratio was 30 wt%, the EMC was decreased by 13.1%. On the other hand, in the case of SiS with 150-250 μm sieving size range at 40 ºC, when the FA mixing ratio was 20 wt %, the EMC was increased by 22.9%. When the FA mixing ratio increased to 30 wt %, the EMC of SiS was even higher. These results also suggest the soil and sand type dependency on the different mixing ratios of the FA amendment on EMC. Increase the FA mixing ratio could not have positive effects on EMC. Suitable FA mixing ratio is recommended for the soil water amendment.

2.3.4 Temperature dependency

According to the above results, the temperature effect on the FA amendment is evident in many cases. For example, in the sieving size range of 150-250 μm, when the FA mixing ratio is 20 wt %, the EMC of DGS was decreased by 0.265% at room temperature, but increased by 22.6% at 40 ºC. In the case of AkS in the sieving size range of 250 μm-500, with the FA mixing ratio is 20 wt%, the EMC was only increased by 3.77%. However, when the temperature was 40 ºC, the EMC was increased by 25.4%. The similar temperature dependency also occurred in the cases of RiS and SiS. In the particle size range of 250 μm- 500 μm, with the FA mixing ratio is 20 wt%, the EMC of SiS was decreased by 1.81%, but increased by 32.3% when the temperature was 40ºC. In the case of RiS in the sieving size range 500 μm-710 μm, when the FA mixing ratio is 30 wt% in the sand samples, the EMC was increased by 2.2% under room temperature but decreased by 18.4% at 40 ºC.

These complicated results can be summarized as follows. At room temperature, the FA

amendment on the EMC of soil/sand is not significantly positive nor negative, which mainly occurs from the low water evaporation. The variation of EMC is tiny at room temperature. Thus the FA amendment on EMC can be negligible. On the other hand, compared to the cases at room temperature, the water evaporation rate is much higher at 40 ºC. The FA amendment effects on EMC of soil/sand samples were much more apparent compared to the samples at room temperature. In the different sieving size fractions, the FA amendment on EMC was either positive or negative. In some sieving size ranges, the EMCs of soil/sand samples were increased by 15%-30% at 40 ºC. Meanwhile, in some particle size ranges, the EMCs of soil/sand mixed with FA were slightly increased at room temperature but decreased a lot at 40 ºC. All of these results suggested there are temperature dependency as well as size dependency.

2.3.5 Effect of FA amendment on soil EMC

According to the above results, when EMC of FA-amended soil/sand was evaluated as water evaporation resistance, complex pseudo-effects on EMC were found. Although FA amendment gave no significant impact on soil/sand EMC at room temperature (see Figure 2-19), it decreases EMC in many cases at 40 ℃ (see Figure 2-20). However, it sometimes increases EMC at 40 ºC (e.g. AkS of 250-500 μm range with 20 % FA amendment). Even when FA amendment apparently increases EMC, however, the increase is not linear with respect to FA mixing ratio except for SS with 150-250 μm size range at 40 ºC. For example, FA amendment at 20 wt% mixing ratio increased EMC of DGS with 500-710 μm size range at 40 ºC, while 30 wt% FA amendment decreased EMC less than that of non-amended soil. Weltch's t-test was used to check the statistical significance of EMC difference among pure soil/sand and FA-amended soil/sand with the same sieving size range. The results of t-test are shown in Table 2-2 and 2-3. P values less than 0.05, which corresponds to significant differences between pure

soil/sand and FA-amended-soil/sand, were found in only a limited number of cases. In contrast, EMC differences among different sieving size fractions were found to be statistically significant in many cases. Therefore, negative/positive effects of FA amendment on EMC can be statistically regarded as negligible or limited. In addition, Figure 2-21 and 2-22 show that EMC variations as a function of soil/sand sieving size range are almost the same regardless of FA mixing ratios. This means that EMC changes significantly depending on sieving size but is not affected by the increase of clay/slit faction through FA amendment. To investigate the impact of physical size of particles/aggregates in soil/sand system on EMC, EMC of non-sieved samples (all sieving size fractions) was predicted using EMC at each sieving size fraction and then compared to measured EMC of non-sieved sample. Comparisons are shown in Figure 23-25. In particular, at 40 °C, measured EMC of DGS and RiS are always larger than predicted EMC. Different optimum sieving size for EMC depending on soil/sand type and drying temperature, limited impact of clay/silt fraction increase (FA amendment), and disagreement of measured and predicted EMC suggest that physical size of particles/ aggregates in soil/sand system is not a controlling factor of EMC.

2.3.6 Effect of organic matter content on sieving size dependency of EMC

The weight ratios of organic matter content in the different sieving size fractions of soils and sands were measured by weight loss on ignition. The results show that the weight ratios of organic matter content varied with the change of soil/sand sieving size (see Table 2-12). Standardized evaporation mitigation capacities (EMCs) and standardized weight ratios of organic matter at each sieving size faction were calculated using their weighted average based on sieving size distributions. Their comparisons are shown in Figure 2-26 and 2-27. It should be firstly noted that data with dotted circle were excluded as outliers in correlation analysis.

Positive or negative correlations were found between EMC and organic matter content. For example, in the cases of DGS and AkS at room temperature, the correlations are positive. This means that EMC of DGS and AkS increase with the increase of organic matter content. In the cases of RiS and SiS at room temperature, however, the correlations are negative. The increase of organic matter content decreased sand EMC. Therefore, the correlation between EMC and organic matter content shows soil/sand type dependency of EMC. On the other hand, the correlation changes conversely at 40 ºC. Although the increase of organic matter content increased EMC of SiS and RiS, it decreased EMC of DGS and AkS. This means that the dependency of soil/sand EMC on organic matter content also depends on drying temperature. These complicated results can be summarized as follows. The distinct correlation between EMC and organic matter content suggests that the sieving size effect on soil/sand EMC is derived partially from different concentration of organic matter in each sieving size fraction. Organic matters play an important role for the size dependency of EMC. In addition, the influence of organic matters to soil/sand EMC depends on temperature. This might be explained by characteristic changes of organic matters induced by temperature. It is expected that high temperature might affect some organic matter components in soil/sand. It might change their wetting properties and thus change the influence of organic matters to EMC. For example, Graber et al. reported that the decrease of soil water repellency with the increase of temperature could be explained by the behavior of fatty acid salts. This means that fatty acid salts make soil more hydrophilic with temperature increase (Graber et al., 2009). Sodium salts of humic and fulvic acids, which are typical organic matter components in soil, changed their hydration state within a temperature range of 5-90 °C (Drastik et al., 2013). Glassy/rubbery state transitions of lignin and humic acids at 60-70 ºC were also reported (Leboeufet al., 2000) although impacts of such state transition on soil hydrophilicity or hydrophobicity is still uncertain. Lin tested

artificial modification of FA surface using chitosan, sodium alginate, or guanidine hydrochloride. However, these modifications gave no impact or decreased EMC at 40 ºC when modified FA was amended (Lin, 2019). According to these trials, it is proposed that polymerized organic matters like the structure of lignin and humic substances might be relevant to EMC mechanisms.

In addition, Lin investigated the correlation between specific surface area, water repellency, capillary water content, and EMC of samples. Their combining effects were analyzed by multi-regression analysis (Lin, 2019). However, when breaking the analysis down on only significant data or data that separated by soil/sand type, no reliable equation was found. This result suggested compared to other factors; organic matter seems to play a dominant part in the effect of EMC.

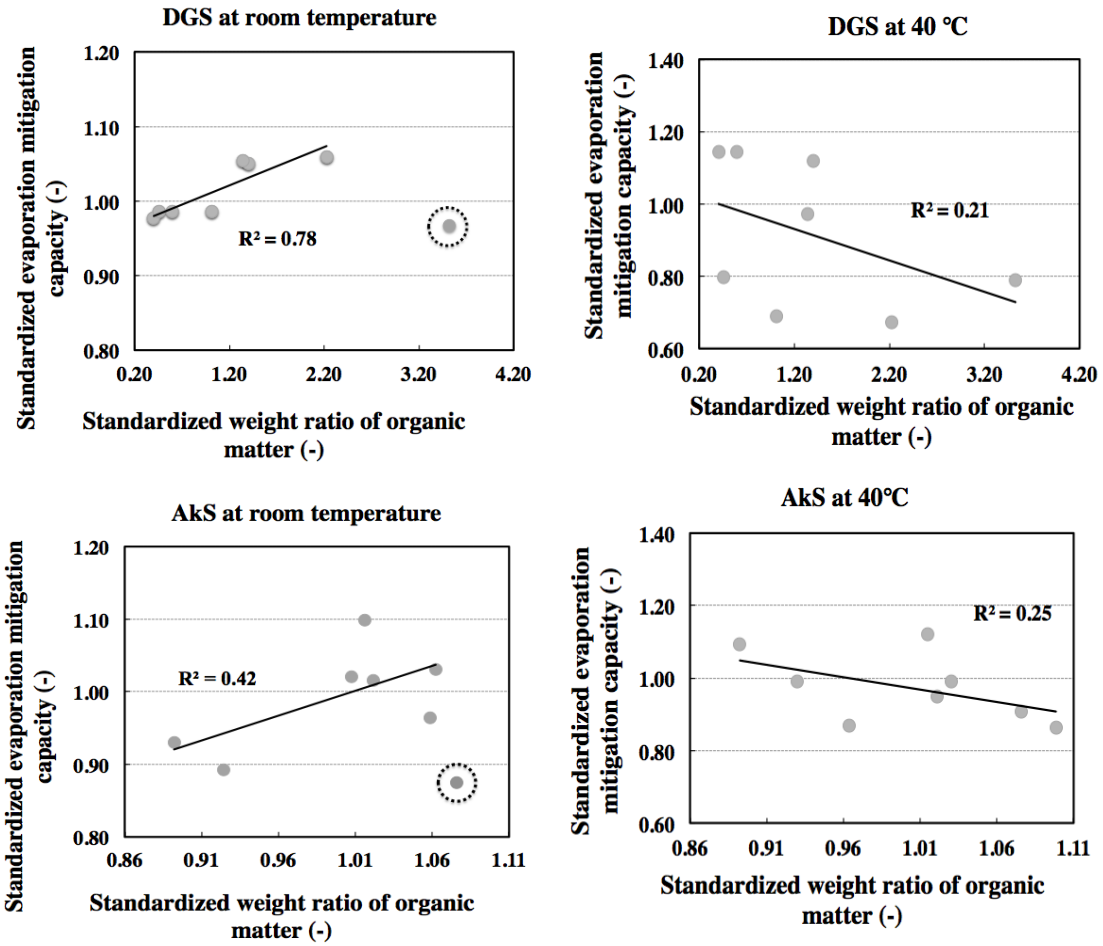

Figure 2-26. Correlation between standardized EMC and standardized organic matter content for DGS and AkS at room temperature and 40 ℃

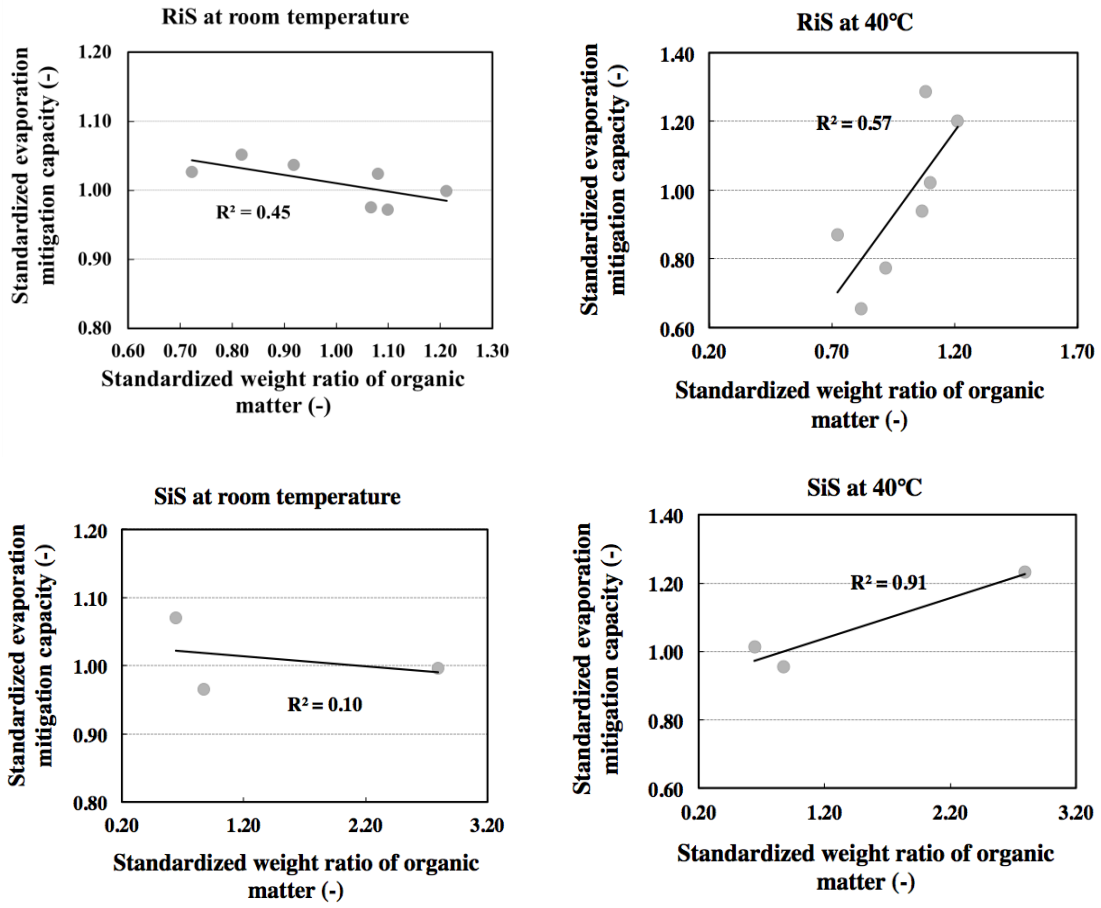

Figure 2-27. Correlation between standardized EMC and standardized organic matter content for SiS and RiS at room temperature and 40 ℃

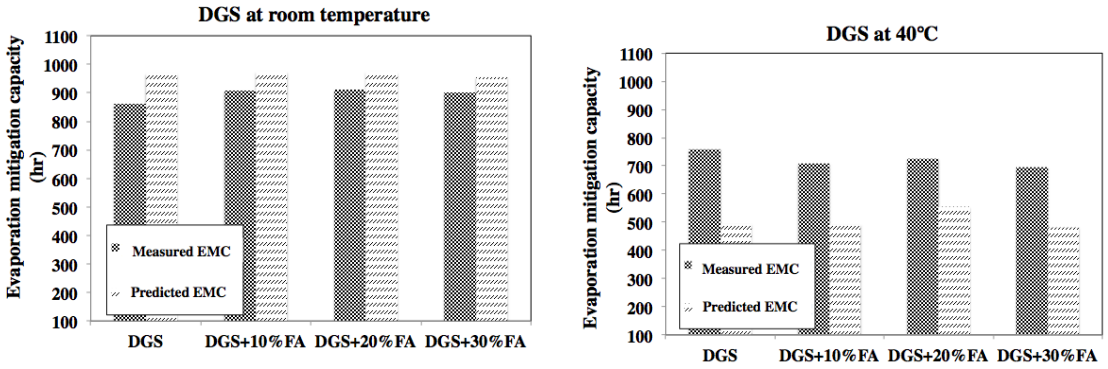

Figure 2-23. Measured and predicted EMC of DGS at room temperature and 40 °C

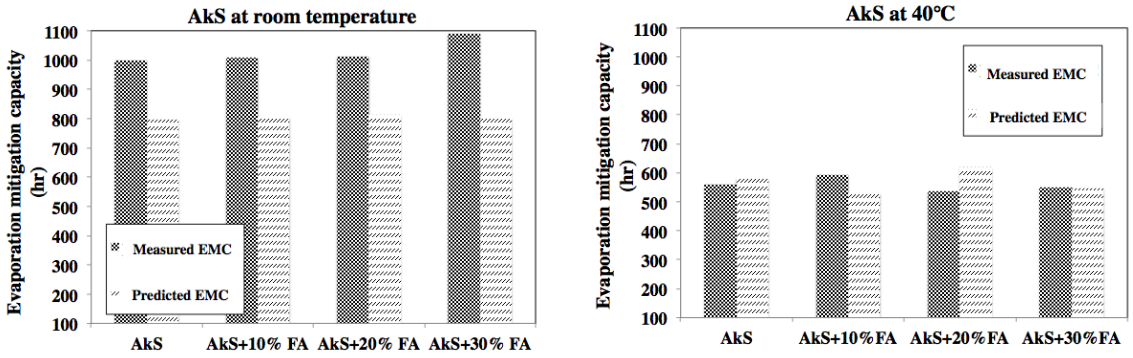

Figure 2-24 . Measured and predicted EMC of AkS at room temperature and 40 °C

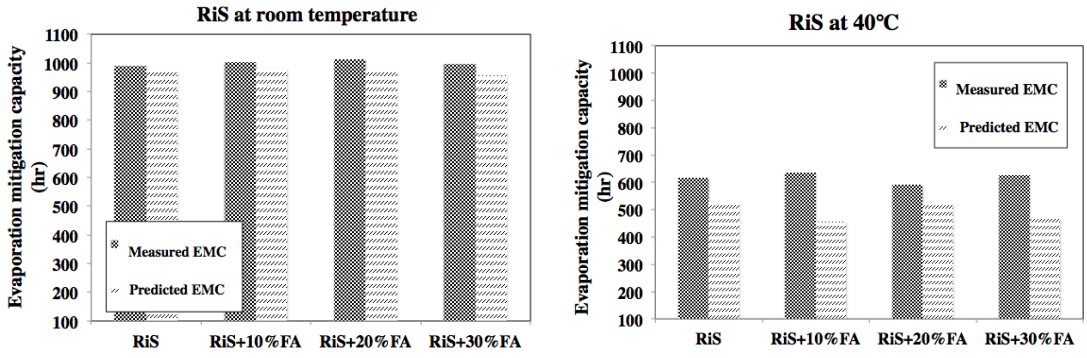

Figure 2-25. Measured and predicted EMC of RiS at room temperature and 40 °C

As a summary, this study found that the effect of soil/sand sieving size on EMC was more significant than the FA amendment effect. However, the sieving size effect could be explained partially by organic matter concentration in the respective soil/sand sieving size fractions. The sieving size effect on EMC depends on soil/sand type and drying temperature. Soil organic matter composition also partially explains drying temperature dependency. According to these results, FA modification is recommended when the FA amendment is used to improve soil/sand EMC.

2.4 Conclusion

The effect of FA amendment on soil/sand moisture was investigated focusing on soil/sand sieving size. Although FA amendment increased WHC of soil/sand slightly, it is much lower than sieving size effect. FA amendment also gave limited impacts on EMC. On the other hand, EMC of tested soil/sand clearly showed sieving size dependency regardless of FA mixing ratio. The effects of FA amendment on EMC are also much smaller than the sieving size effect. The sieving size effects on EMC are very complicated with depending on soil/sand type and drying temperature. This study found that the sieving size dependency of EMC could be explained partially by organic matter content in each soil/sand sieving size fraction. Correlations between organic matter contents and EMC are contrast depending on drying temperature. The increase of organic matter in DGS and AkS increased EMC of DGS and AkS at room temperature but decreased them at 40 ºC. EMC of sands shows opposite trends at both temperature. This study proposes temperature-dependent hydraulic properties of organic matter components in soil/sand to explain the temperature dependency. According to the results, it is concluded that organic matter plays an important part on EMC although physical sieving size is important for WHC. If FA is used in the arid/semi-arid areas to increase EMC of sandy soil, proper modification of FA

properties using organic compounds will be necessary to suppress water evaporation from soil system.

Reference

1. Adriano, D. C., Weber, J. T. (2001). Influence of fly ash on soil physical properties and turfgrass establishment. J. Environ. Qual. 30(2), 596-601
2. Campbell, D. J., Fox, W. E., Aitken, R. L., Bell, L. C. (1983) Physical characterization of sands amended with fly ash. Aust. J. Soil Res. 21(2), 147-154
3. Drastik, M., Novak, F., Kucerik, J.: Origin of heat-induced structural changes in dissolved organic matter. Chemosphere. 90(2), 789-795 (2013)
4. Gangloff, W. J., Ghodrati, M., Sims, J. T., Vasilas, B. L. (2000). Impact of fly ash amendment and incorporation method on hydraulic properties of a sandy soil. Water, Air Soil Poll. 119(1-4), 2331-245
5. Graber, E. R., Tagger, S., Wallach, R.: Role of Divalent Fatty Acid Salts in Soil Water Repellency. Soil Sci. Soc. Am. J. 73(2), 541-549 (2009)
6. Gupta, S.C., Larson, W.E. (1979) Estimating soil water retention characteristics from particle size distribution, organic matter percent, and bulk density, Water Resources Research, Vol.15,No.6.
7. Hollis, J.M., Jones, R.J A., Palmer, R.C. (1977) The effect of organic matter and particle size on the water retention properties of some soils in the west midlands of England, Geoderma, 17(1977) 225-238.
8. Jong R. DE, Campbell C.A., Nicholaichuk W. (1983) Water retention equations and their relationship to soil organic matter and particle size distribution for disturbed samples. Can, J.Soil Sci. 63: 291-302.
9. Leboeuf, E. J., Weber, W. J.: Macromolecular characteristics of natural organic matter. 1. Insights from glass transition and enthalpic relaxation behavior. Environ. Sci. Technol. 34(17), 3623-3631 (2000)

10. Lin, S. L., Takahashi, F. (2015). Raw and Treated Coal Fly Ash Amendment Aiming for Water Holding Capacity Adjustment of Natural Soils. J. Residuals Sci. Technol. 12(2), 73-84
11. Lin, S.L. (2018). Effect of raw and treated coal fly ash amendment on water retention capacity of soils and sands. Doctoral Dissertation. Tokyo Institute of Technology, Japan,
12. Parker F. W. (1922). The classification of soil moisture. Soil Science. Volume 13 - Issue 1 - ppg 43-54
13. Pathan, S. M., Aylmore, L. A. G., Colmer, T. D. (2001). Fly ash amendment of sandy soil to improve water and nutrient use efficiency in turf culture, International Turfgrass Society Research Journal, 9, 33-39
14. Simpson, Daniel,Corde. (2014). Behavioral Thresholds in Mixtures of Sand and Clay. A thesis submitted to Oregon State University, Citeable URL: https://ir.library.oregonstate.edu/concern/graduate_thesis_or_dissertations/bg257j16m
15. Tracy, SR; Daly, KR; Sturrock, CJ; Crout, NMJ; Mooney, SJ; Roose, T. (2015). Three-dimensional quantification of soil hydraulic properties using X-ray Computed Tomography and image-based modeling. Water Resources Research, 51(2), 1006-1022
16. World Reference Base for Soil Resources 2014. http://www.fao.org/3/i3794en/I3794en.pdf (Accessed on 2nd Jun. 2019)

Chapter 3

Evaporation mitigation capacity of soil/sand mixed with/without polymer-treated fly ash

3.1 Background

As mentioned in previous chapter, the raw-FA amendment is not significantly effective, but organic matters are influential greatly. Therefore, chemical modification of the FA surface can be useful to suppress water evaporation from unsaturated soil/sand. Researchers have confirmed that hydrogels, also called superabsorbent polymers are helpful and suitable for improving water retention capacity, especially for sandy soils (Bakass, et al., 2002; Narjary et al., 2012; Montesano et al., 2015; Demitri et al., 2013). The synthetic superabsorbent polymers are commonly three-dimensional cross-linked. Their central ability is water absorption, for they are more effective in water retention than mineral soil amendments. And also they can be used as fertilizer carriers. Superabsorbent polymers are often directly mixed or injected into the soil for the soil amendment. In general, one gram of superabsorbent polymer can absorb up to 1000 g of distilled water. Most plants can take up 95% of the water retained within the superabsorbent polymer (Lejcus et al., 2018).

The primary reason for conducting polymer-modification is as followed. Modifying the surface of FA particles with superabsorbent polymers can promote the coagulation of FA particles, and thus it generates aggregated structure in the soil system. It might increase the water retention capacity of soil in the “orders of magnitude” level. Besides, there are other researchers suggested that the desaturation of mixed superabsorbent polymers could lower the

soil bulk density and increase its porosity (Han et al., 2010). And also, there are other studies about using hydrogel such as polyvinyl alcohol for heavy metal removal. For instance, Wang has reported that removal of heavy metal ions by polyvinyl alcohol and carboxymethyl cellulose composite hydrogels (Wang et al., 2016). It might provide another potential alternative for the immobilization of the heavy metals of the coal fly ash.

In this chapter, to investigate the effects of the polymer modified-FA on the soil/sand water retention, the values of evaporation mitigation capacities of soils, sands, raw FA and polymer treated FA were measured and compared in corresponding groups. The effect of the polymer treated-FA on the water retention of soil/sand would be reported and discussed.

3.2 Experimental materials & methods

3.2.1 Polymers used in this study and their properties

3.2.1.1 Polyethylene glycol

Polyethylene glycol is a water-soluble linear polymer which consists of hydrophilic oxygen and hydrophobic ethylene units. Its chemical formula is (C2H4O)n+1H2O, and the structural formula is HOCH2-(CH2-O-CH2)n-CH2OH. The polyethylene glycols are classified into various categories by their molecular weights. PEG is commercially available from 200 to 10,000,000 g/mol molecular weight. The high MW grades (>20,000 g/mol) are commonly referred to as polyethylene oxide (PEO). As the molecular weights differ, the properties of polyethylene glycols also change. PEG of molecular weights of 200–600 g/mol is transparent or slightly yellow liquids at room temperature. PEG of molecular weights 1000 and more g/mol is white or almost white solids of a wax appearance (Zdeňka et al., 2016). As the molecular weight of the glycols increases, their solubility, and hygroscopicity decrease. PEG has a wide variety of applications in various industrial processes because of its favorable properties, such as excellent absorbing and hygroscopicity, low vapor pressure, high chemical stability, low toxicity, and low

melting temperature. Polyethylene glycols (PEO-4,000,000 and PEG-200) used in this study were purchased from Wako Pure Chemical Industries, Ltd, Japan. Their molecular weights are 4,000,000 g/mol, and 200 g/mol, respectively.

3.2.1.2 Polyvinyl alcohol

Polyvinyl alcohol (PVA) is a water-soluble and biodegradable polymer. Its idealized formula is [CH2CH-(OH)]n. It is white in color and odorless. PVA is widely used in the fabrication of compatible composites, such as colloidal stabilizers, textiles, adhesives, and coatings. PVA used in this study was purchased from Wako Pure Chemical Industries, Ltd, Japan. It is completely hydrolyzed, and its molecular weight is around 1,000 g/mol.

3.2.1.3 Polyacrylic acid

Polyacrylic acid (PAA) is a large molecular weight compound that consists of small repeating monomers. It can be used in a variety of household and personal care products. For example, it is capable of absorbing many times its weight in water, and hence is used in disposable diapers. In a water solution at neutral pH, many of the side chains of PAA lose their protons and acquire a negative charge. The ionization of the carboxyl side chains makes PAA soluble in aqueous media at neutral pH. The length of the polymer chain and the properties of the polymer may be changed by varying the reaction conditions and can change the characteristics of the polymer. PAA used in this study was purchased from Wako Pure Chemical Industries, Ltd, Japan. One type is the PAA solution (abt.25%), another type is PAA with its molecular weight of 25,000 g/mol.

3.2.1.4 Cellulose

Cellulose as a polysaccharide is an organic compound with the formula (C6H10O5)n.

Powdered cellulose is colorless, odorless, and tasteless. It has an average degree of polymerization of 150 to 450; an average particle diameter of 30 to 250 μm; an apparent specific volume exceeding 7cm^3/g. The cellulose used in this study was purchased from Wako Pure Chemical Industries, Ltd, Japan. The particle range is around 38 μm (through 38 μm-400 mesh).

3.2.2 Surface modification of FA by polymer treatment

Polymer modifications on the surface of the FA particles were conducted. All the mixtures of FA and polymer are made into solutions, and each solution of the treated FA was dried at 105 ºC, crushed softly, and then utilized for experiments on the evaporation mitigation capacity. In the treatment of cellulose-modified FA (C-FA), 190 g of FA was treated by 500 ml of 2.0 wt % of cellulose powder solution. In the treatment of polyethylene glycol-modified FA (PEO-FA and PEG-FA), 10 g of the polymer was mixed with 190 g of raw FA particles. In the treatment of cellulose-polyethylene glycol-modified FA (C-PEO-FA), 8 g of the PEO was mixed with 2 g cellulose and 190 g of raw FA. In the treatment of polyacrylic acid-modified FA (PAA-FA), 10 g of PAA powder was mixed with 190 g of FA particles. In the treatment of polyacrylic acid solution modified FA (PAA_S-FA), 50g of 25 wt% polyacrylic acid solution was mixed with 237.5 g of raw FA. In the polyacrylic acid with calcium chloride (PAA-CaCl2-FA) treatment, 200g of the polyacrylic acid solution treated-FA was mixed with 100ml of 0.5 mol/L calcium chloride and dried. In the treatment of polyvinyl alcohol-modified FA (PVA-FA), 10 g of PVA powder was mixed with 190 g of raw FA particles. Details of the chemical composition on each polymer-treated FA and the properties of the polymers were shown in Table 3-1 and Table 3-2. In general, the weight ratio of FA is 95 wt %, in order for comparison in the controlled groups.

Table 3-1 Chemical composition of polymer-treated FA

Types of treated fly ash	Weight ratio of raw fly ash (wt %)	Weight ratio of polymer and chemical compound (wt %)				
		Cellulose	Polyethylene glycol	Polyacrylic acid	Polyvinyl alcohol	Calcium chloride
C-FA	95	5.0	--	--	--	--
PEG-FA	95	--	5.0	--	--	--
PEO-FA	95	--	5.0	--	--	--
C-PEO-FA	95	1.0	4.0	--	--	--
PAA-FA	95	--	--	5.0	--	--
PAA_S-FA	95	--	--	5.0	--	--
PVA-FA	95	--	--	/	5.0	--
PAA_S-CaCl$_2$-FA	92.4	--	--	4.8	--	2.7

Table 3-2 Selected Properties of the studied polymers

Name	Structural unit	Formula	Molecular weight (g/mol)	Form	Viscosity (mPa.s)
Polyethylene glycol (PEO)	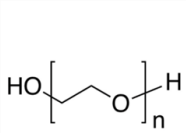	$(-CH_2CH_2O-)_n$	4,000,000	Powder	1% AQ=1650-5500 mPa.s
Polyethylene glycol (PEG)		$(-CH_2CH_2O-)_n$	200	Liquid	~60 mPa.s (20 ºC)
Polyacrylic acid (PAA)	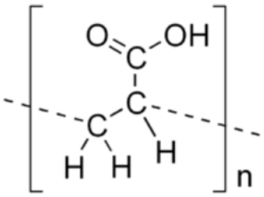	[-CH2CH(COOH)-]n	25,000	Powder	1000~2000 mPa.s (40 %, 25 ºC)
Polyacrylic acid solution (PAA_S)		[-CH2CH(COOH)-]n	Not available	Liquid	8000~12000 mPa.s (30 ºC)
Polyvinyl alcohol (PVA)	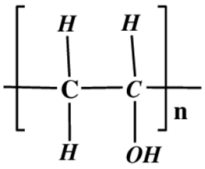	[-CH(OH)CH2-]n	900~1100	Powder	9~15 mPa.s (40 %, 25 ºC, calculated on the dried basis)
Cellulose	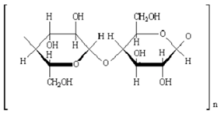	(C6H10O5)n	Not available	Powder	Not available

3.3 Results and discussion

3.3.1 Evaporation mitigation capacity (EMC) of polymer treated-FA mixed in soil/sand

Evaporation mitigation curves of the PEG-treated FA, PEO treated FA, PAA-treated FA, PVA treated FA mixed in soils (DGS and AkS), sands (SiS and RiS) were measured though drying experiment for 12 hours. Each polymer treated-FA was manufactured by wet treatment as described above. Drying experiments were conducted at room temperature and 40 ℃ for comparison. EMC of each sample was calculated according to the EMC curves. Error bars in all figures are standard deviation of 3 or more than 3 times repeated measurement data (see Figure 3-1 to Figure 3-28).

3.3.1.1 Effect of PEG treated-FA amendment on EMC of soils and sands

EMC of soil/sand mixed with PEG-treated FA of 10 wt%, 20 wt% and 30 wt% at room temperature and 40 ºC were investigated. The results are shown in Figure 3-1 to Figure 3-7. The PEG-treated FA gave a positive effect on the EMC of soils and sands at room temperature and 40 ℃. For example, the EMC of DGS was increased by 6.45% at the mixing ratio of 20 wt%, at room temperature. The EMC of AkS was increased by 5.76% and 6.02% at room temperature, at the mixing ratio of 20 wt% and 30 wt%, respectively. Compared with soils, PEG-FA showed a more effective amendment on water retention in sands. For the SiS and RiS at room temperature, PEG-treated FA increased the EMC of the sands in all the cases at the mixing ratio of 10 wt%, 20 wt%, and 30 wt%. At 40 ºC, The EMC of DGS was increased by 10.42% and 8.85% at the mixing ratio of 20 wt% and 30 wt%, while the EMC of AkS was merely increased by 2.30% at the mixing ratio of 30 wt%. As for SiS and RiS at 40 ºC, the EMCs were all increased at the different mixing ratios of FA. The biggest relative positive change of EMC was 18.98 % when the SiS mixed with 20 wt% PEG treated FA at 40 ºC. T-test was used to check all these relative positive changes as described above, and it suggested they were statistical

significance (Table 3-3).

Table 3-3 The effect of PEG-treated FA on the EMC of soil/sand

PEG-FA treatment	Relative change of EMC (%)					
Temperature	**Room Temperature**			**40 ºC**		
FA ratio	10 wt%	20 wt%	30 wt%	10 wt%	20 wt%	30 wt%
DGS	+2.77	+6.45 *	-1.89	+1.74	+10.42*	+8.85 *
AkS	+2.15	+5.76 *	+6.02 *	+2.31	+7.51	+2.30 *
SiS	+7.37 *	+11.16 *	+10.39 *	+11.77 *	+18.98*	+14.63*
RiS	+9.07 *	+13.14*	+10.11*	+9.43 *	+15.91*	+15.20*

All data was conducted by t-test, and "*" stand to "p value < 0.05".

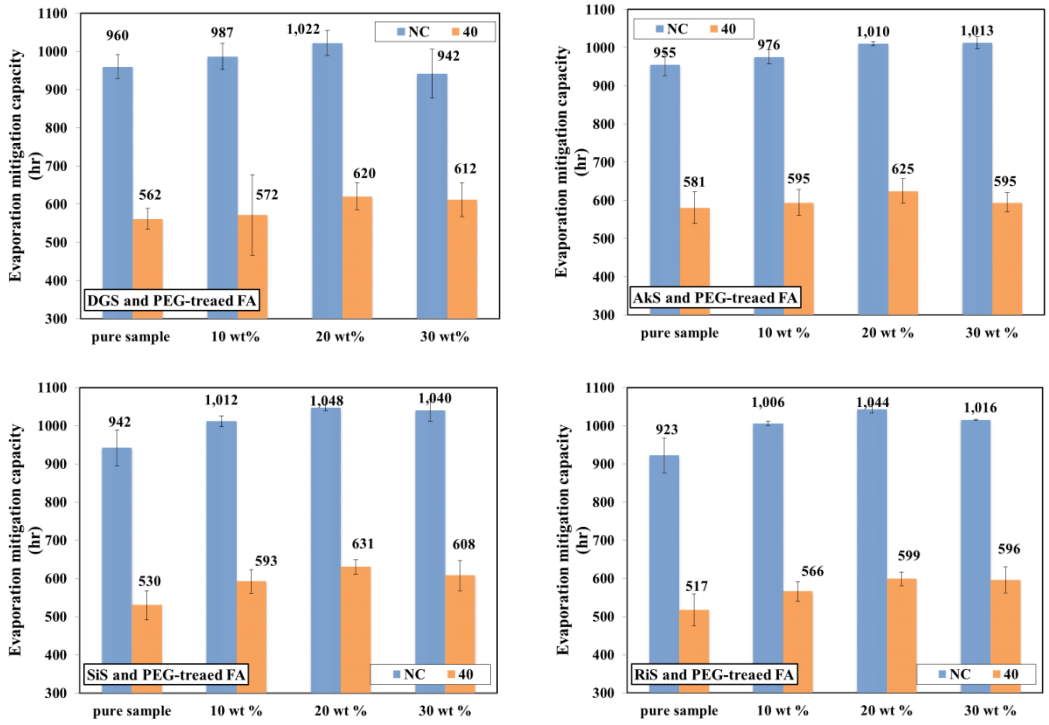

Figure 3-1 Effect of PEG modified FA on EMC of DGS AkS, SiS, and RiS at room temperature and 40 ºC.

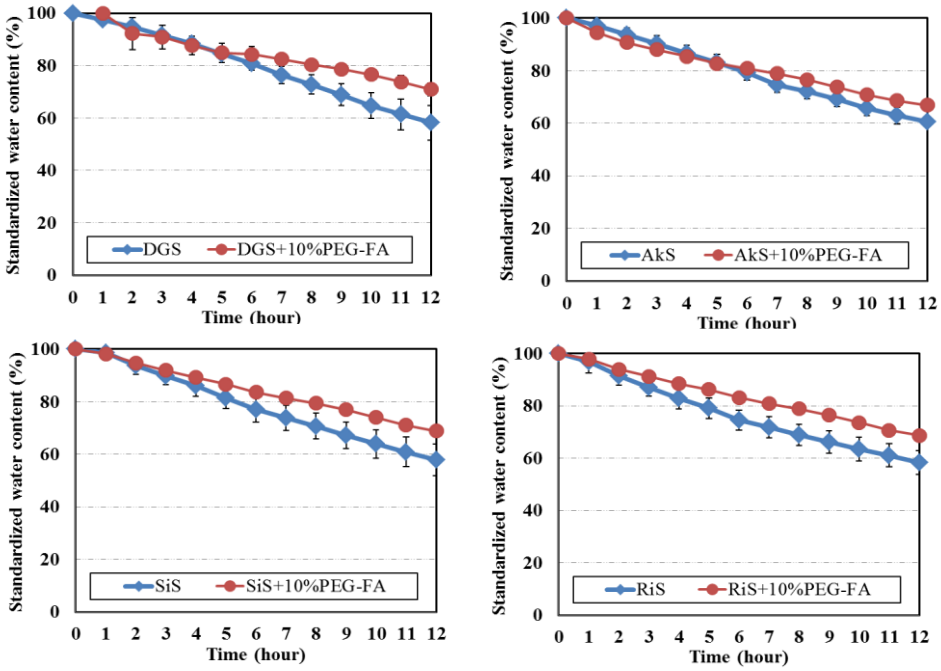

Figure 3-2 Evaporation mitigation capacity curves of DGS, AkS, SiS, RiS mixed with PEG-treated FA at 10 wt% mixing ratio and room temperature.

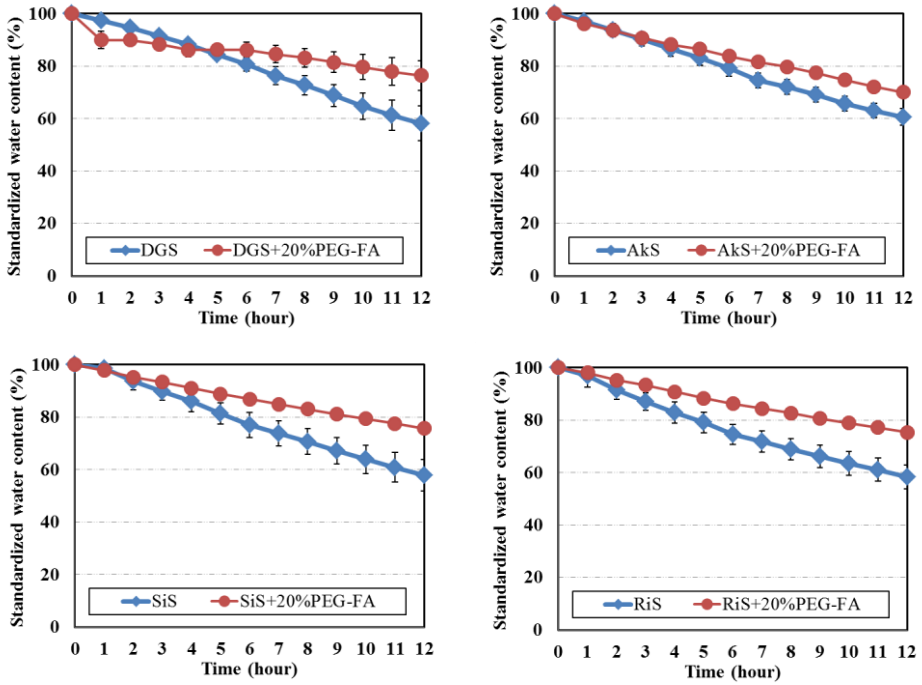

Figure 3-3 Evaporation mitigation capacity curves of DGS, AkS, SiS, RiS mixed with PEG-treated FA at 20 wt% mixing ratio and room temperature.

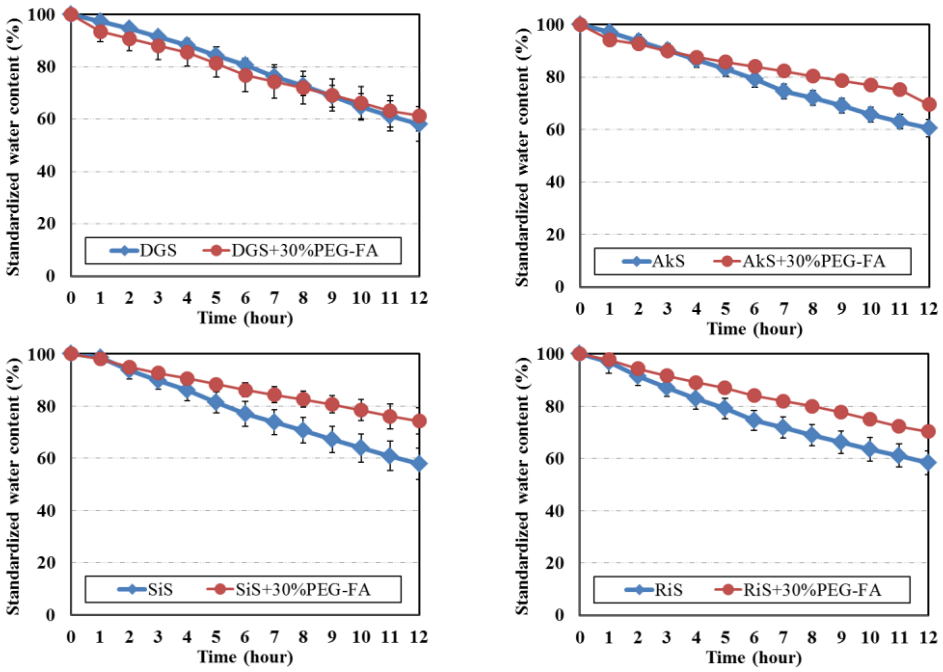

Figure 3-4 Evaporation mitigation capacity curves of DGS, AkS, SiS, RiS mixed with PEG-treated FA at 30 wt% mixing ratio and room temperature.

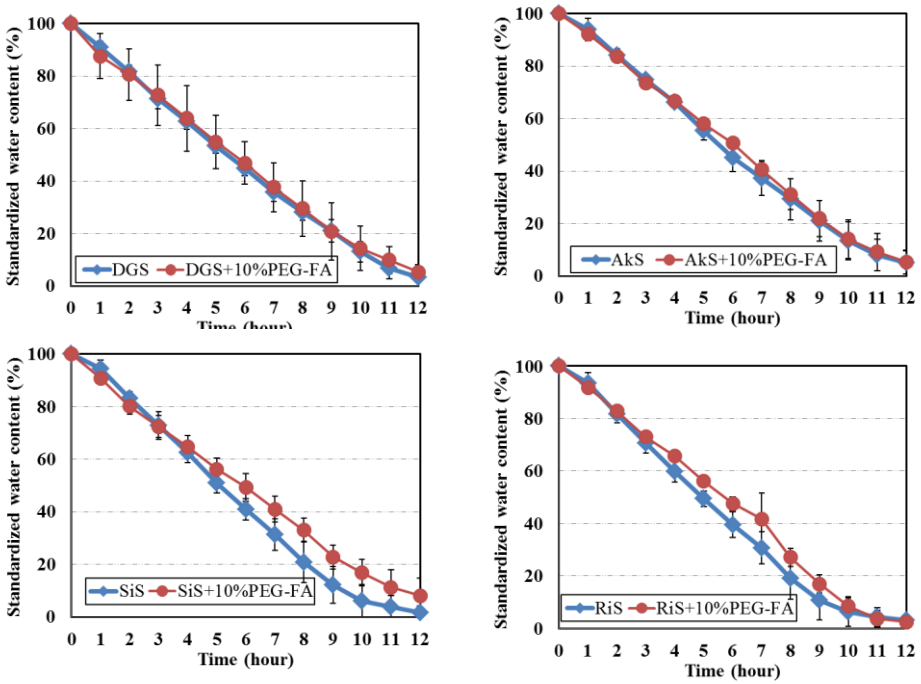

Figure 3-5 Evaporation mitigation capacity curves of DGS, AkS, SiS, RiS mixed with PEG-treated FA at 10 wt% mixing ratio and 40 ℃.

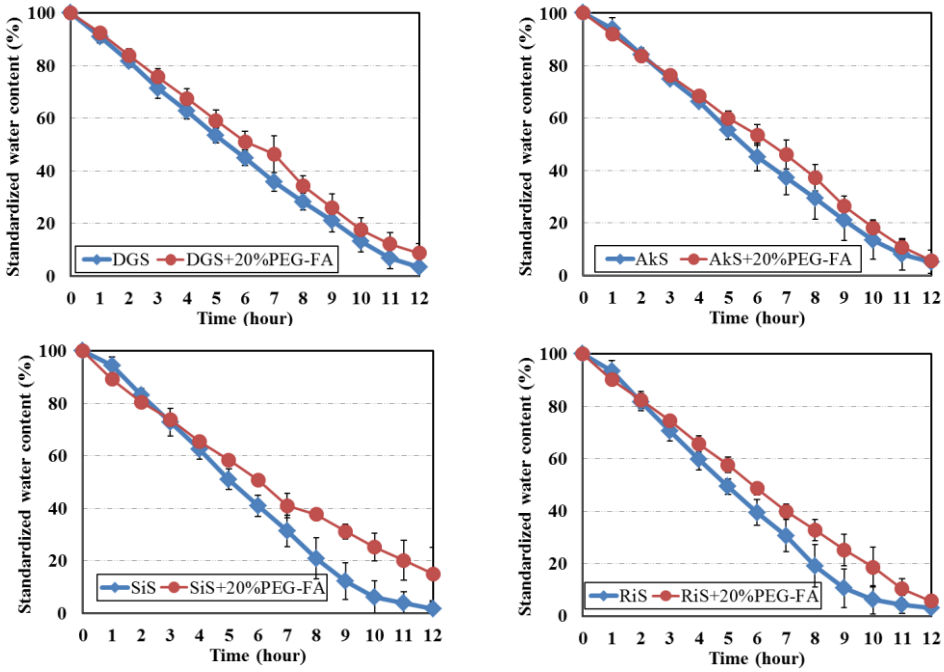

Figure 3-6 Evaporation mitigation capacity curves of DGS, AkS, SiS, RiS mixed with PEG-treated FA at 20 wt% mixing ratio and 40 ºC.

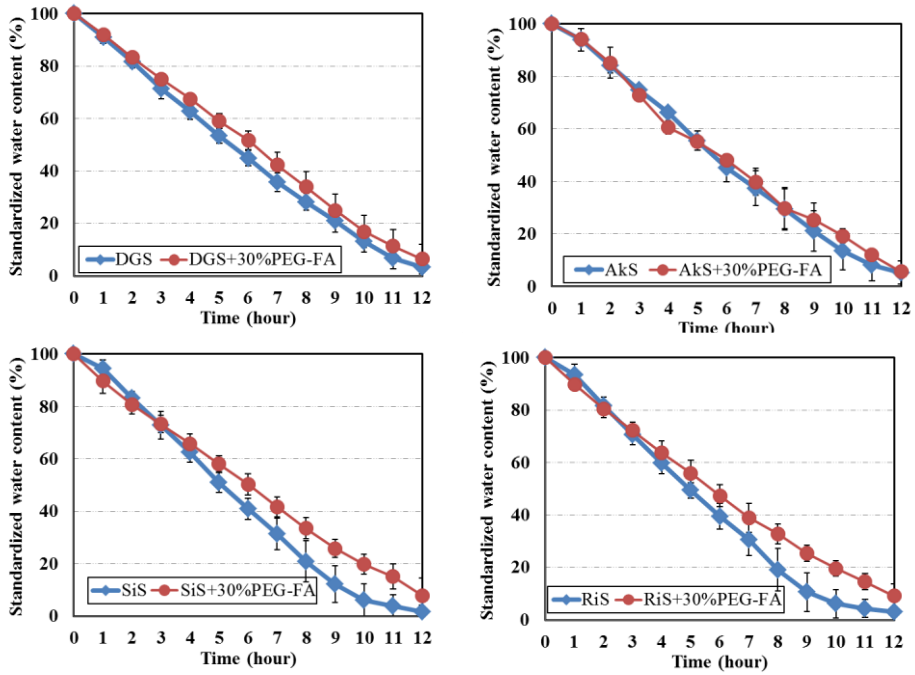

Figure 3-7 Evaporation mitigation capacity curves of DGS, AkS, SiS, RiS mixed with PEG-treated FA at 30 wt% mixing ratio and 40 ºC.

3.3.1.2 Effect of PEO treated-FA amendment on EMC of soils and sands

EMC of soil/sand mixed with PEO-treated FA of 10 wt%, 20 wt% and 30 wt% at room temperature and 40 ºC were investigated. The results are shown in Figure 3-8 to Figure 3-14. The molecular weight of PEO is 4,000,000 g/mol, which is much larger compared to the PEG of which the molecular weight is 200 g/mol. The results are shown in Figure 3-8 to Figure 3-14. Compared to the PEG-treated FA in the previous section, the amendment of POE treated–FA on the EMC of soil/sand is not effective. Under both temperature conditions, the POE modified FA amendment performed limited improvement on the EMC of soil/sand. The most considerable relative positive change of EMC was merely 9.81 % when the RiS mixed with 20 wt% PEO treated FA at 40 ºC, which was statistically significant. Nevertheless, Welch's t-test suggested that in most cases, the increase of EMC was not statically significant (see Table 3-4).

Table 3-4 The effect of PEO-treated FA on the EMC of soil/sand

PEO-FA treatment	Relative change of EMC (%)					
Temperature	**Room Temperature**			**40 ºC**		
FA ratio	10 wt%	20 wt%	30 wt%	10 wt%	20 wt%	30 wt%
DGS	-1.73	+0.98	-2.14	+0.37	+6.44	+2.31
AkS	+3.59	+3.01	-0.63	-5.53	+5.60	-3.27
SiS	+0.50	+0.46	-1.52	-7.01	+2.56	+5.68
RiS	+1.05	0.32	-1.58	-0.585	+9.81*	+9.10

All data was conducted by t-test, and "*" stand to "p value < 0.05".

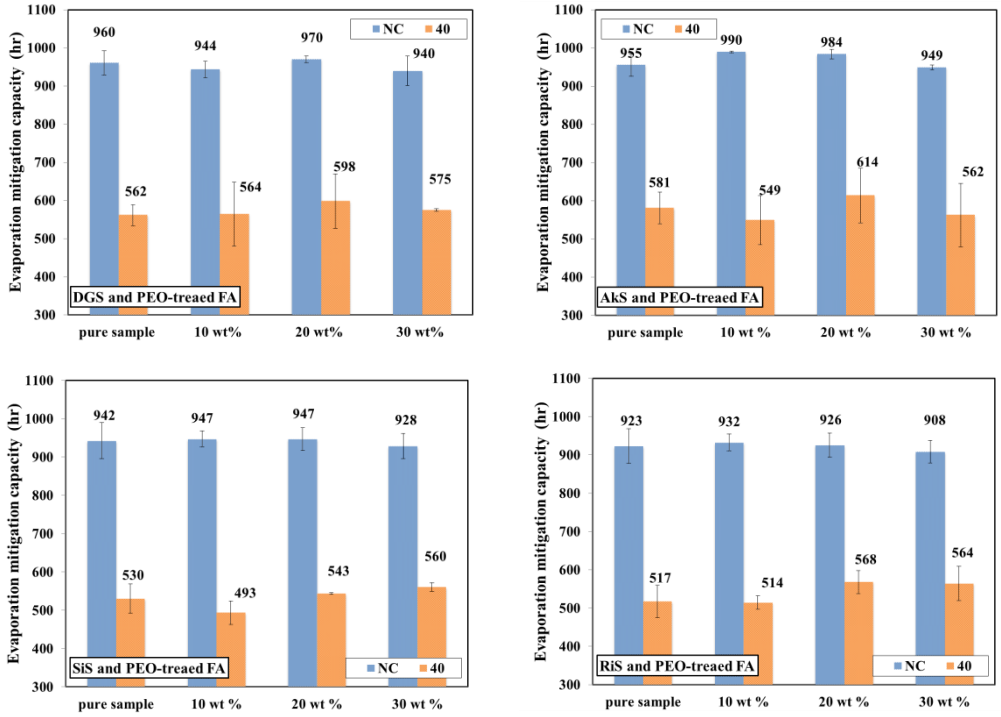

Figure 3-8 Effect of PEO modified FA on EMC of DGS AkS, SiS, and RiS at room temperature and 40 ºC.

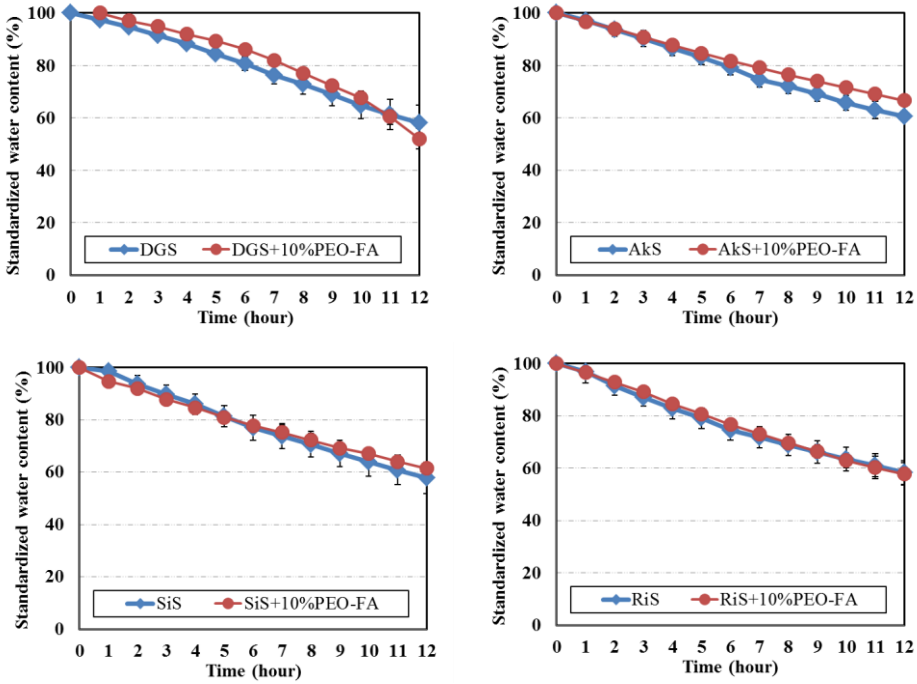

Figure 3-9 Evaporation mitigation capacity curves of DGS, AkS, SiS, RiS mixed with PEO-treated FA at 10 wt% mixing ratio and room temperature.

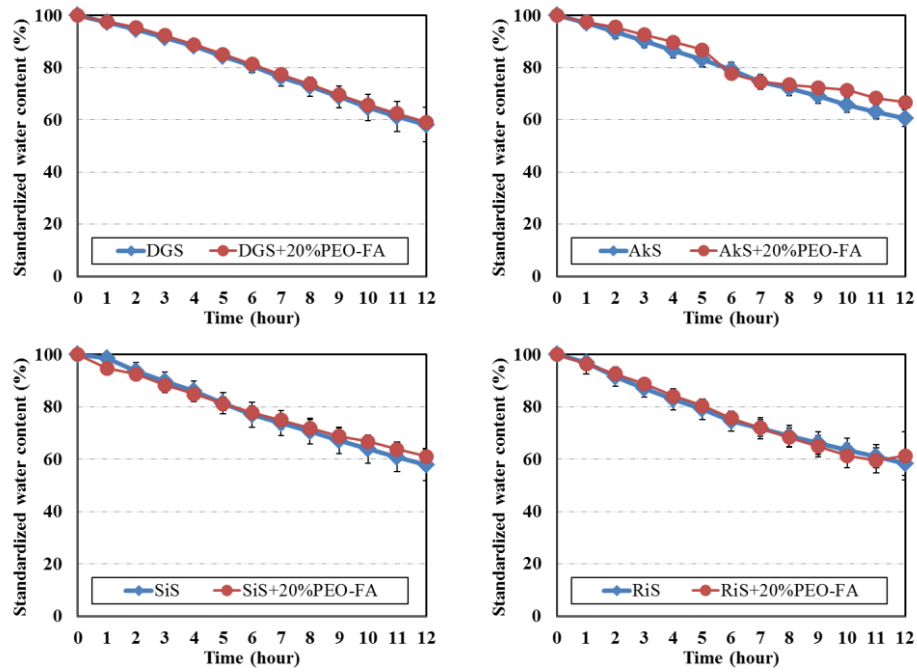

Figure 3-10 Evaporation mitigation capacity curves of DGS, AkS, SiS, RiS mixed with PEO-treated FA at 20 wt% mixing ratio and room temperature.

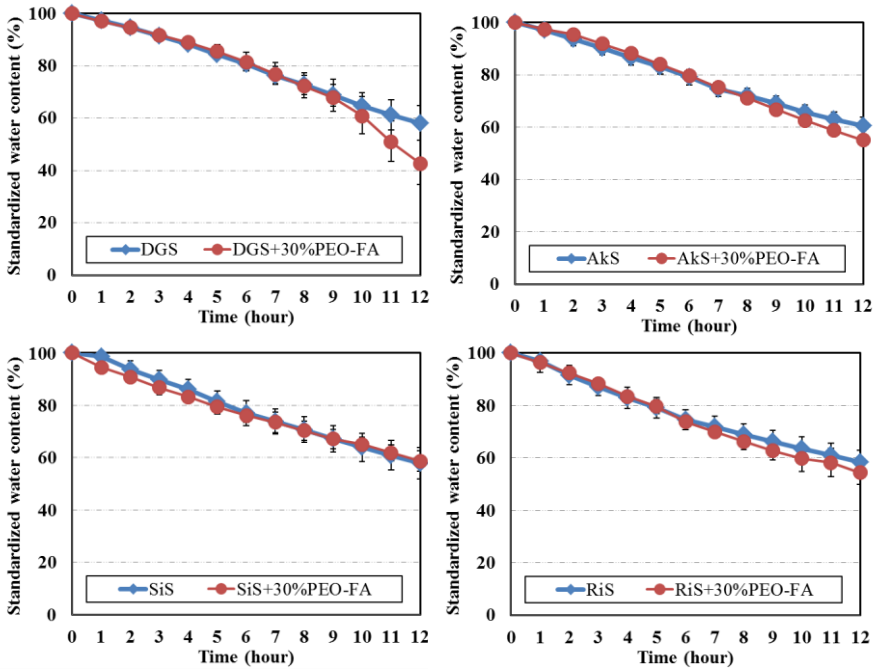

Figure 3-11 Evaporation mitigation capacity curves of DGS, AkS, SiS, RiS mixed with PEO-treated FA at 30 wt% mixing ratio and room temperature.

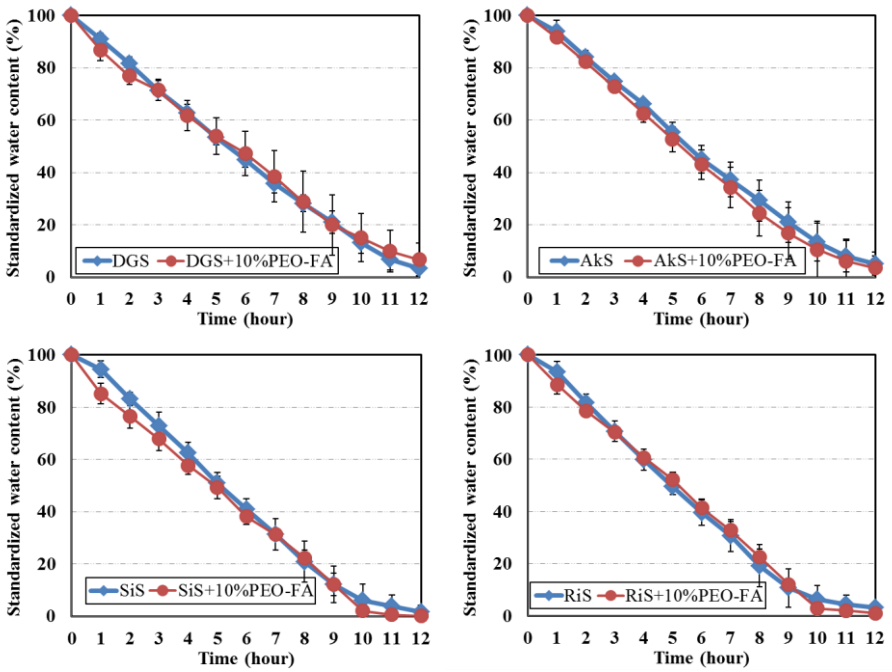

Figure 3-12 Evaporation mitigation capacity curves of DGS, AkS, SiS, RiS mixed with PEG-treated FA at 10 wt% mixing ratio and 40 ºC.

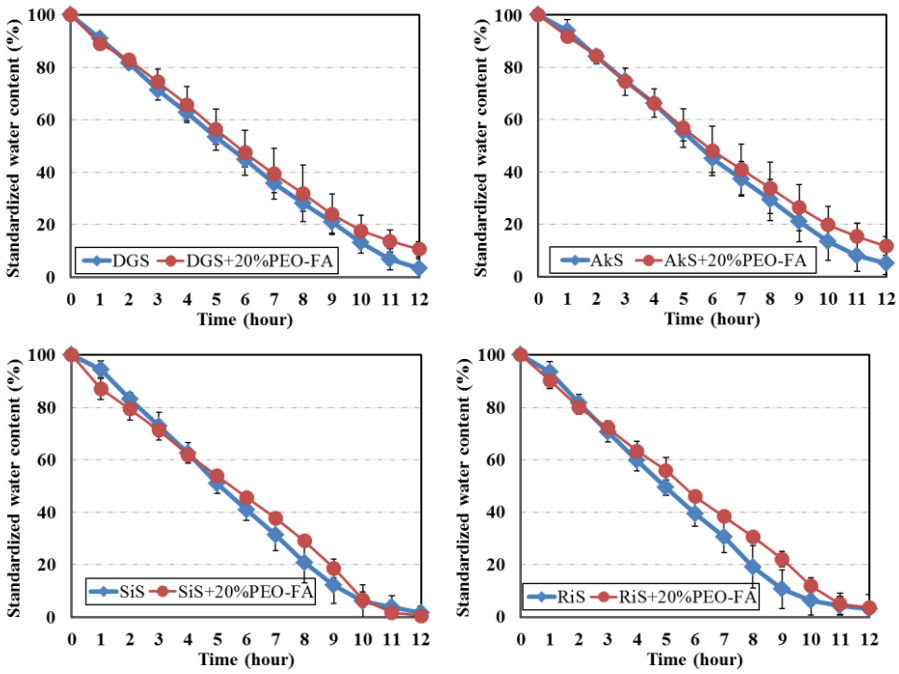

Figure 3-13 Evaporation mitigation capacity curves of DGS, AkS, SiS, RiS mixed with PEG-treated FA at 20 wt% mixing ratio and 40 ºC.

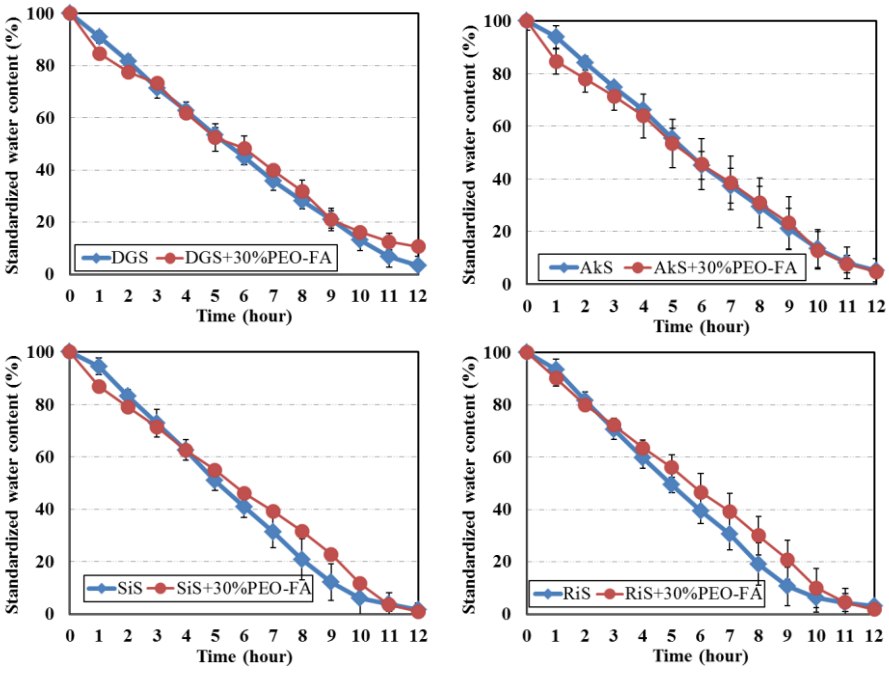

Figure 3-14 Evaporation mitigation capacity curves of DGS, AkS, SiS, RiS mixed with PEG-treated FA at 10 wt% mixing ratio and 40 ºC.

3.3.1.3 Effect of PVA treated-FA amendment on EMC of soils and sands

EMC of soil/sand mixed with PVA-treated FA of 10 wt%, 20 wt% and 30 wt% at room temperature and 40 ºC were investigated. The results are shown in Figure 3-15 to Figure 3-21. The PEG-treated FA gave a positive effect on the EMC of soils and sands at room temperature and 40 °C. For example, at room temperature, the EMC of DGS was increased by 3.89% and 5.61% at the mixing ratio of 10 wt% and 20 wt%, respectively. At 40 ºC, the EMC of DGS was increased by 9.79% and 8.86% at the mixing ratio of 20 wt% and 30 wt%. The EMCs of AkS were increased at room temperature in all the cases regardless of the different mixing ratios. At 40 ºC, The EMC of AkS was increased by 8.85% and 9.21% at the mixing ratio of 20 wt% and 30 wt%. In addition, PVA treated-FA performed an eligible amendment on the water retention of sand. For the SiS and RiS at room temperature, PEG-treated FA increased the EMC of the sands in all the cases at the mixing ratio of 10 wt%, 20 wt%, and 30 wt%. As for SiS and RiS at 40 ºC, the EMCs were all increased at the different mixing ratios of FA. The most significant relative positive change of EMC was 24.80% when the SiS mixed with 20 wt% PVA treated FA at 40 ºC. T-test was used to check all these relative positive changes as described above, and it suggested they were statistical significance (Table 3-5).

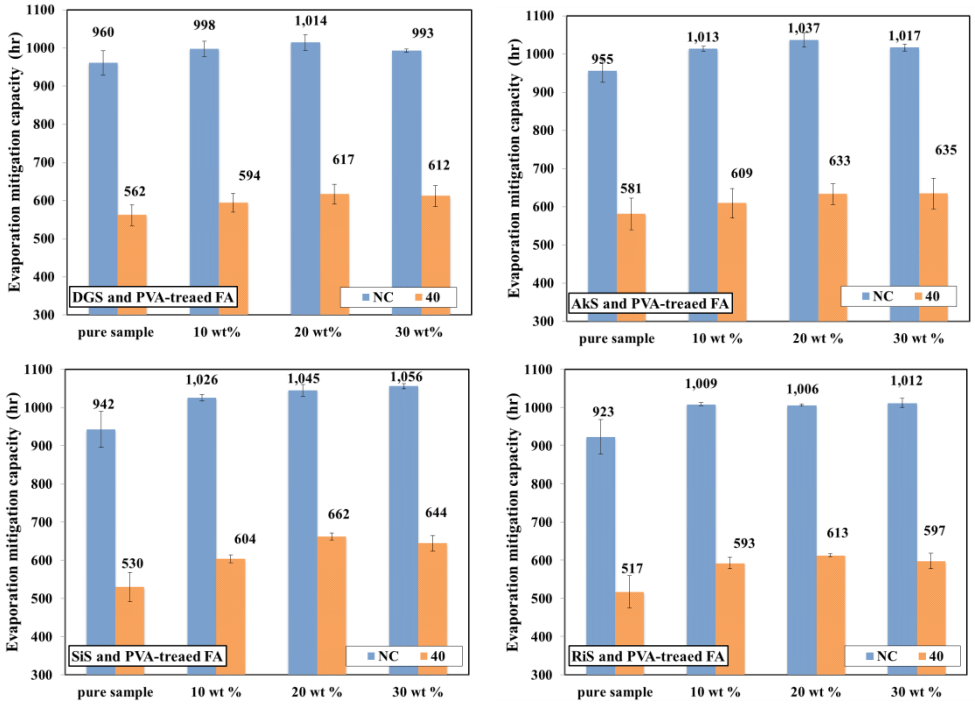

Figure 3-15 Effect of PVA modified FA on EMC of DGS AkS, SiS, and RiS at room temperature and 40 ºC.

Table 3-5 The effect of PVA-treated FA on the EMC of soil/sand

PVA-FA treatment	**Relative change of EMC (%)**					
Temperature	**Room Temperature**			**40 ºC**		
FA ratio	10 wt%	20 wt%	30 wt%	10 wt%	20 wt%	30 wt%
DGS	+3.89 *	+5.61 *	+3.41	+5.67	+9.79 *	+8.86 *
AkS	+6.07 *	+8.51 *	+6.41 *	+4.80	+8.85 *	+9.21 *
SiS	+8.83 *	+10.86 *	+12.04*	+13.87 *	+24.80 *	+21.55 *
RiS	+9.29 *	+9.03 *	+9.66 *	+14.56 *	+18.54 *	+15.49 *

All data was conducted by t-test, and "*" stand to "p value < 0.05"

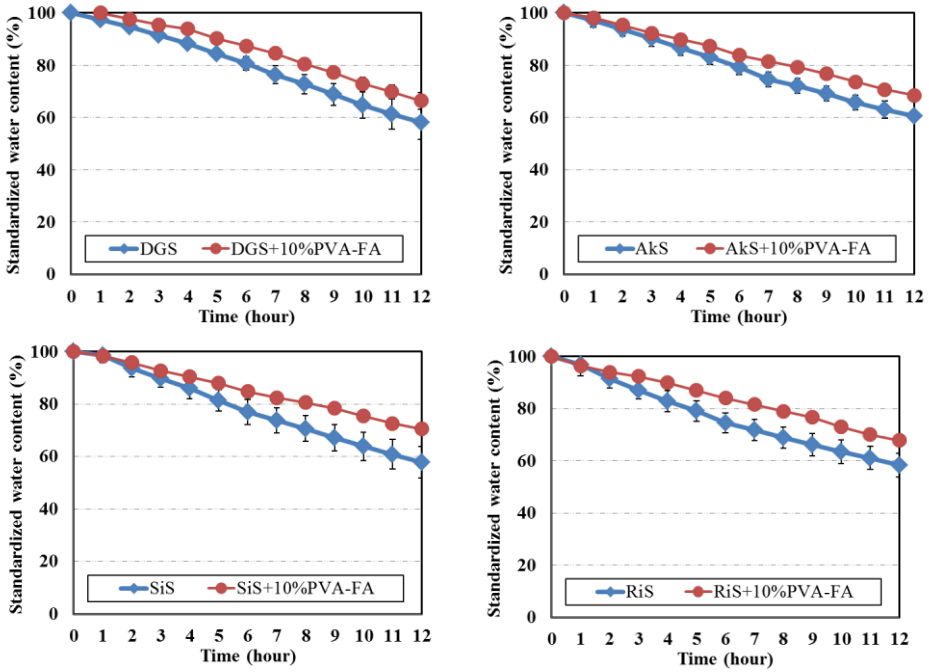

Figure 3-16 Evaporation mitigation capacity curves of DGS, AkS, SiS, RiS mixed with PVA-treated FA at 10 wt% mixing ratio and room temperature.

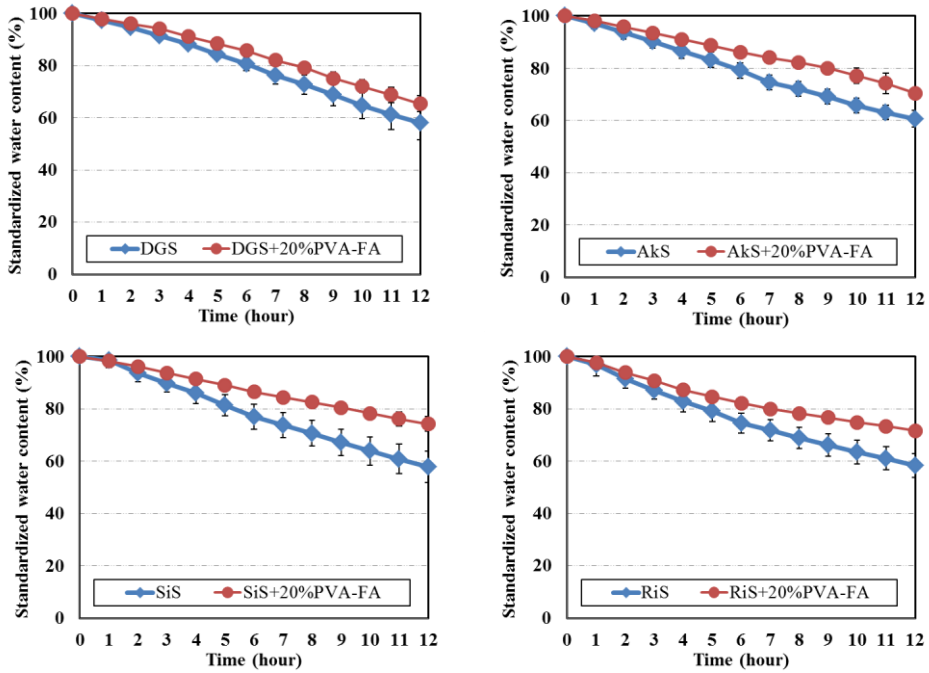

Figure 3-17 Evaporation mitigation capacity curves of DGS, AkS, SiS, RiS mixed with PVA-treated FA at 20 wt% mixing ratio and room temperature.

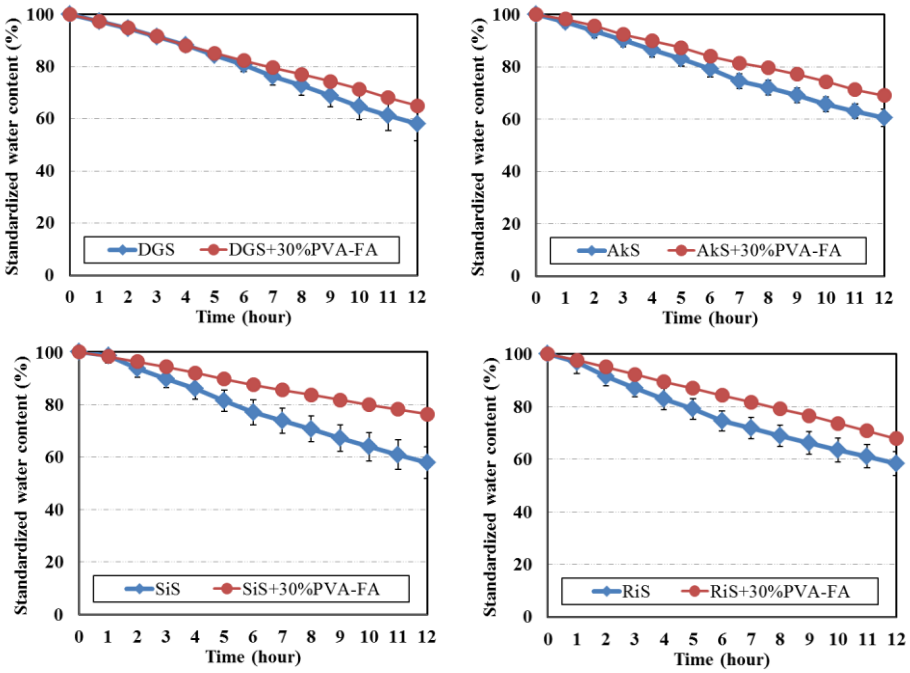

Figure 3-18 Evaporation mitigation capacity curves of DGS, AkS, SiS, RiS mixed with PVA-treated FA at 30 wt% mixing ratio and room temperature.

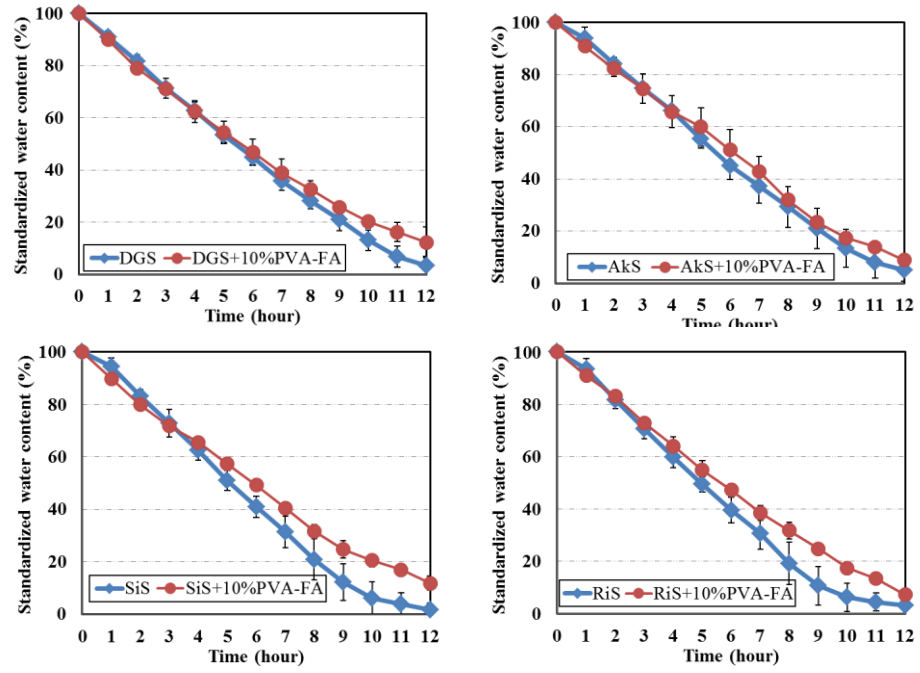

Figure 3-19 Evaporation mitigation capacity curves of DGS, AkS, SiS, RiS mixed with PVA-treated FA at 10 wt% mixing ratio and 40 °C.

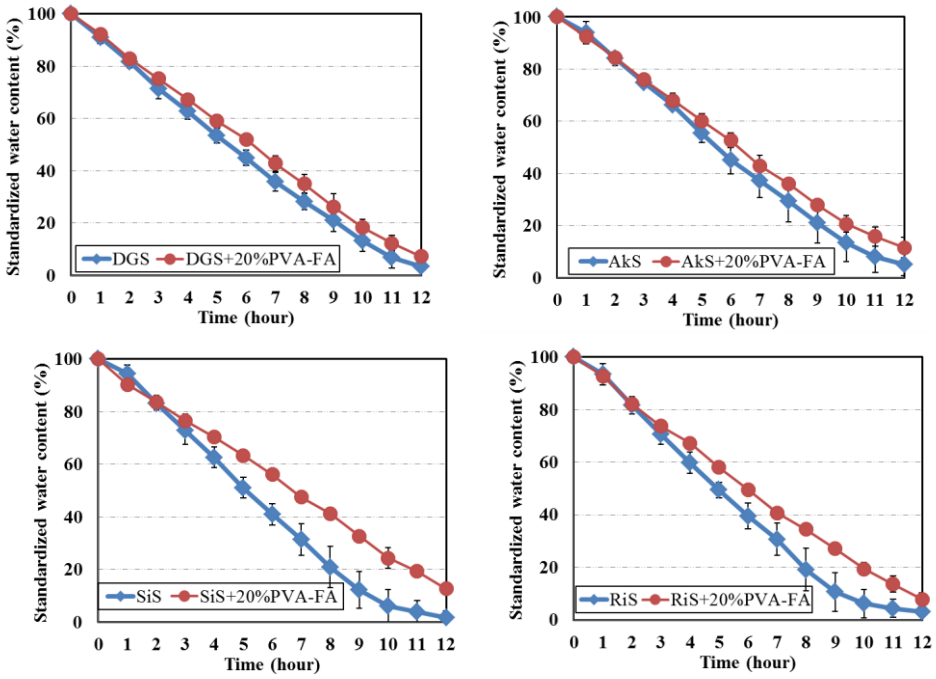

Figure 3-20 Evaporation mitigation capacity curves of DGS, AkS, SiS, RiS mixed with PVA-treated FA at 20 wt% mixing ratio and 40 °C.

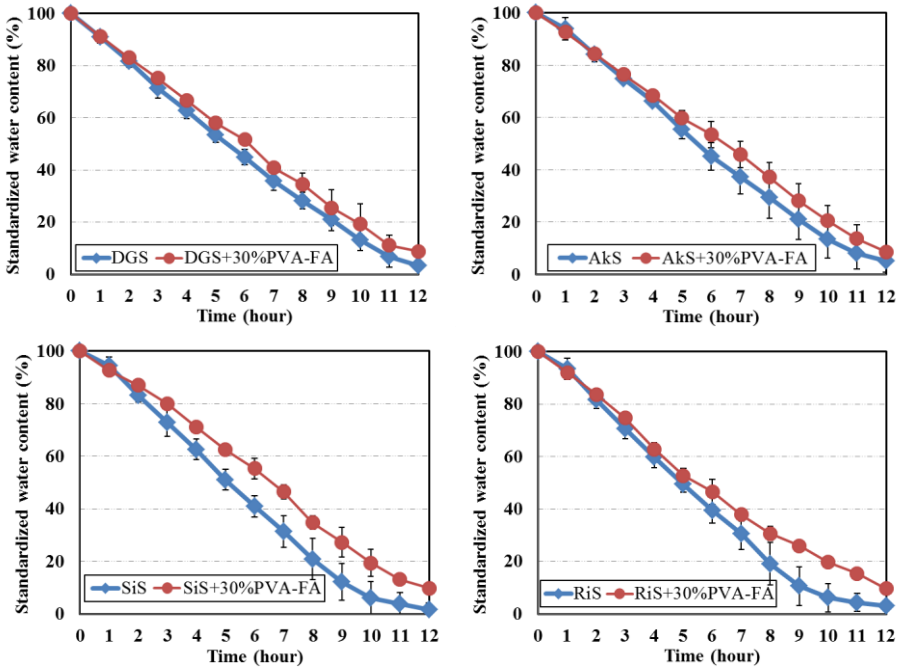

Figure 3-21 Evaporation mitigation capacity curves of DGS, AkS, SiS, RiS mixed with PVA-treated FA at 30 wt% mixing ratio and 40 °C.

3.3.1.4 Effect of PAA treated-FA amendment on EMC of soils and sands

EMC of soil/sand mixed with PVA-treated FA of 10 wt%, 20 wt% and 30 wt% at room temperature and 40 ºC were investigated. The results are shown in Figure 3-22 to Figure 3-28. The PAA-treated FA generally increased on the EMC of soils and sands at room temperature and 40 °C and at different treated-FA mixing ratios. For example, at room temperature, the EMCs of DGS and AkS were increased by around 5% and 7%, respectively. At 40 ºC, the most significant positive change for the EMC of DGS was 12.84% at the mixing ratio of 20 wt%, and for AkS was 12.57% at the mixing ratio of 30 wt%. PAA treated-FA also gave a decent positive effect on the EMCs of Sis and RiS. As for SiS and RiS at room temperature and 40 ºC, the EMCs were all increased by the PAA-FA amendment at all the different mixing ratios. The most substantial positive change of EMC was 28.31% when the SiS mixed with 30 wt% PAA treated FA at 40 ºC. T-test was used to check all these relative positive changes, and it suggested they were statistical significance (Table 3-6).

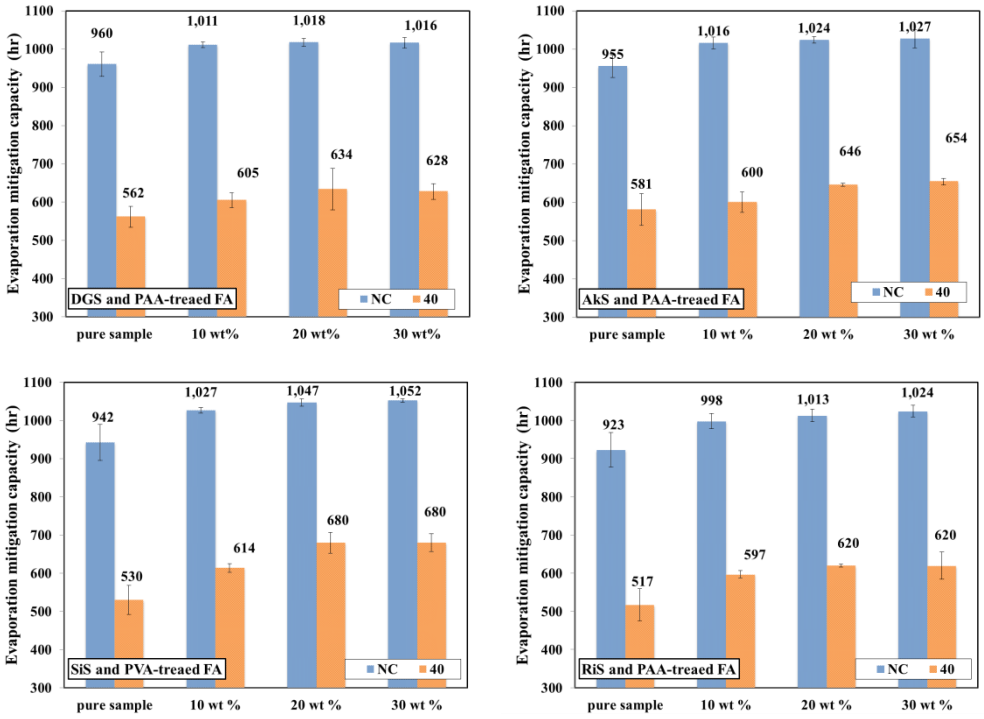

Figure 3-22 Effect of PAA modified FA on EMC of DGS AkS, SiS, and RiS at room temperature and 40 ºC.

Table 3-6 The effect of PAA-treated FA on the EMC of soil/sand

PAA-FA treatment	Relative change of EMC (%)					
Temperature	**Room Temperature**			**40 ºC**		
FA ratio	10 wt%	20 wt%	30 wt%	10 wt%	20 wt%	30 wt%
DGS	+5.32 *	+5.96 *	+5.84 *	+7.65 *	+12.84 *	+11.71 *
AkS	+6.36 *	+7.18*	+7.54 *	+3.26	+11.09 *	+12.57 *
SiS	+8.96 *	+11.07 *	+11.68*	+15.82 *	+28.21*	+28.31 *
RiS	+8.18 *	+9.79*	+10.97 *	+15.40*	+19.88 *	+19.84*

All data was conducted by t-test, and "*" stand to "p value < 0.05"

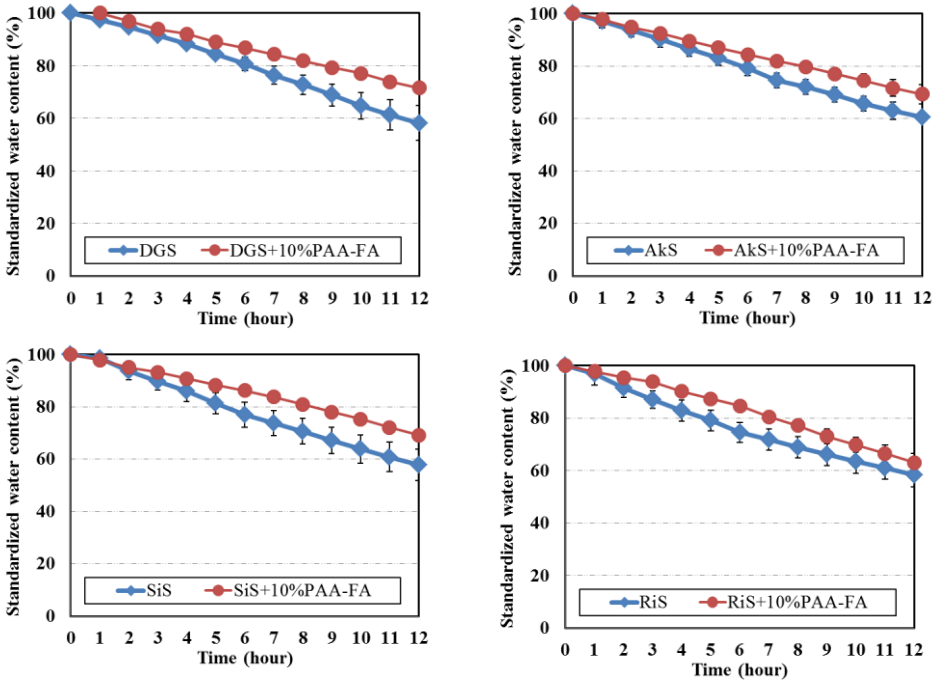

Figure 3-23 Evaporation mitigation capacity curves of DGS, AkS, SiS, RiS mixed with PAA-treated FA at 10 wt% mixing ratio and room temperature.

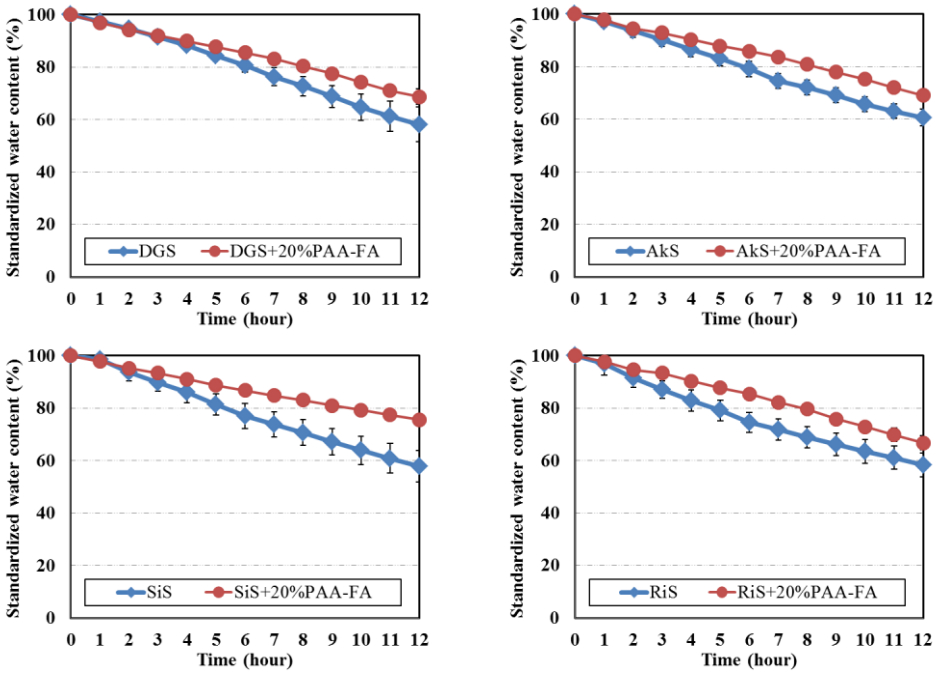

Figure 3-24 Evaporation mitigation capacity curves of DGS, AkS, SiS, RiS mixed with PAA-treated FA at 20 wt% mixing ratio and room temperature.

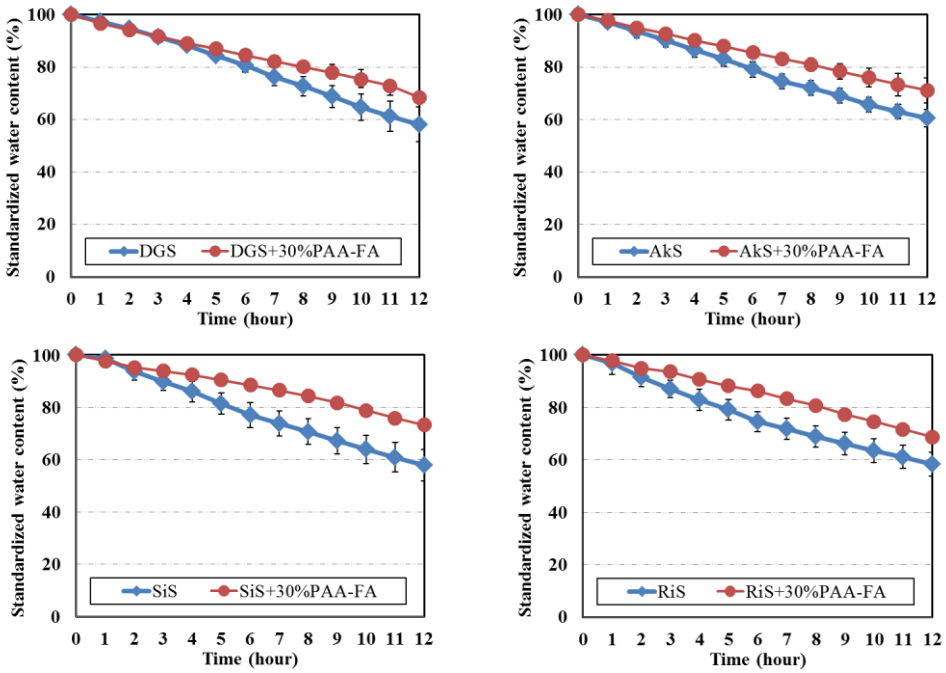

Figure 3-25 Evaporation mitigation capacity curves of DGS, AkS, SiS, RiS mixed with PAA-treated FA at 30 wt% mixing ratio and room temperature.

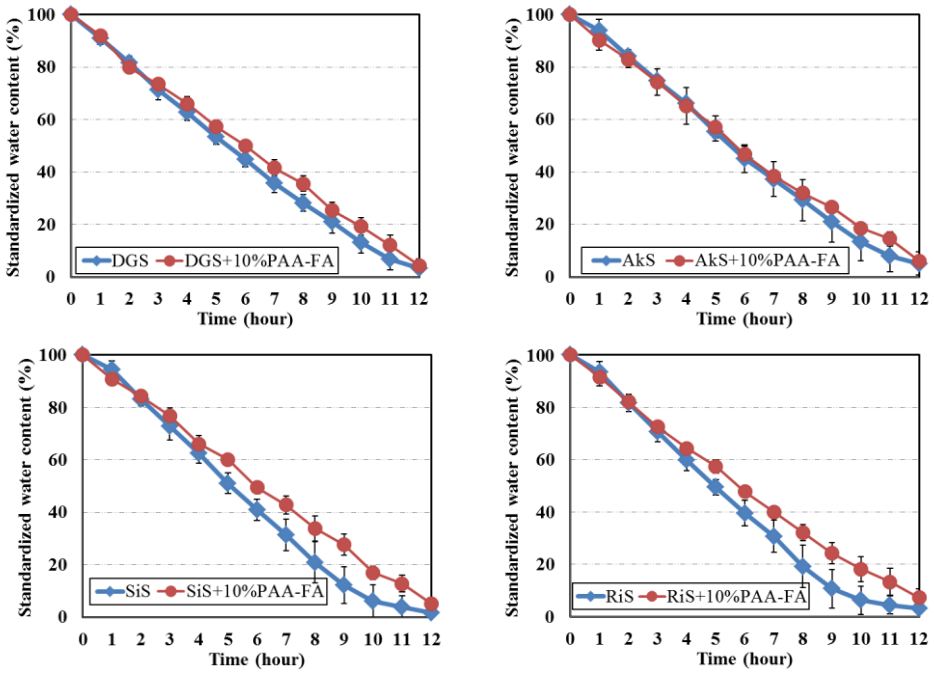

Figure 3-26 Evaporation mitigation capacity curves of DGS, AkS, SiS, RiS mixed with PAA-treated FA at 10 wt% mixing ratio and 40 ℃.

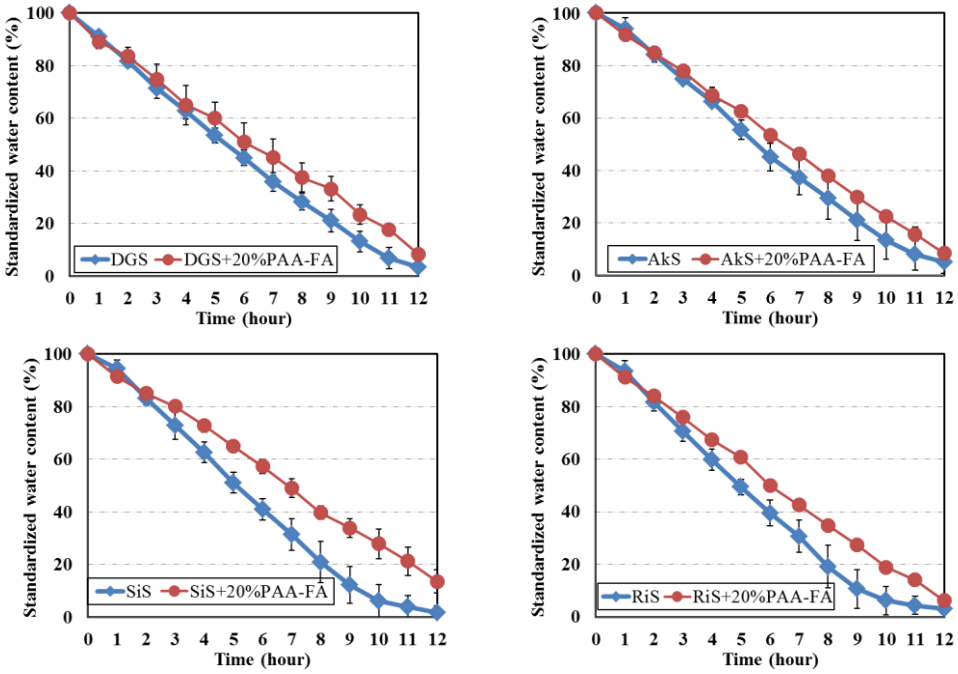

Figure 3-27 Evaporation mitigation capacity curves of DGS, AkS, SiS, RiS mixed with PAA-treated FA at 20 wt% mixing ratio and 40 °C.

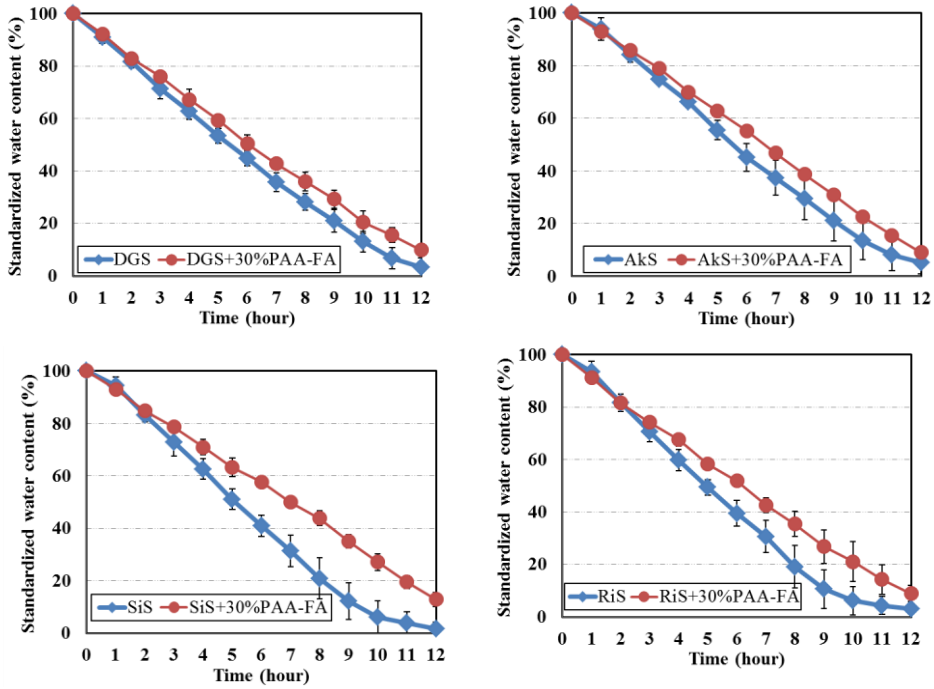

Figure 3-28 Evaporation mitigation capacity curves of DGS, AkS, SiS, RiS mixed with PAA-treated FA at 30 wt% mixing ratio and 40 °C.

3.3.1.5 The comparison of wet-treatment and dry-treatment of polymer-FA mixed in soils and sands at 40 ºC.

In the wet treatment of polymer-FA, the polymer was mixed with fly ash by water, then dried and used for drying experiment on the EMC of soil/sand. As a comparison, the drying experiment of polymer and FA, which directly mixed into the soil/sand, was conducted.

In general, the EMC values of dry-treatment of polymer-FA mixed in the soil/sand were higher than the wet-treatment. For example, in the case of the PEO-treated FA amendment, the dry-treatment of the PEO-FA showed slightly higher EMC values compared to the wet-treatment, regardless of the mixing ratios of the polymer treated FA in soil/sand (see Figure 3-29, Figure3-30). However, the differences are not statistically significant. Although the results of dry-treatment showed higher EMC values, the t-test suggested that only in a few cases were statistically significant. These results can be explained as followed. After wet-treatment, the polymer and fly ash particles are usually connected by hydrogen bonding. However, the hydrogen bonding between the FA particle and polymer may cost the overall water absorption ability of the polymer, because it reduced the amount of the hydrophilic groups such as –OH. As mentioned previously, the hydrophilic groups have a significant influence on the EMC value; as a result, the EMC values would be decreased if the total amount of the hydrophilic groups reduced. On the other hand, in the wet-treatment, polymer and FA mixed in water could make the surface morphology of the FA particle more complicated. Polymer modified FA can form polymer-FA aggregates which might improve the amendment of soil/sand structure, and influence on the EMC value. Therefore, the EMC value is impacted by complicated factors. As conclude, the results of drying treatment and wet treatment had no significant difference. The mixing of the polymer-FA in the water had no significant effect on the changes in EMC values.

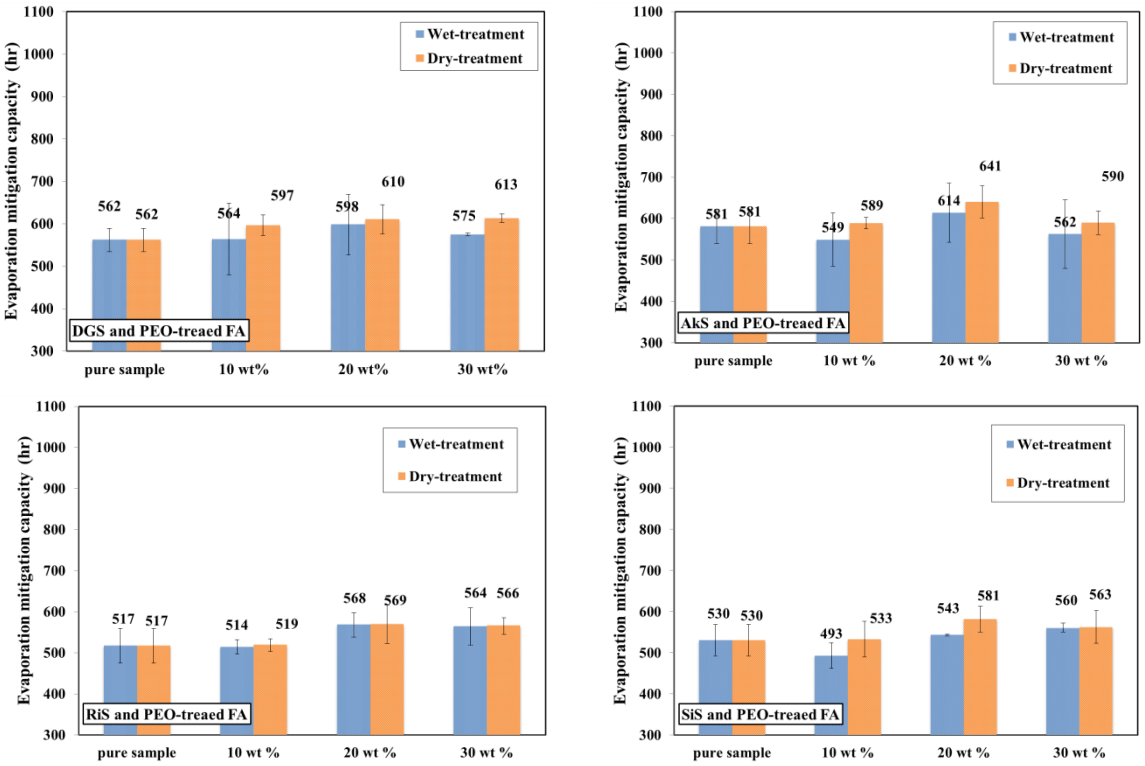

Figure 3-29. The comparison of wet-treatment and dry-treatment of PEO-FA mixed in soils and sands at 40 ºC.

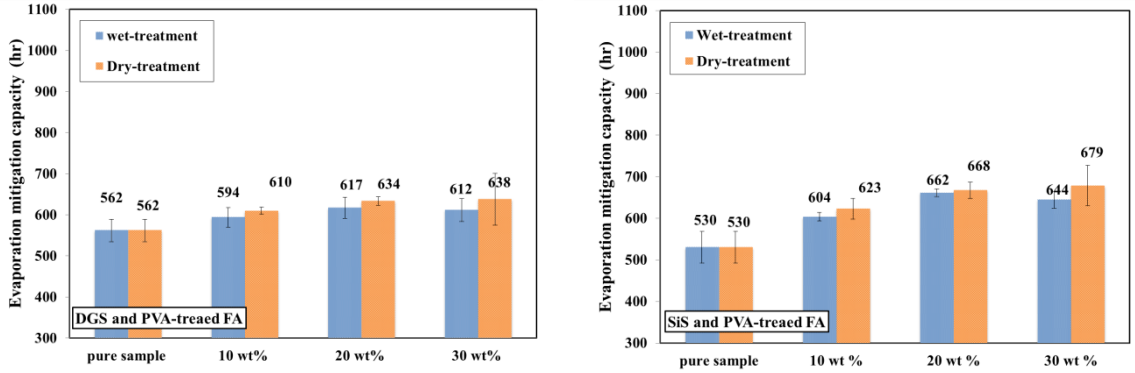

Figure 3-30. The comparison of wet-treatment and dry-treatment of PVA-FA mixed in DGS and SiS at 40 ºC.

3.3.1.6 The comparison experiments on the EMC values of solo polymer mixed in soils and sands at 40 ºC.

The polymer of PVA and PEO were mixed in the soil/sand samples in different groups, respectively. The mixing ratios of the polymers ranged from 10 wt% to 30 wt%. The drying experiment was conducted at 40°C.

According to the results shown in Figure 3-31, the polymers of PVA and PEO can significantly increase the EMC values. The EMC increased as the mixing ratio of the polymer increased. Compared to the EMC of the polymer treated-FA mixed in the soil/sand, the EMC of solo polymer mixed in the soil/sand was much higher because, at the same mixing ratio, the polymer itself contains a large amount of hydrophilic functional groups such as –OH or –COOH-.

Besides, in the same type of soil/sand, the PVA mixed soil/sand has relatively higher EMCs than the PEO mixed soil/sand, which indicated that at the same mixing weight ratio of the polymers, the PVA contained more hydrophilic functional groups than the PEO. In conclude, the hydrophilic functional groups can have a significant impact on the EMC. And compared to the previous results, the raw-FA amendment on the EMC of soil/sand didn't have a considerable effect because of FA is a lack of hydrophilic functional groups. Therefore, to improve the performances of the FA amendment on the EMC of soil/sand, the modification of hydrophilic functional groups on the surface of the FA particles is necessary.

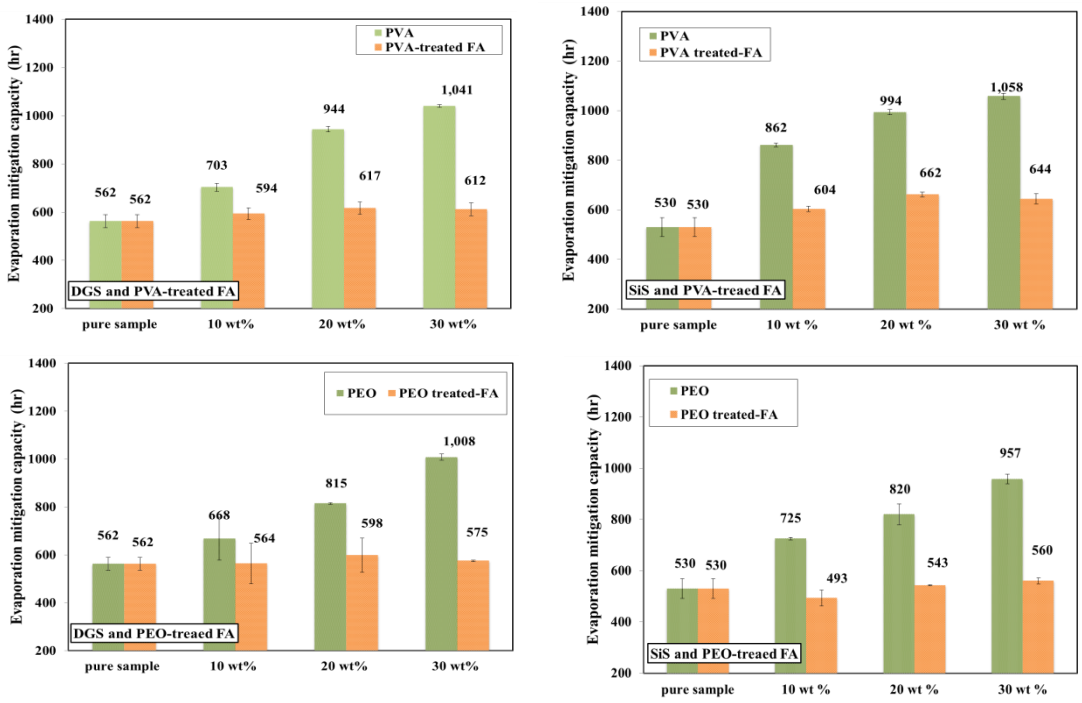

Figure 3-31. The comparison of EMC values of polymer-mixed soil/sand and polymer-treated FA mixed soil/sand.

3.3.1.7 Summary of the polymer treated-FA amendments on EMCs of soils and sands

The optimal EMCs of soil/sand amended by polymer–treated fly ash were compared with the EMCs of the pure soil/sand samples. The relative change of the EMC of each sample was shown in Figure3-32. The relative positive change of the EMC values of silica sand and river sand was more significant than the other two types of soils. This result showed that polymer treated-FA gave a superior improvement in the evaporation mitigation capacity of sandy soil. Temperature also influenced the EMC value. The variation of the EMC value is relatively small because the water evaporation rate is low at room temperature. At high temperature, the polymer-treated FA added in the soil/sand samples inhibited the water evaporation, thus increased the EMC value significantly. PVA-FA amendment is relatively active compared to the PEG-FA amendment on EMC. Compared to the other polymer treatments, PAA-treated FA performed the optimal improvement on the EMC of soils and sands. As for soil/sand at room temperature and 40 ºC, the EMCs were all increased by the PAA-FA amendment at all the different mixing ratios. The most significant change of EMC was 28.31% when the SiS mixed with 30 wt% PAA treated FA at 40 ºC. In contrast, PEO-treated FA had a limited impact on the EMC of soil/sand. The T-test suggested that most of the amendments by PEO-FA were not statistically significant. Although PEO and PEG have the same structural unit, they have a big difference in the molecular weight. Compared to the POE treatment, the PEG-treated FA had a significant impact on the EMC of soil/sand. The dependency of molecular weight on the properties of the water-absorption polymer would be illustrated in the following section.

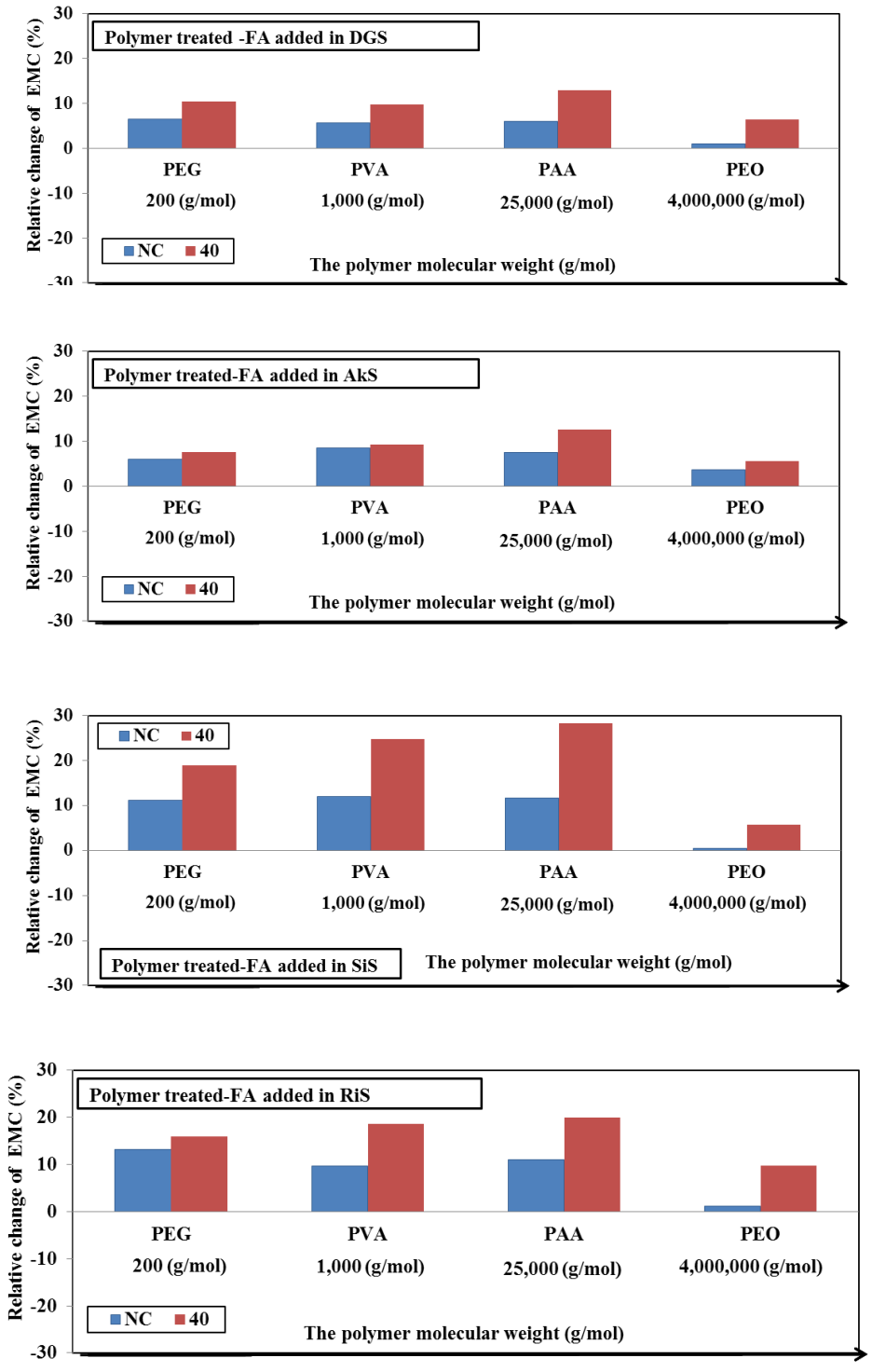

Figure 3-32 Optimal EMCs changes of polymer-FA amended soil/sand compared with the pure soil/sand samples.

3.3.2 The impact of hygroscopic groups of the polymer- treated FA on the EMC

3.3.2.1 The dependency of the polymer chemical structure on the EMC

According to the previous result, the effect of polyethylene glycol (PEG, PEO) treated FA on the soil/sand EMC decreased considerably as the molecular weight (MW) of the polymer increased. POE treated (which the molecular weight is 4,000,000) FA gave limited effect on the EMC. On the other hand, PAA treated FA had a significant effect on the EMC of soil/sand. This phenomenon could be explained by the chemical structure of the polymers (see Figure 3-33). The hydrophilicity of polymer is owed to several water-solubilizing groups such as –OH, –COOH, –COO−, >C=O, >CHNH2, –CONH2, and–SO3H, which are on the backbone or side chains. When water is added to the polymer, the formation of hydrogen bonds along with cross-link chain swelling is taking place in superabsorbent polymer (Kumar, 2018). As for the PEG or PEO, the hydroxyl (-OH) end groups in the polymer can form many hydrogen bonds with water, which makes the polyethylene glycol can sorb large amounts of moisture (Baid, 2009). However, as the molecular weight increases, the relative fraction of hydroxyl end groups decreases, and the hydrophobic groups such as -CH- increases. Therefore, the higher the molecular weight, the polyethylene glycol would become less hydrophilic. As a result, the POE treated-FA had a negligible effect on the EMC of the soils and sands.

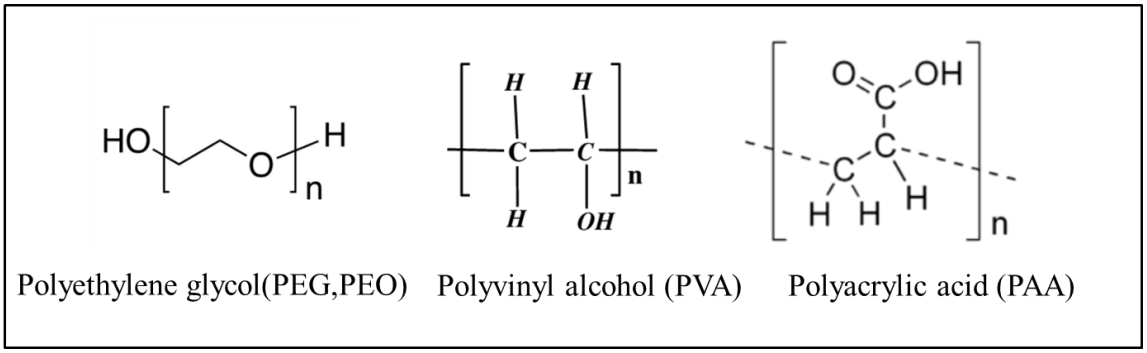

Figure 3-33 Chemical structure of PEG, PEO, PVA, and PAA

The dependency of the polymer chemical structure on the EMC could also explain that the PVA-FA amendment is relatively active compared to the PEG-FA amendment, although the molecular weight of PVA (1000g/mol) is larger than the PEG (200g/mol). This is because of the high density of the hydroxyl groups of PVA are located on its side chains other than the backbone, making it can form quantiles of hydrogen bonding or self-cross-linking even at the sizeable molecular weight.

3.3.2.2 The priority of the hydrophilic groups on hydrogen bonding and its impact on the EMC

Compared to other treatments, the PAA-treated FA gave the most significant positive impact on the EMC. This is most likely due to the facilitated formation of hydration shells around the polymer. The polymer with more hydrogen-bond accepting groups is more likely to form hydration shells. Therefore the material with the hydrogen-bond accepting groups has superior ability to up-take water, compared to materials with hydrogen-bond donor groups (Hanneke, 2007). The groups such as –OH, $–NH_2$, –CONH–, $–CONH_2$, –COOH and $–SO_3H$ act as hydrogen-bond donors, while the carbonyl groups from the acid moiety of the PAA is known as the primary H-bond acceptor. The carboxylic acid can act as both hydrogen-bond acceptors due to the carbonyl groups act as hydrogen bond acceptors, and the hydroxyl groups act as the hydrogen donor. Compared to other polymers, PAA has stronger hydrogen-bond accepting groups, resulting in higher water uptake. Therefore, the PAA-treated FA gave an optimal amendment on the EMC of soil/ sand..

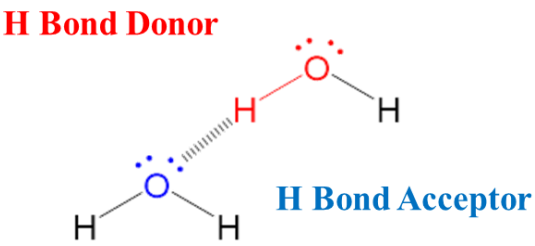

Figure 3-34 Concept of hydrogen bonding groups.

3.3.2.3 The analysis of the chemical groups on the polymer through IR-spectrum

The chemical groups on the surface of polymer-modified FA particles were investigated by IR spectrum, and the result was shown in Figure 3-35. According to the FTIR spectra, the broad absorption band between 2700 cm^{-1} to 3550 cm^{-1} of PVA was attributed to the –OH stretching, which can be commonly found in the compound class of alcohol. In particular, in the frequency range of 2700cm^{-1}-3200 cm^{-1} is the intramolecular bonded O-H stretching, The weak broadband at the range of 3200-3550 cm-1 is the intermolecular bonded O-H stretching. The intermolecular bonded O-H and intramolecular bonded O-H both exist in the PVA- treated FA. This result accorded with the fact that the high density of the hydroxyl groups is located on PVA side chains, making it form hydrogen bonding or self-cross-linking. The weak waves around 2000 cm^{-1} could be the C-H bending, which exists in the unit structure of all the polymers. The band at the frequency around 2940 cm^{-1}, was mostly recognized as stretching vibration of –(CH)n structure, which obviously exists in the PVA-treated FA. The band at around 1760 cm^{-1} implied the stretching vibration of –C=O in the carboxylic, which can be recognized in the spectra of PAA-treated FA. The band at around 1650 cm^{-1} was attributed to the C=C stretching, which is in the backbone structure of the polymers. The band at around 1330 cm^{-1} to 1440 cm^{-1} is the O-H bending. In particular, the O-H bending of carboxylic is at the range of 1440 cm-1to1395 cm^{-1};

and the O-H bending of alcohol is at the range of 1330 cm^{-1} to1420 cm^{-1}. The strong broadband at around 1050 cm^{-1}, was corresponded to the C–O–R stretching structure. This peak could also be ascribed to the –Si-O stretching. This peak could also be ascribed to the –Si-O stretching. The peak at around 795 cm^{-1} was attributed to the C=C bending or C-H bending stretching

As a summary, according to the IR spectra, PVA-modified-FA exhibits abundant types of O-H groups, from the frequency range 2700 cm^{-1} to 3200 cm^{-1}, 3200-3550 cm^{-1}, and 1330 cm-1 to 1420 cm^{-1} to1330 cm^{-1}. These O-H groups can form hydrogen bonding and hence amplify the the ability of water-absorbing, On the other hand, the spectra of PAA-treated FA didn't show the O-H stretching at the frequency range of 2700cm^{-1}-3550 cm^{-1}, but there is an evident peak at 1760 cm^{-1}, which is attributed to the C=O group in the carboxyl acid. The carboxyl groups are the main chemical factor that attributes to the high EMC vale of the PAA-treated FA mixed in soul/sand. When the hydrophilic groups in the PVA-FA and PAA-FA were compared with their effects on the EMC of soil/ sand, it can be concluded that the carboxyl group is superior for water retention than the hydroxyl group. As a comparison, the FTIR spectra showed that PEO treated FA has fewer types of O-H group and C=O group, which is the chemical factor that the PEO-treated FA is not effective in the EMC of soil/sand.

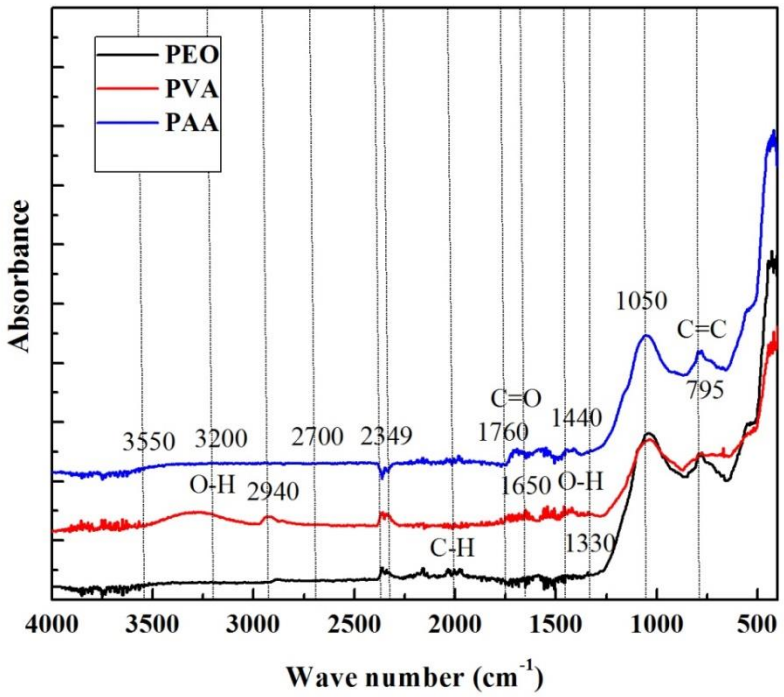

Figure 3-35. IR spectra of polymer treated FA (PEO-FA, PVA-FA, PAA-FA)

3.3.2.4 The influence of the metal ions on the hydrophilicity of the polymer solution-treated FA

The effect of polyacrylic acid solution (PAA_S)-treated FA amendment and PAA solution with calcium chloride-treated FA amendment were conducted. The effect of the polyacrylic acid solution with/ without Ca^{2+} modified FA on EMC of DGS, AkS, RiS, and SiS are shown in Table 3-7 to Table 3-8. At natural temperature, the PAA solution-treated FA amendment had nearly no significant effect on the EMC of most samples. At 40ºC, however, the PAA-treated FA amendment increased EMC in most cases. For example, the EMC of AkS, SiS, and RiS were increased when the mixing ratio of FA was 20 wt%. When the mixing ratio of FA was 10 wt %, the EMC of DGS and SiS were increased. When the mixing ratio of FA was 30 wt %, the EMC of DGS and SiS were increased by 28% and 12% respectively. T-test suggested in some cases, the increase of EMC caused by the FA amendment was regarded as significant. For example, the

21% increase of SiS EMC at a 20% mixing ratio was statistically significant. On the other hand, in the case of DGS at 40ºC, although the EMC was increased by 34% and 28% when the FA mixing ratios were 10 wt% and 20 wt % respectively, the t-test suggests that the differences of EMC between pure samples and FA-amended samples are not significant. Temperature dependency is evident in the soil/sand sample with the same mixing ratio of FA. For example, in the case of AS with the FA mixing ratio of 10 wt %, the EMC was increased by 3% at room temperature but decreased by 9% at 40 ºC. In the case of SiS with the FA mixing ratio of 30wt %, the EMC was decreased by 2% at room temperature but increased by 12% at 40 ºC.

As a comparison, the PAA solution+$CaCl_2$ treated-FA amendment on EMC was also tested, in the hope of generating a microporous structure on the surface of PAA treated-FA by adding Ca^2+. It was expected to serve as a water-holding space to increase the EMC. However, the results were different from the expectation. At 40ºC, it showed that the EMC of all the soil/sand samples were decreased by mixing with the PAA+$CaCl_2$-treated-FA, except SiS with the FA mixing ratio of 30 wt %. Compared to the previous results of the PAA solution-treated FA amendment, the PAA+$CaCl_2$ treatment was not positive; it decreased the EMC of soil/sand at 40ºC. Although at the room temperature, the PAA+$CaCl_2$ treated-FA amendment slightly increased the EMC of almost all the samples, except AS with the FA mixing ratio of 30 wt%. It could be concluded that the temperature may have an essential impact on the hydraulic properties of PAA+$CaCl_2$-treated-FA. There is a temperature dependency on the PAA+$CaCl^{2-}$treated-FA amendment. Compared to the RiS and SiS, the temperature dependency is more significant in the cases of DGS and AS. This result might relate to the complex reactions between–COO- groups and metal ions in a polymer solution. Decades of research have revealed that even small amounts of Ca^{2+} tend to have a significant effect on polymer solutions. For example, Mao (Mao et al., 2018) reported that there is a solubility product balance among –

COO− groups and Ca^{2+}/Mg^{2+} ions that can lead to precipitation of the hydrophobic associating polymer solubility product, and then the precipitate acts as a core and grows continuously. As for FA particles contain many different types of metals and heavy metals, there might be sophisticated reactions between the metal ions and the hydrophilic groups such as –COO−. These reactions might lead to the disfunction of the hydrophilic chemical groups, and as a result, the amendment on the water retention of soil/sand is invalid.

Table 3-7 The effect of polyacrylic acid solution -treated FA amendment on EMC of DGS, AkS, RiS and SiS.

PAA_S treatment	Relative change of EMC (%)					
Temperature	Room Temperature			40 ºC		
FA ratio	10 wt%	20 wt%	30 wt%	10 wt%	20 wt%	30 wt%
DGS	+0.443*	-0.0102	-0.284	+33.55	-3.657	+27.56
AkS	+3.148	+3.219	+2.822	-9.012	+13.38	-8.797
RiS	-2.210	-1.466	-0.9631	-7.762	+4.864	-15.84
SkS	+1.160*	+1.857*	-1.732	+6.965	+21.31*	+11.92*

All data was conducted by t-test, and "*" stand to "p value < 0.05"

Table 3-8. The effect of polyacrylic acid solution with alcium chloride-treated FA amendment on EMC of DGS, AkS, RiS and SiS.

PAA_S+$CaCl_2$ treatment	**Relative change of EMC (%)**					
Temperature	**Room Temperature**			**40 ºC**		
FA ratio	10 wt%	20 wt%	30 wt%	10 wt%	20 wt%	30 wt%
DGS	+1.445	+1.624	+0.881	-7.373	-11.47	-11.93
AkS	+1.522	+0.322	-1.257	-5.188	-8.325 *	-5.272
RiS	+2.206	+4.320	+3.060	-3.350	-0.440	-5.115
SiS	+1.202	+1.946	+5.154	-4.182	-4.710 *	+0.381

All data was conducted by t-test, and "*" stand to "p value < 0.05"

3.3.3 The morphology on the surface of polymer modified FA particles

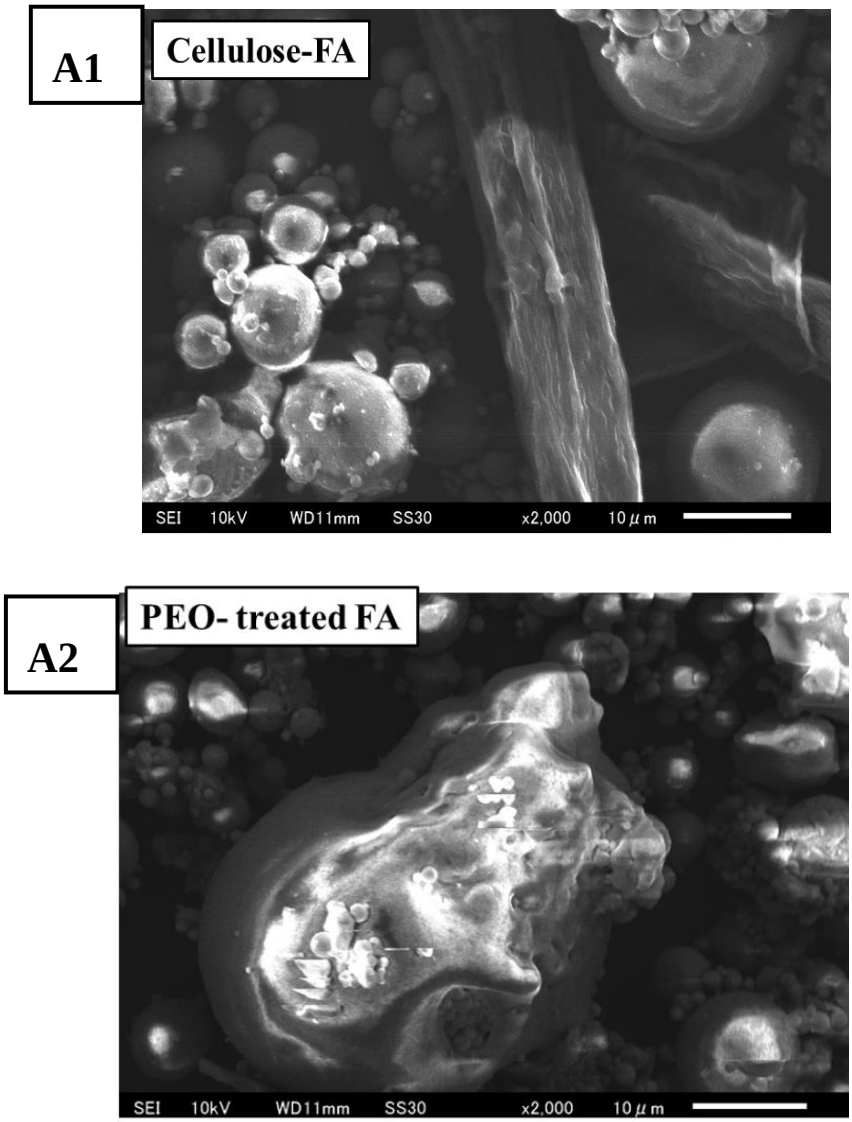

Figure 3-36. The morphology on the surface of cellulose modified FA (A1) and PEO-modified FA (A2).

As shown in Figure 3-36, cellulose-treatment of FA is unlikely to generate aggregates with FA particles (Figure 3-36 A1). The adhesive polymer is needed for binding cellulose and FA particle into aggregates. Semi-crystalline of PEO was founded in the POE- treated FA, which indicated the insufficient modification of POE-FA particles.

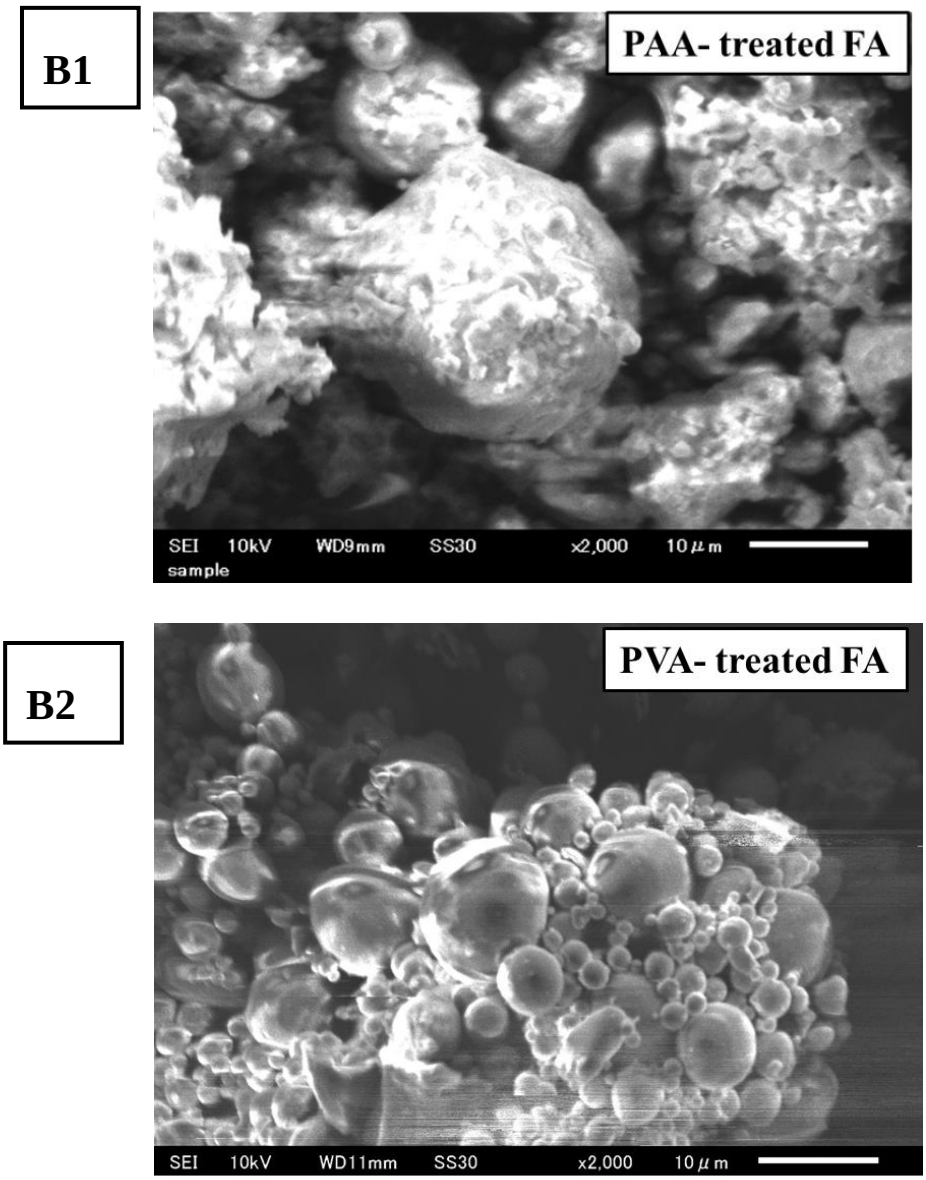

Figure 3-37. The morphology on the surface of PAA modified FA (B1) and PVAmodified FA (B2).

The surface of PAA-treated FA and PVA- treated FA is coarser, compared to the other treatment such as PEO-FA, and cellulose-FA. The enhancement of the surface area might be one of the factors that improved the EMC value of PVA-FA, and PAA-FA amendment on the soil/ sand. Compared with cellulose-FA and PEO-FA, the cellulose-PEO-FA has a more complexed aggregates-structure, which may lead to an increase of the EMC value on soil/sand.

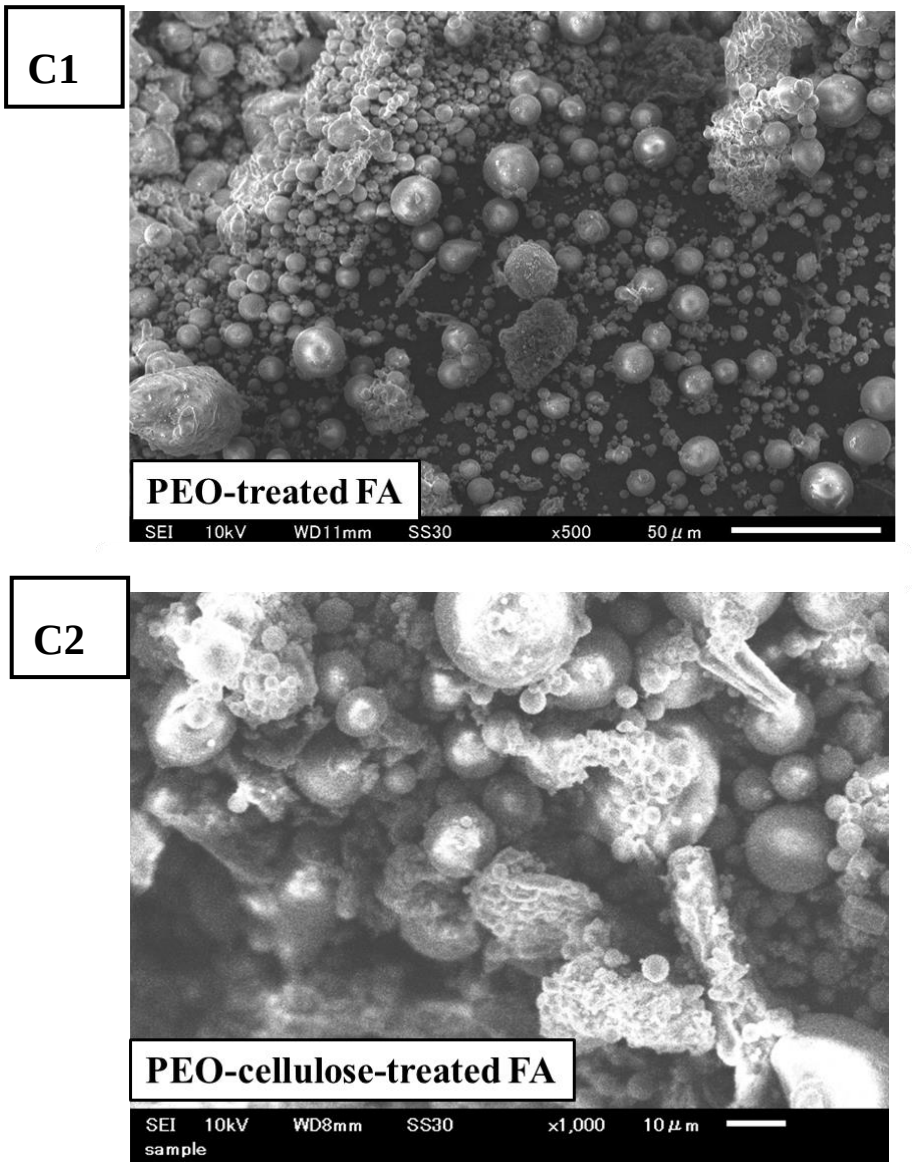

Figure 3-38. A plausible diagram of hydrogen bonding between PVA and FA

3.3.3.1 The comparison of cellulose-modified FA and cellulose-polymer-modified-FA

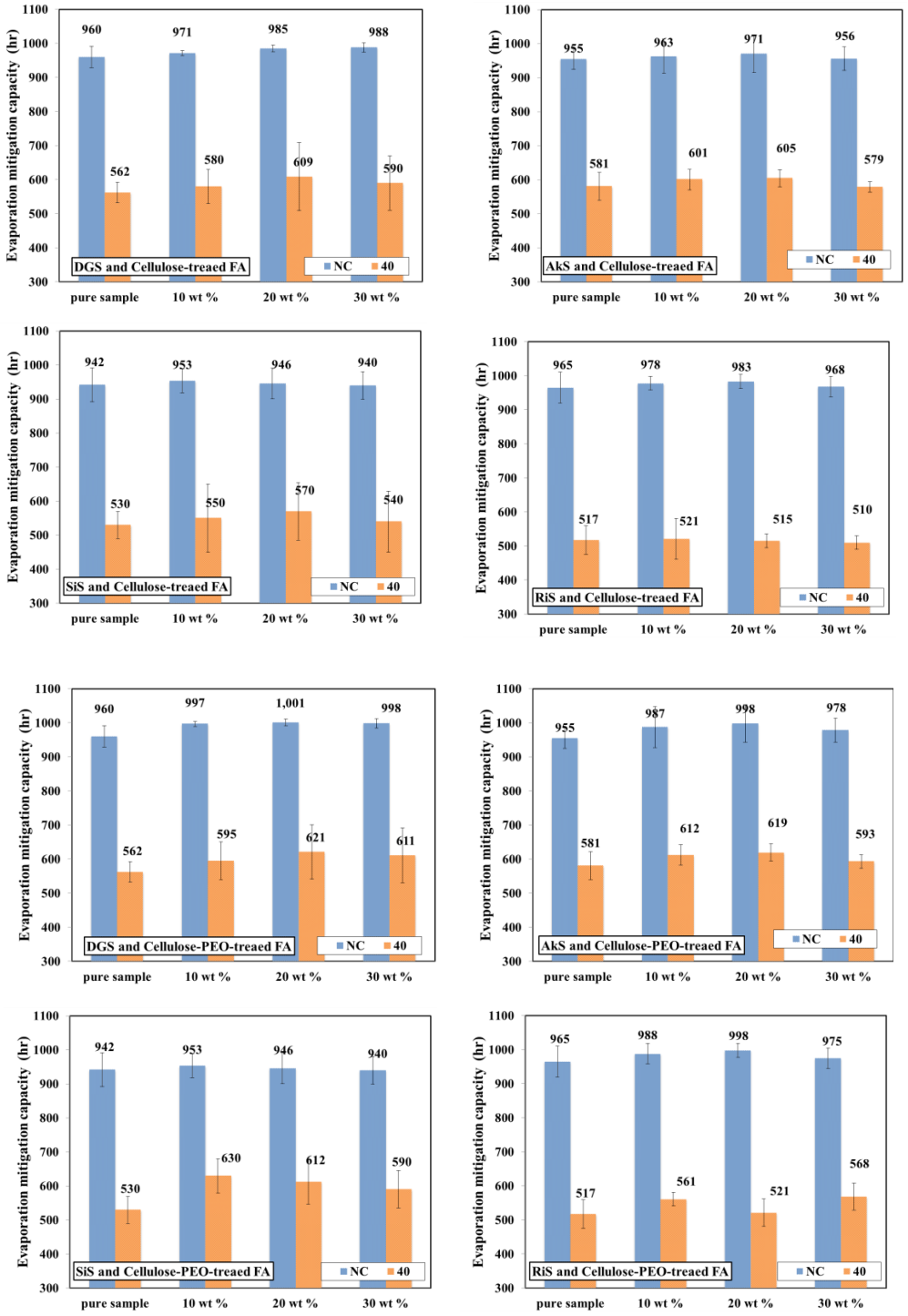

Figure 3-39 Effect of cellulose modified FA and cellulose-PEO modified FA on EMC of DGS AkS, SiS, and RiS at room temperature and 40 ºC.

The effect of cellulose treated FA, and PEO-cellulose treated-FA amendment on EMC of soils and sands was shown in Figure 3-39. According to the results, at natural temperature, the cellulose-treated FA amendment had nearly no significant effect on the EMC of most samples (DGS, AkS, RiS, and SiS). At 40 ºC, the cellulose-treated FA increased EMC of DGS by 8.36 % when the mixing ratio of FA was 20 wt%, but generally, the EMC effect of cellulose-treated FA on soil/sand is not significantly positive in all samples. Temperature dependence is not apparent among all the soil/sand samples with the cellulose-treated FA amendment. Also, when the mixing ratio of FA was 20 wt %, the EMC of the sample was relatively higher with other samples.

The cellulose treatment of FA on the EMC is not significant favorable, which can be the result of lacking aggregates formation and sufficient hydrophilic groups on the surface of the FA particles. Compared to the PEO-treatment and cellulose treatment, the PG-cellulose treated FA amendment was relatively more effective. For example, in the case of DGS and AS at 40ºC, the optimal EMCs were increased by 10.49% and 6.54 % respectively. EMC of RS was increased by 9.86 % when the mixing ratio of FA was 30 wt%. In particular, the EMC of SiS was increased by by18.86% when the mixing ratio of FA was 10 wt%. Polymer-cellulose modified FA mixture can increase the retention of water against evaporation losses. These results suggested that multiple treatments on the FA modification would be necessary to increase the effect of the FA amendment on soil water retention. Using a low concentration of biopolymers from plant fibers is helpful to increase water retention. Adding cellulose fiber together with the polymer could accelerate the complexed aggregates surrounding the FA particles (see Figure 3-38), which can enhance the surface area of the FA particles. To keep water holding for a longer time, further potentially suitable FA modification is required to improve the physical properties as well as the chemical properties.

3.4 Conclusion

The effects of the polymer-FA amendment on the EMC of soils and sands were investigated. In majority cases, when the mixing ratio of raw-FA was 20 wt%, the effect of the FA amendment on EMC was positive. PAA-treated FA amendment increases the EMC of soil/sand more effectively compared to the other treatments. And also, there are molecular weight and temperature dependencies on the polymer-FA amendments. Further study showed that the hydrophilic groups such as –OH and –COO- on the polymer-modified FA play the vital roles in the EMC value of soil/sand. The molecular weight dependence was caused by the fraction of the hydrophilic groups on the polymer, and the temperature can have an influence on the hydrogen kinetic energy. Therefore, sufficient surface modification with hydrophilic groups could greatly increase the water retention ability of FA particles. The SEM results showed that polymer treated fly ash could generate aggregates. The polymer and fly ash particles are usually connected by hydrogen bonding. However, the hydrogen bonding between the FA particle and polymer may cost the overall water absorption ability of the polymer. Besides, the aggregates formed by FA particle and polymers may contain capillary-size pore structure, which is suitable for water retention; but it was destroyed by crashing the aggregates into powder. Therefore, multiple modifications on the fly ash could be conducted. One of the applicable methods is to make the fly ash and polymer into composites. The porosity of the FA composites could be improved. Moreover, the surface modification could also be added to increase the chemical functional groups such as hydroxyl and carbonyl, which are hydrophilic. The concept of the water-absorbent material was shown in Figure 3-40. The experiment on porous FA composites synthesis and the properties analysis shall be described in the next chapter.

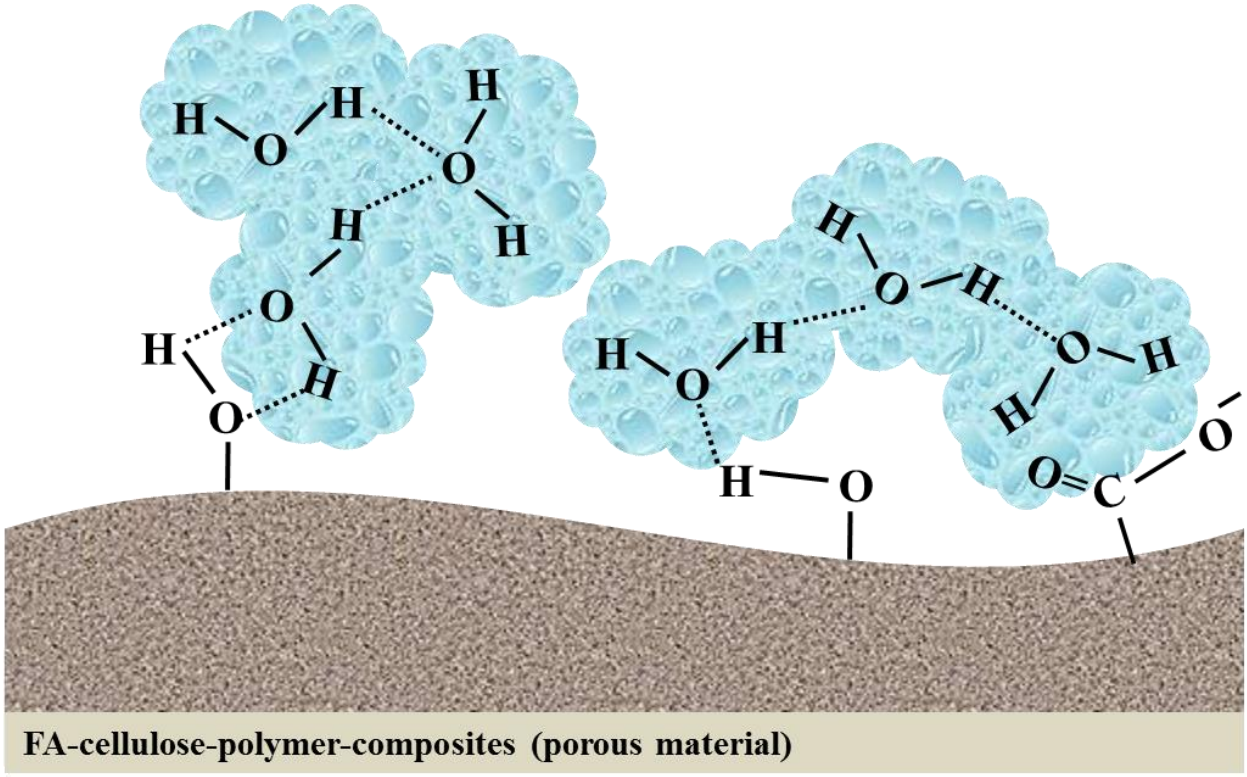

Figure 3-40 Concept of building water retention material by the surface modification.

References

1. Baid. A Jared.; et al. (2009). Effect of molecular weight, temperature, and additives on the moisture sorption properties of polyethylene glycol, Wiley InterScience. DOI 10.1002.
2. Bakass, M.; Mokhlisse, A.; Lallemant, M. (2002). Absorption and desorption of liquid water by a superabsorbentpolymer: Effect of polymer in the drying of the soil and the quality of certain plants. J. Appl. Polym. Sci., 83, 234–243.
3. Demitri, C.; Scalera, F.; Madaghiele, M.; Sannino, A.; Maffezzoli, A. (2013). Potential of Cellulose-BasedSuperabsorbent Hydrogels as Water Reservoir in Agriculture. Int. J. Polym. Sci.
4. Gunko, V., et al. (2017). Properties of Water Bound in Hydrogels. et al. (2016). Gels 2017, 3, 37.
5. Han, Y.G.; Yang, P.L.; Luo, Y.P.; Ren, S.M.; Zhang, L.X.; Xu, L. (2010) Porosity change model for watered super absorbent polymer-treated soil. Environ. Earth Sci. 61, 1197–1205.
6. Hanneke M. L., et al. (2007). Water uptake of hydrophilic polymers determined by a thermal gravimetric analyzer with a controlled humidity chamber. J. Mater. Chem., 2007, 17, 4864–4871
7. Kumar Panda Arun., et al. (2018). Role of water absorbing materials in vegetable production. Journal of Pharmacognosy and Phytochemistry. 7(2): 3639-3644

   Lejcus, K.; Spitalniak, M.; Dabrowska, J. (2018). Swelling Behaviour of Superabsorbent Polymers for Soil Amendmentunder Different Loads. Polymers, 10, 271
8. Mao, Jincheng., et al.(2018). Novel Hydrophobic Associating Polymer with Good Salt Tolerance. Polymers, 10(8), 849;
9. Montesano, F.F.; Parente, A.; Santamaria, P.; Sannino, A.; Serio, F. (2015). Biodegradable

Superabsorbent HydrogelIncreasesWater Retention Properties of Growing Media and Plant Growth.Effic. Irrig. Manag. Eff. UrbanRural Landsc, 4, 451–458.

10. Narjary, B.; Aggarwal, P.; Singh, A.; Chakraborty, D.; Singh, R. (2012). Water availability in different soils in relationto hydrogel application.Geoderma,187, 94–101.
11. Wang, Liang-Yi., Wang, Meng-Jiy. (2016). Removal of Heavy Metal Ions by Poly(vinyl alcohol) and Carboxymethyl Cellulose Composite Hydrogels Prepared by a FreezeÔÇôThaw Method. ACS Sustainable Chemistry & Engineering. 4 (5), 2830-2837
12. Zdeňka, K.; Petr, V.; et al. (2016). Refract metric study of systems water-poly (ethylene glycol) for preparation and characterization of Au nanoparticles dispersion. Arabian Journal of Chemistry. Accepted 12 November 2016

Chapter 4

Fly ash based polymer composites synthesis and properties analysis

4.1 Introduction

Composite is made from two or more constituent materials with significantly different physical or chemical properties that when combined, produce a substance with characteristics different from the individual components. Researches on the formation and development of FA-based polymer composites have been conducted in recent years. FA is a valuable reinforcing filler because of its potentiality, excellent particle size, and plenty of availability. Functionalized polymers are promising candidates in the fabrication of high-performance composites because they can maximize the interaction between the filler and polymer matrix. Such fly ash filled polymer composites can possess attractive thermal and mechanical properties and better dimensional stability (Satapathy et al., 2013; Kumar et al., 2012; Singla et al., 2010; Acharya and Mishra, 2007; Sahai and Pawar, 2014; Sheriff et al., 2017).

Fly ash based polymer composites present significant applications to basic science and technology, environment, and economy. The production of fly ash is increasing year by year, posing a severe problem with its safe disposal and utilization. FA disposal is a great challenge faced by the environmentalists and techniques to use it effectively are a concern worldwide. The usage of FA as filler material in the polymer matrix can result in the reduction of the production cost of the finished products. If Fly ash can be used as reinforcing filler in high density, it would benefit both the economy and waste management. The polymer-FA composite can be made into a value-added product with different properties. For example, it is a promising adsorbent for the

removal of various pollutants. Also, as mentioned in Chapter 3, modification of the porous structure and the hydrophilic chemical groups could increase the EMC value. Therefore, it is an appropriate way to make fly ash based polymer composites as a water-retentive material.

4.2 Fly ash based polymer composites synthesis

4.2.1 Details of the materials

a) The physical and chemical properties of the FA were described in Chapter 2. The particle size of the FA is ranging from 0.5 to 15 μm in diameter (see Figure 2-5). FA is mainly a mixture of inorganic metal oxides such as SiO_2, $Al2O_3$, Fe_2O_3, CaO, MgO, et, al. The elemental content of tested FA was analyzed by XRF, which is shown in Table 2-1. According to the elemental content, FA tested in this study is classified into Class F. FA utilized in this study was taken from one coal-fired power plant in Japan.

b) Polyvinyl alcohol (PVA) is a water-soluble and biodegradable polymer, which is white in color and odorless. Its idealized formula is [CH2CH (OH)]n. PVA is widely used in the fabrication of compatible composites. PVA used in this study was purchased from Wako Pure Chemical Industries, Ltd, Japan. It is a completely hydrolyzed type, and its molecular weight is around 1000g/mol. PAA contains many types of functional groups, which could improve the chemical and mechanical properties of the FA composites. In particular, the O-H groups on the side chains of PVA are suitable for water absorbing. Besides, compared to the other polymers used in Chapter 3, PAA has a relatively low viscosity, which convenient the sample fabrication process.

c) Cellulose is an organic compound with the formula $(C6H10O_5)n$. It has an average degree of polymerization of 150 to 450; an average particle diameter of 30 to 250 μm; an apparent specific volume exceeding $7cm^3/g$. The cellulose used in this study was purchased from Wako Pure Chemical Industries, Ltd, Japan. The particle range is around 38 μm (through

38 μm-400 mesh). The purpose for using cellulose is for the improvement and adjustment of the porous structure of the FA composites

4.2.2 Preparation of the FA composites materials

A quantified amount of FA, cellulose, and PVA was mixed in the beaker, and distilled water was added into the mixture (see Figure 4-1). The suspension was heated and under vigorous stirring until the suspension became into a gluey form. The mixture prepared was transferred to the mold cavity by care. The mold (3.3 cm*3.3 cm*3.3 cm) should be thoroughly filled. The samples were kept in the incubator until dried. The composition and the production conditions of the FA composites are shown in Table 4-1.

Table 4-1. The composition of FA composites

The composition of FA composites			
Samples	**FA (%)**	**PVA (%)**	**Cellulose (%)**
PFA90	90	10	0
PCFA90	90	5	5
PFA80	80	20	0
PCFA80	80	10	10
PFA70	70	30	0
PCFA70	70	15	15
PCFA60	60	20	20
PFA60	60	40	40

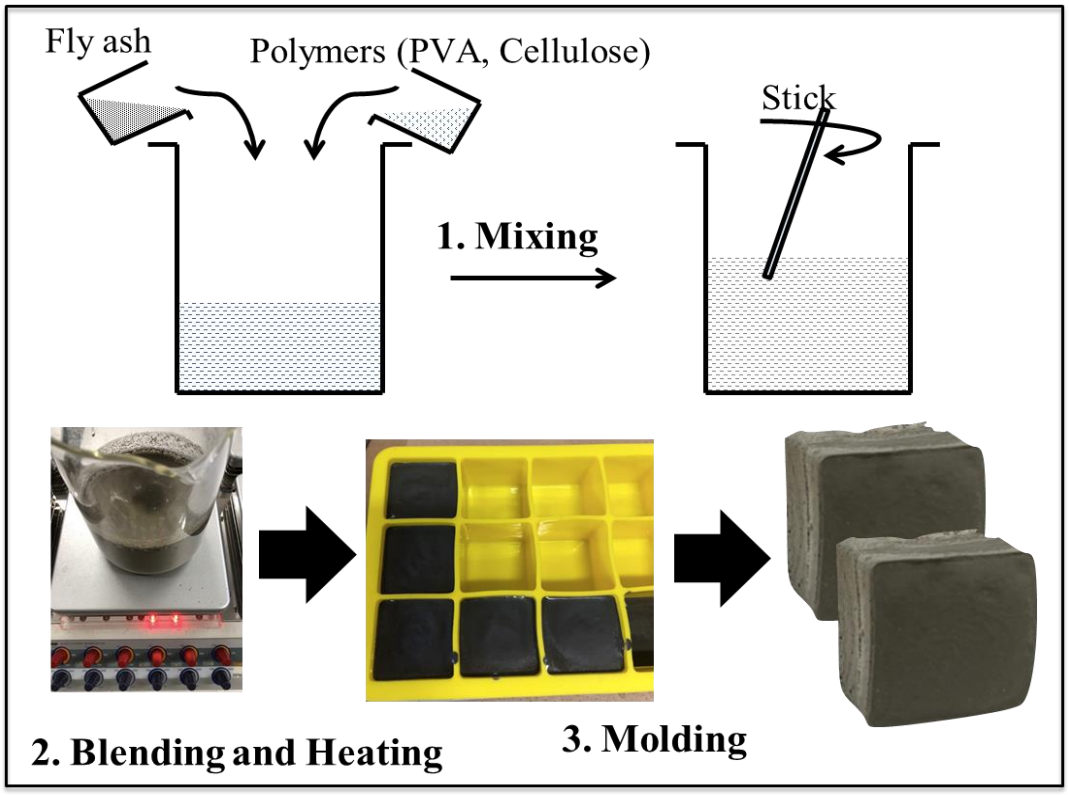

Figure 4-1 Process of the samples manufacture

4.3 Testing and analytical instruments

4.3.1 Unconfined compression test

The unconfined compression test is the most popular method of measuring shear strength, which is one of the essential mechanical characteristics. The sample is placed in an apparatus while the side stress is not applied, and the vertical stress gradually increases until the excessive deformation of the specimen occurs. The details of the equipment (see figure 4-2) and the experimental procedure are as followed:

1. The loading frame consists of two metal plates. The sample will be placed horizontally between the bottom plate and a disc shape metal probe (10cm of diameter). The top plate gradually descends; the stationary bottom plate provides the resistance. The top plate is attached to a load-measuring device and applies an axial force to the sample.

2. The measurement will be carried out at a specific deformation rate. Commonly the

vertical strain rate is 1% per minute for the height of the sample. Therefore, before the compression test, we need to measure the initial height of the sample and determine the deformation rate. During the measurement, the loading head of the top plate is descending at a specified rate so that there is a constant strain rate. The loading continues until the load values decrease or remain consistent with increasing strain, or until reaching 20% (sometimes 15%) vertical strain.

3. The load and deformation values are automatically recorded using the data logger for obtaining a complete load-deformation curve. The measured data is used to determine the strength of the specimen and the stress-strain characteristics. The stress applied to the sample is computed as follows: σ_1 =F/A, where A is the cross-sectional area of the specimen. The unconfined compressive strength (σ_c) is the maximum value of σ_1. If σ_1 continues to increase up until 20 % vertical strain and does not reach a maximum, in this case, σ_c is defined as the value of σ1 measured at 20% strain.

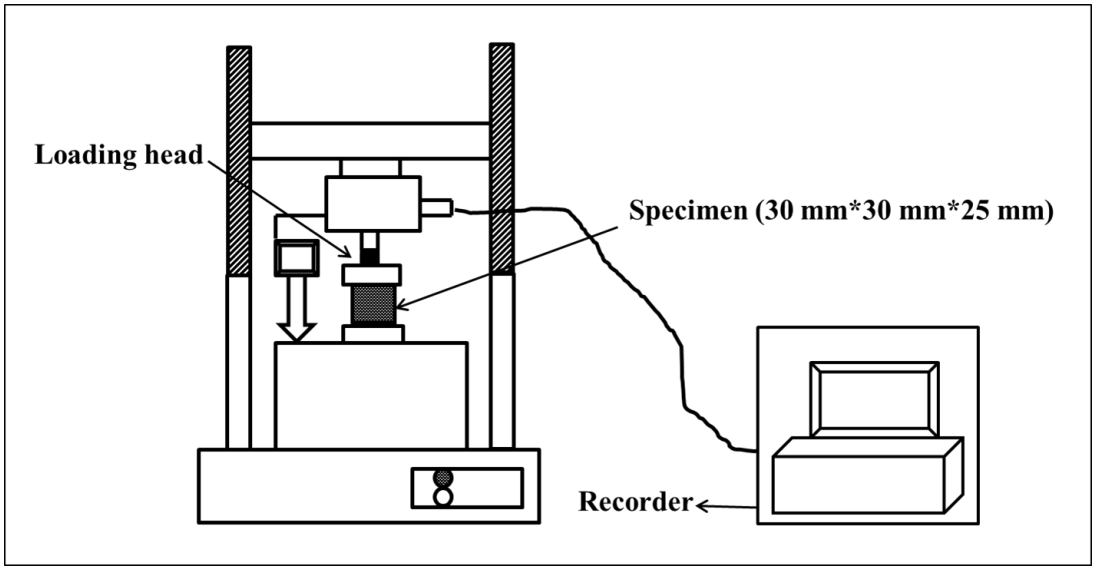

Figure 4-2 Illustration of the unconfined compression tester.

4.3.2 Mercury intrusion porosimetry testing

4.3.2.1 Porosity and pore structure

Porosity, pore size, pore shape, and specific surface area are the necessary parameters for the porous material. Porosity refers to the ratio of the volume of pores and voids to the total volume occupied by a given amount of the solid. It is one of the essential parameters due to its significant influence on the mechanical, physical, and chemical properties of the materials.

There are various categorizations of pores described in the literature, but it is difficult to give a consistent global classification of porous substances (Zdravkov et al., 2007). Pores can be classified according to their accessibility in the porous material (see Figure 4-3). For example, an open pore is a cavity or channel that communicates with the external surface. Some pores may be accessible only at one end; they are described as blind pores. Others may be open at two ends; they are called through pores. Closed pores are inside the material, and cannot connect to the surface. These open and closed pores are called intra-particular porosity of the material. Space between particles is called inter-particular porosity of the material (Westermarck, 2000). Also, there are various categories of pore sizes described in the literature (IUPAC, 1972; Kaneko, 1994; Zdravkov et al., 2007; Mays, 2007). According to the IUPAC classification, pores are classified into three categories; micropores (pore diameter smaller than 2 nm), mesopores (pore diameter 2–50 nm) and macropores (pore diameter larger than 50 nm). However, the IUPAC classification of pore size in each range is rather broad to distinguish many porous solids. Mays has proposed a new classification for further divisions of each pore size range, which is regarding the sub-divisions of the main pore size classes (Mays, 2007). The new pore size classification compared with the IUPAC scheme is showed in Figure 4-4.

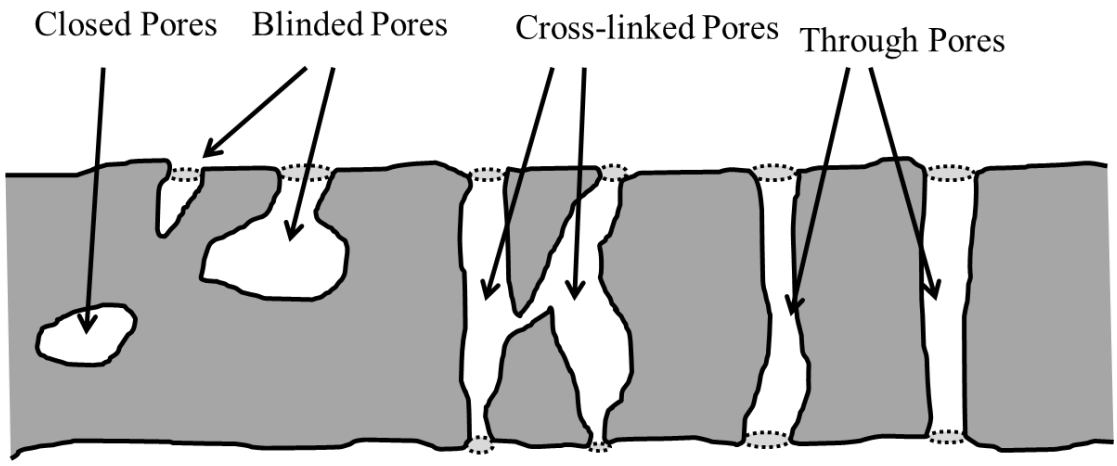

Figure 4-3 Types of the porous structure

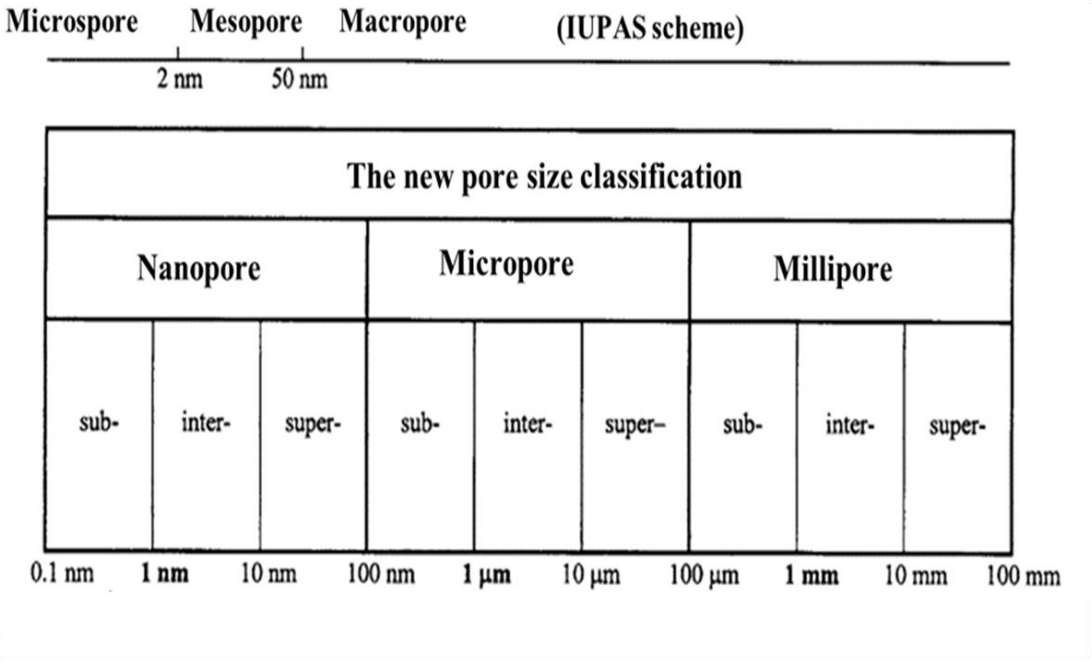

Figure 4-4 Pore size classification

4.3.2.2 Theory and key-parameter of mercury porosimetry

The determination of pore size following the technique of mercury intrusion is based on the behavior of "non-wetting" liquids in the capillary. Mercury is considered the best example of a non-wetting phase. Compared to other wetting liquid, it exhibits a high contact angle ranging between 112º and 142º. Since mercury will not spontaneously penetrate pores by capillary action, it must be forced into the pores by external pressure. The mercury porosimeter commonly consists of a low-pressure system and a high-pressure system (Figure 4-5). The low-pressure system of the porosimeter initially fills the sample container with mercury and characterizes the large pore size range of the material. The sample container is then placed in the high-pressure vessel that can increase up to approximately 60,000 psi (414 MPa). The required equilibrated pressure is inversely proportional to the size of the pore, according to the Washburn equation:

$$p \cdot r = -2 \cdot \gamma \cdot \cos\theta,$$

Where r is the radius of the pore where mercury intrudes, γ is the surface tension of mercury and θ is the contact angle of the mercury on the surface of a solid sample. Generally, used value contact angle of mercury is 140° (Leon, 1998). From the pressure versus intrusion data, the mercury intrusion porosimetry can characterize the pore structure features, particularly the size distribution of porous material. The mercury porosimeter can measure a wide range of pore sizes, from the micron scale (up to about 350 μm) to the nano-scale (below 1 μm to about 2 nm) (Anovitz and Cole, 2015). Also, it can indicate various characteristics of the pore space and reveal a variety of physical properties of the solid material. However, the mercury porosimetry also has limitations. First, it is not ideal for measuring micropores that usually smaller than 2 nm. Second, the method has the possibility that it will distort, compress, and damage the pore structure of the samples at the high intrusion pressures. Besides, it cannot measure the closed

pores that isolated from the surface of the porous material (Leon, 1998; Giesche, 2006).

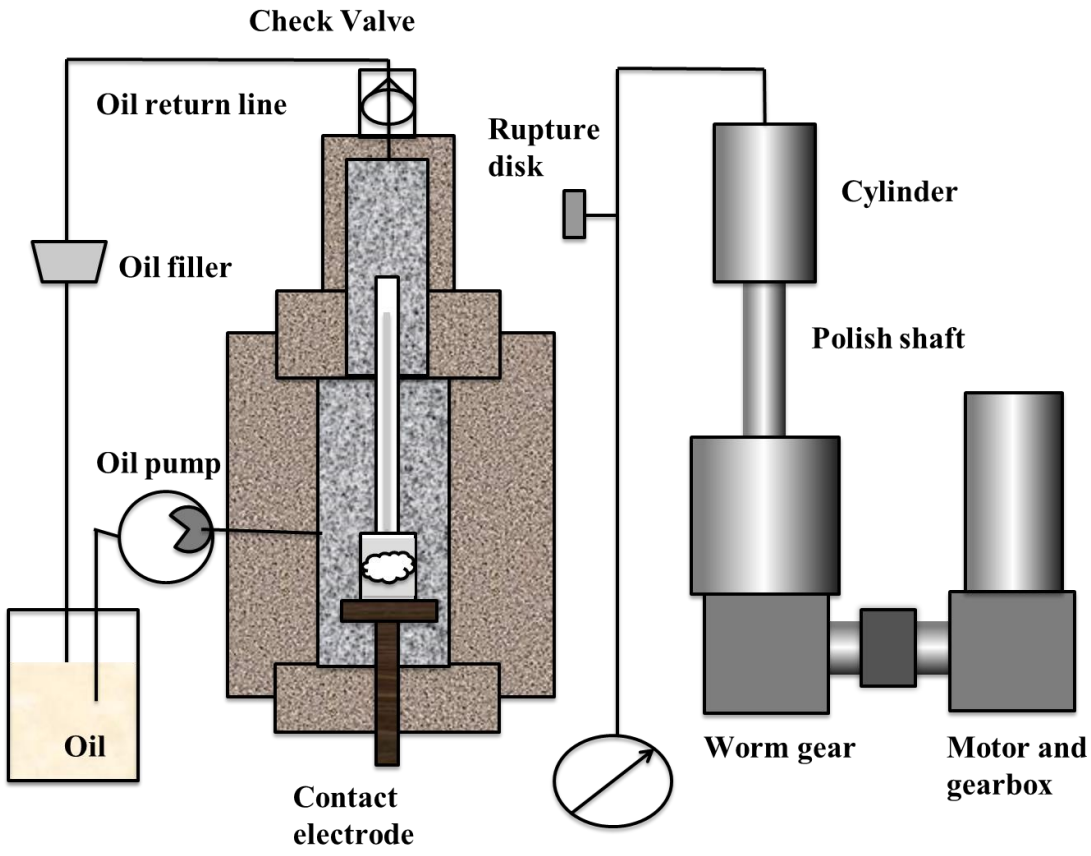

Figure 4-5 Block diagram of an FTIR spectrometer.

4.3.3 Scanning electron microscope (SEM)

A scanning electron microscope (SEM) is a method scanning a focused electron beam over a surface to create a high-resolution image. The electrons in the beam interact with the sample, producing various signals that can be used to obtain information about the surface topography and composition. Qualitative and quantitative chemical analysis information can also be achieved using an energy dispersive x-ray spectrometer with the SEM. In this study, SEM was used to examine the morphology of fly ash, polymers, and composites.

4.3.4 Fourier transform infrared (FT-IR) spectrometer

Fourier transform infrared (FT-IR) spectrometer is an instrument that can acquire broadband near-infrared (NIR) to far-infrared (FIR) spectra. Figure 4-5 is a block diagram of an FTIR spectrometer. FTIR spectrometer commonly consists of a source, interferometer, sample compartment, detector, amplifier, A/D converter, and a computer. The interferometer consists of a beam splitter, a fixed mirror, and a mirror that can precisely translate back and forth. The beam splitter is made of a unique material that transmits half of the radiation and reflects the other half. Radiation from the source strikes the beam splitter and separates into two beams. One beam is transmitted through the beam splitter to the fixed mirror and the second is reflected off the beam splitter to the moving mirror. The mirrors reflect the radiation to the beamsplitter. Again, half of this reflected radiation is transmitted, and half is reflected at the beam splitter, resulting in one beam passing to the detector and the second back to the source. Eventually, the signal is amplified and converted to a digital signal by the amplifier and analog-to-digital converter, respectively. The computer receives the signal and shows the Fourier transform. (Griffiths, 1983). Different functional groups can absorb the characteristics frequencies of IR radiations. In this study, the main goal of FT-IR analysis is to analyze the chemical functional groups in the samples.

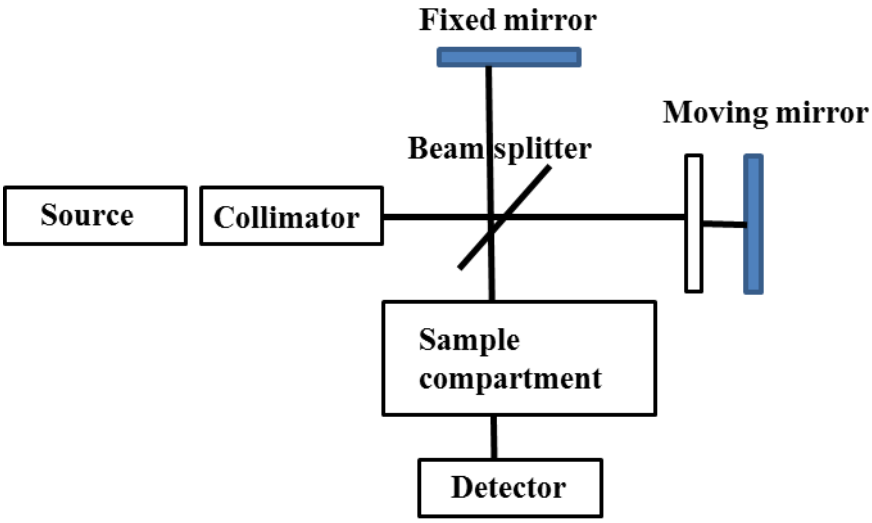

Figure 4-6 High pressure system of mercury porosimeter

4.3.5 Methylene blue absorption test

4.3.5.1 Materials and adsorbent

Methylene blue is a basic dye that easily solutes in water, ethanol, and chloroform. Its molecular weight is 373.9 g mol−1, and the formula is C16H18N3SCl·3H2O. The chemical structure of the dye is shown in figure 3-9. A stock solution of methylene blue was prepared (100mg/L) by dissolving the required amount of methylene blue in distilled water. The stock solution was diluted with distilled water to obtain the desired concentration. The concentration of methylene blue in each aqueous solution was measured using UV–vis spectrophotometer (SHIMADU2450, Japan) at its maximum wavelength of 664nm. The calibration curve of methylene blue was obtained for the determination of the dye concentration (Figure 4-7). In this study, it was aimed to remove the MB dye from aqueous solutions using the composites consisted of different proportions of polymers and fly ash.

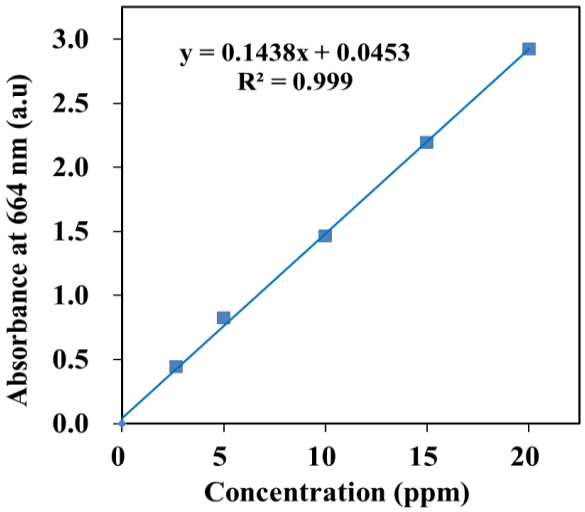

Figure 4-7 Calibration curve of methylene blue

4.3.5.2 Preparation of activated polymer-FA composites

The treated FA composite (PCFA80) consists of 80 wt % of fly ash, 10 wt % of cellulose, and 10 wt% of PVA. The prepared FA composites were transferred to beakers containing the solution of the relevant sulfuric acids and sodium hydroxide, respectively. The chemical activation of polymer-FA composites was divided into three different types of treatments: 1. Concentrated sulfuric acid treated polymer-FA composite; 2. Diluted sulfuric acid (0.25mol/L) treated polymer-FA composite; 3. Sodium hydroxide (0.5mol/L) treated polymer-FA composite. The mixtures kept in the incubator at 60°C for 4 hours and then washed several times with distilled water to remove the remaining chemical. After totally dried in an oven, they were stored in the containers for further use.

4.3.5.3 Adsorption equilibrium sand adsorption isotherm studies

Adsorption tests were performed in batch experiments to obtain the equilibrium data. For isotherm studies, a series of solutions in 30-mL plastic tubes were used. Each plastic tube was filled with 30 mL of a dye solution at varying concentrations (10 mg/L-50mg/L). The

adsorbent dosage is 2.0g/L, and the temperature condition is 25°C. A known amount of adsorbent was added to each plastic tube, and the tubes were put on the shaker vibrating for 24 hours. The solutions were then spectroscopically analyzed by UV-vis for the dye concentration remained in the solution. The adsorption equilibrium capacity is calculated as followed:

$$q_e = [(C_0-C_e)V]/m,$$

where q_e is the absorption equilibrium capacity (mg/g); C_0 and C_e are the initial and equilibrium concentrations (mg/L) of the dye in solution, respectively; V is the solution volume (L), and m is the mass (g) of the adsorbent. The results of the adsorption experiments were analyzed using the models of Langmuir and Freundlich to investigate the parameters associated with the adsorption. Langmuir isotherm is theoretically based on the assumption that the adsorbent surface is homogeneous, and each site can only adsorb one solute molecule. Only a monolayer of adsorbate is formed on the adsorbent surface, and there are no interactions among adsorbate molecules on the adsorbent surface. The adsorption is dynamic, and adsorbed molecules can transform back to liquid phased through thermal motion (Zhang et al., 2009; Khoshbouy et al., 2019; Meroufel et al., 2013).

The Langmuir isotherm equation is:

$$q_e=b*q_m*C_e/(1+b*C_e).$$

The linear form of the Langmuir's model is calculated as follows:

$$C_e/q_e= 1/(b*q_m) + C_e/q_m,$$

where C_e (mg/L) and q_e (mg/g) are the concentration of MB at equilibrium and the absorption equilibrium capacity respectively; q_m (mg/g) is maximum adsorption capacity; b is the coefficient of Langmuir isotherm. The separation factor (R_L) of the Langmuir isotherm, which is a dimensionless parameter, can be calculated as follows:

$$R_L= 1/ (1+b*C_0),$$

where C_0(mg/L)is the initial concentration of the solution. The RL value indicates the characterizations of Langmuir isotherm as follows (Khoshbouy et al. 2019;):

1) If R_L=0, the adsorption onto the adsorbent is reversible.

2) If 0<R_L<1, the adsorption onto the adsorbent is favorable.

3) If R_L=1, the adsorption onto the adsorbent is linear.

4) If R_L>1, the adsorption onto the adsorbent is unfavorable.

The Freundlich model is based on the absorption occurs on the heterogeneous surface. It assumes the enthalpy of adsorption will logarithmically decrease if the fraction of occupied sites increases. The Langmuir isotherm equation is as follows (Zhang et al., 2009; Khoshbouy et al., 2019; Meroufel et al., 2013).:

$$q_e=(1/n) *(k_f*C_e)$$

The linear form of the Freundlich model is calculated as follows:

$$\ln q_e= \ln k_f + (1/n)*\ln C_e,$$

where C_e (mg/L) and q_e (mg/g) are the concentration at equilibrium and the absorption equilibrium capacity respectively; k_f (mg/L) and n are the Freundlich adsorption constants. In the linear form, the slope and the intercept correspond to (1/n) and k_f, respectively. The favorable adsorption of this model can be characterized by the Freundlich adsorption constants. If the value of n is >1, it indicates that the adsorption process is favorable.

4.3.6 X-ray photoelectron spectroscopy.

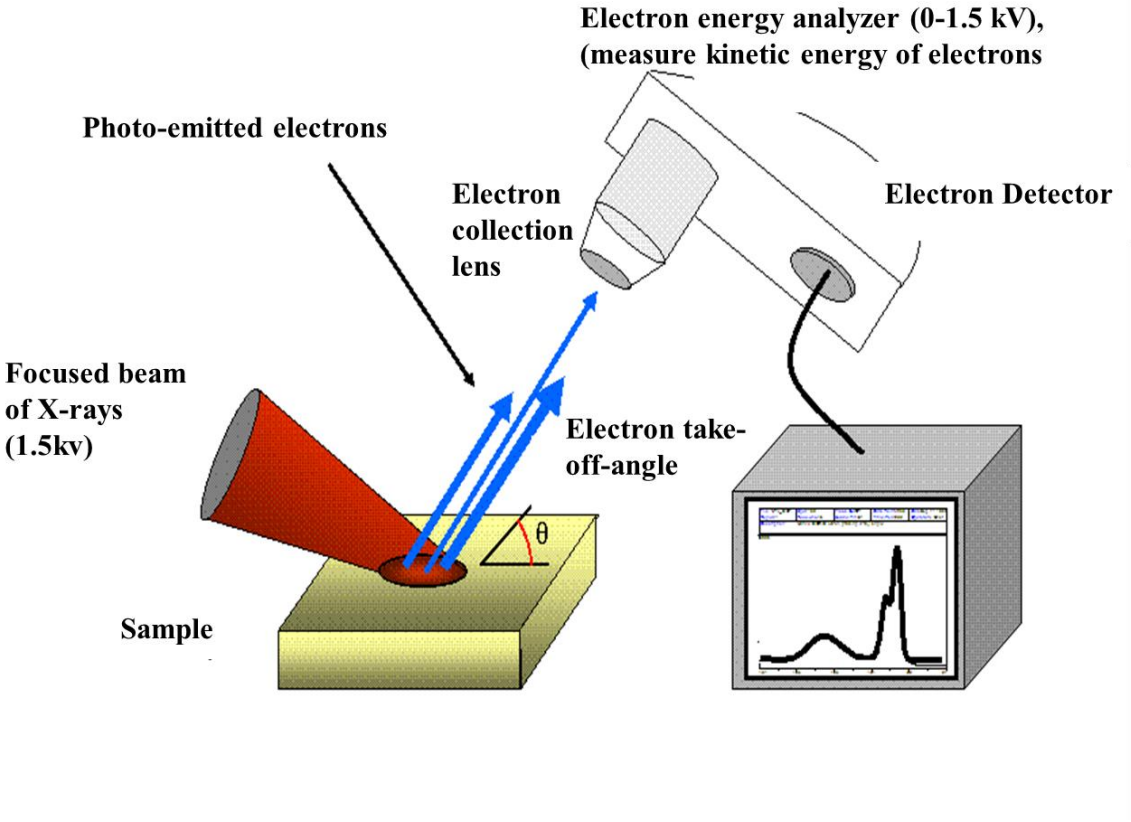

Figure 4-8 The principle illustration of XPS

X-ray photoelectron spectroscopy (XPS) is a quantitative and surface chemical analysis technique. The principle of XPS is shown in Figure 4-8, in which the XPS instruments consist of an X-ray source, energy analyzer for the photoelectrons, and electron detector. The process of XPS is irradiating a sample with monochromatic X-rays, while measuring the kinetic energy (KE) and number of electrons that escape from the top of the analyzed material. The balance between hν and KE is expressed as:

$$h\nu=KE+BE+\phi$$

where EB is a binding energy of electron to nucleus relative to the Fermi level and ϕ is a work function of specimen (Konno, 2016). The energies from emission of photoelectrons are characteristic of the elements, thus the value of BE and chemical shift are utilized for the identification of element and chemical bonding. In this study, XPS experiment was conducted to investigate the surface chemistry of the poly-FA composites.

4.4 Results and discussions

4.4.1 Mechanical properties of polymer-FA composites

The effect of modification of FA in terms of the mechanical behavior was investigated. The results were compared to the PVA-FA composites with the different weight ratios of PVA, and drying temperature of the sample manufacture process (Figure 4-9). In general, the PVA-FA composites the compression strength decreased as the percentage of FA in the composites increased, and increased as the weight ratio of PVA increased (Figure 4-11). Drying temperature during fabrication process is also significant impact factor to the mechanical properties of FA composites. The compression strength of the FA composites dried at 40 °C is relatively much higher than those FA composites dried at 80 °C. For example, in the case of FA composite with 60 wt% FA, and 40 wt% PVA, the compression strength is about 8Mpa, while the compression strength of the FA composite with the same mixing ratio, dried at 80 °C is only 3.4 MPa.

According to the formulation of the strength–porosity dependenc (Kai, 2008): $\sigma = \sigma_0 \exp(-bp)$, where σ_0 is the strength of a nonporous structure, σ is the strength of the porous structure at a porosity p, and b is an empirical constant. The strength of porous material shows an exponential increase with a decrease of the porosity. As compared the relation between porosity and strength, the results do match up to the strength–porosity formulation (Figure 4-12).

These results showed that PVA modification can increase the mechanical strength of the FA composites. The increased weight ratio of PVA enhanced the chemical bonds among FA particles and the polymer matrix, which also cause the decrease in porosity. On the other hand, high temperature can activate chemical reaction and effective water evaporation, which could increase the interstitial voids and cracks of the composites, thus significantly decreased the compression strength.

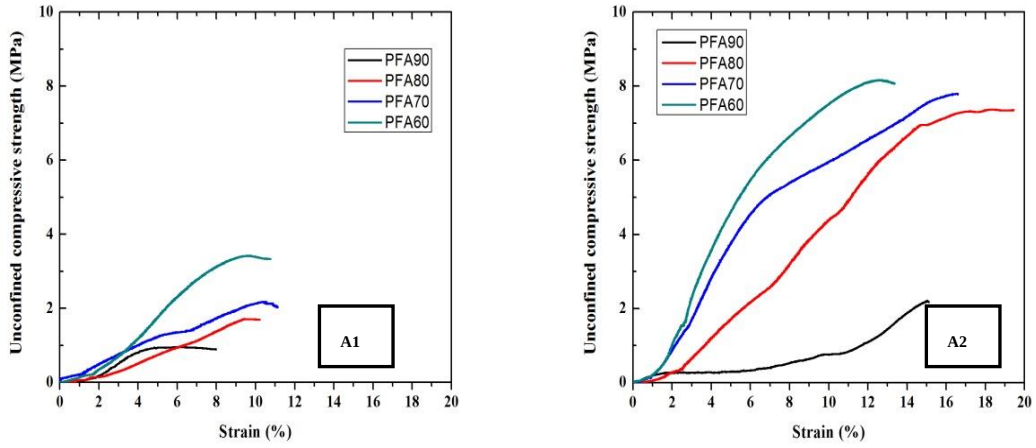

Figure 4-9 Compression strength of the FA composites with different mixing ratios and dried at 80 (A1) and 80 (A2) °C

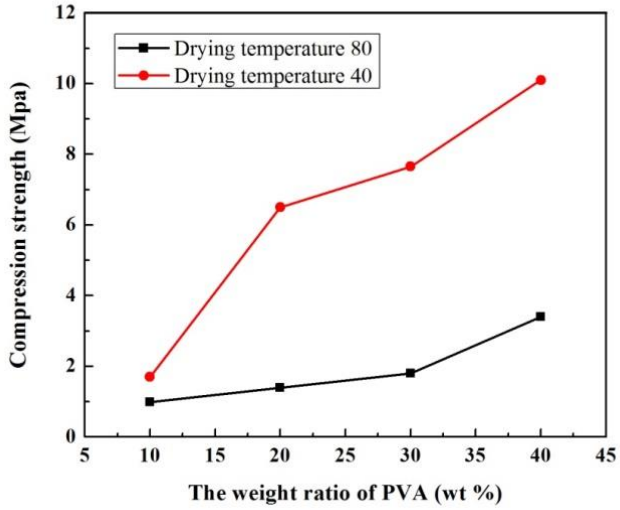

Figure 4-10 Compression strength of the FA composites with different mixing ratios and dried at 80 °C and 40°C

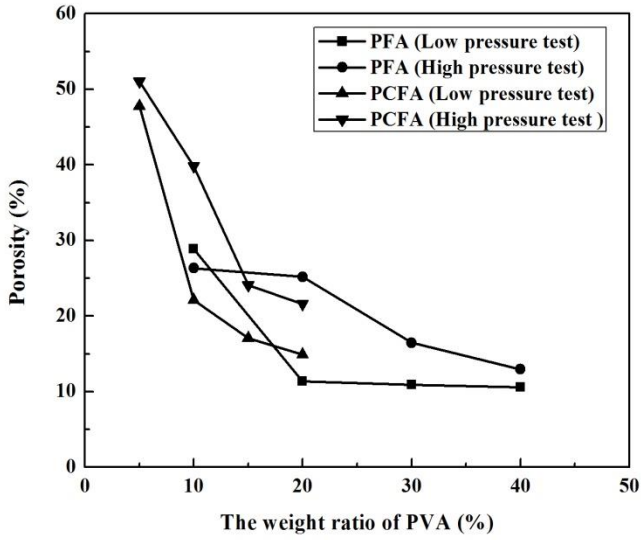

Figure 4-11 The porosity of the FA composites with different mixing ratios and dried at 80 °C

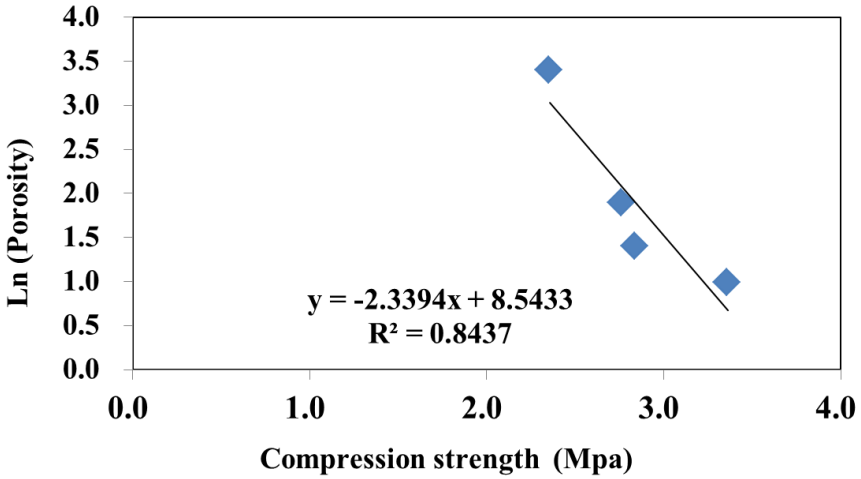

Figure 4-12 Correlation of compression strength with the porosity of the FA composites dried at 80 °C

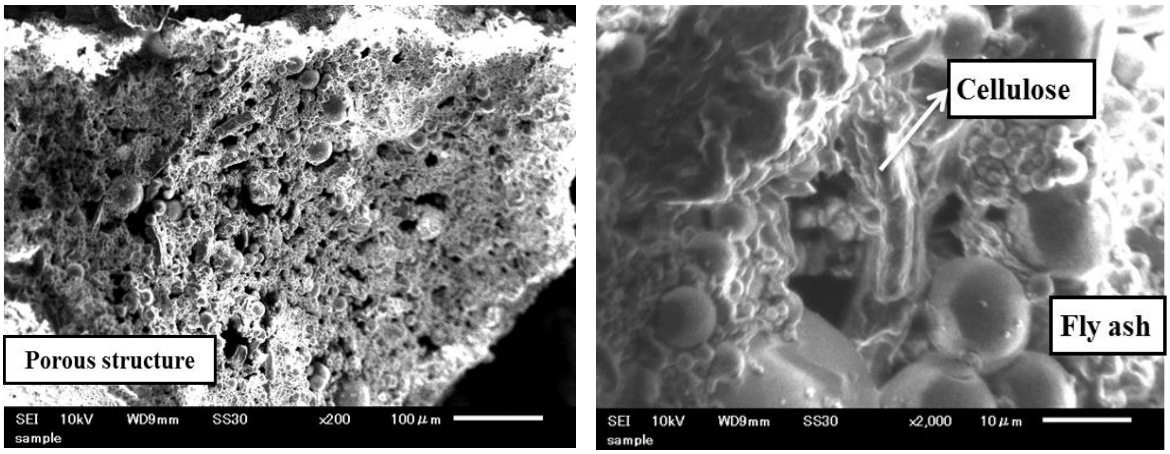

Figure 4-13. SEM image morphology of the porous structure of cellulose-PVA modified FA composites.

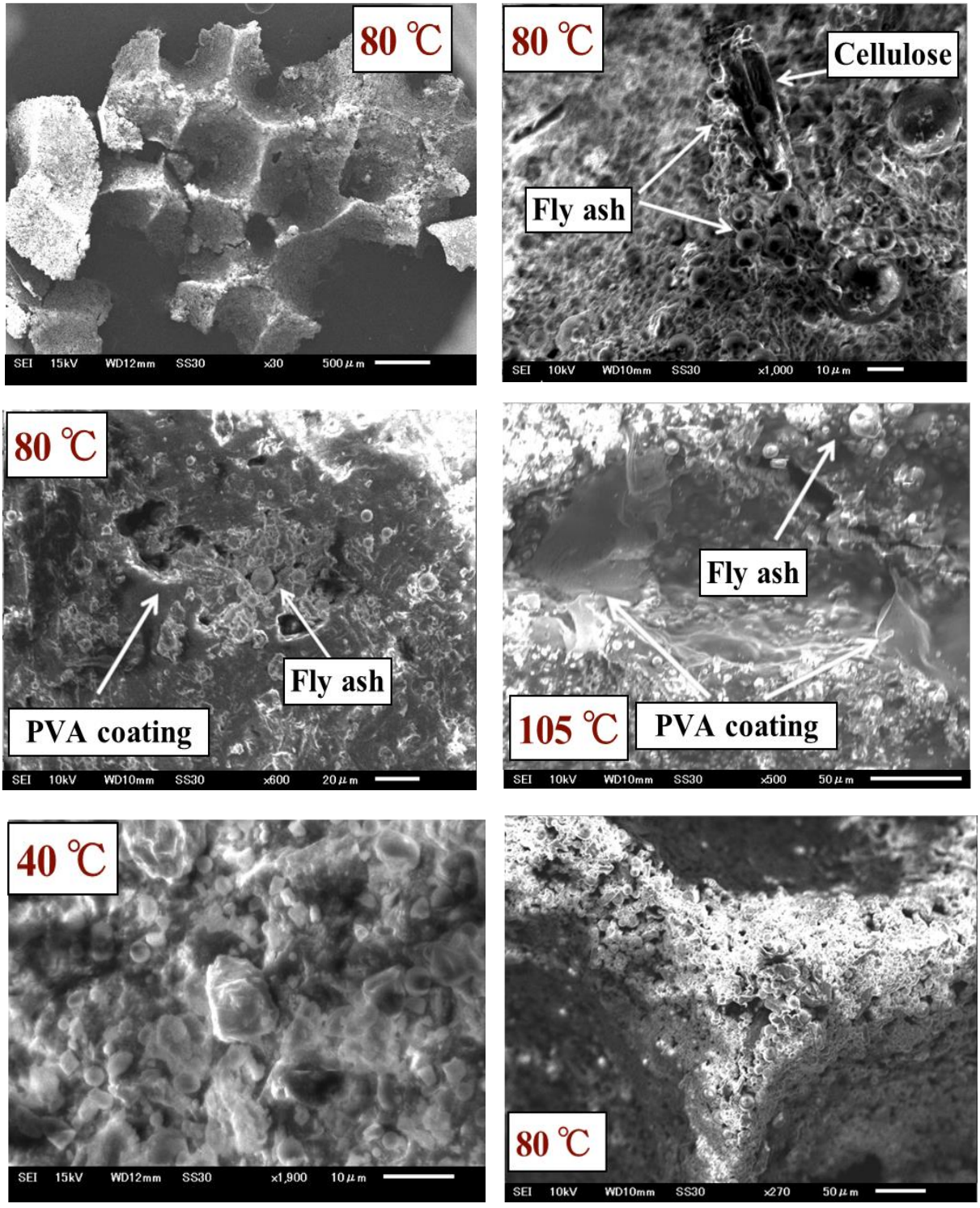

Figure 4-14. SEM image morphology of cellulose-PVA modified FA composites dried at 40°C , 80 °C and 105 °C

4.4.2 Morphology of FA composites observed by SEM

The representative SEM images of cellulose-PVA modified FA composites dried at 40°C, 80 °C and 105 °C are displayed in Figure 4-14. According to the SEM observation, three-dimensional structure of hexagon, which is a structure in stable state as crystalline with lower energy, was found in the specimen. Cellulose combined FA-aggregates are formed, in which PVA chains facilitated the intimated contact. In the aggregate, cellulose was served as anchor, and PVA was served as adhesive, thus this structure could be reinforced with FA particles stick to the cellulose matrix.

In general, most of the unmodified FA particles look like scattered spherical, or some are non-spherical shape. In comparison, the polymer modified FA becomes multiple stacked layers with mostly irregular shape, such as the FA particles were dried at 40 °C during the fabrication process (Figure 4-14). The PVA may coat on the surface of FA particles and give contribution to the superior light reflecting quality of the particles in the SEM. The thin layers may reduce the attraction forces of particle-particle and help to disperse in matrix media. At 80 °C, the entire micrograph shows efficient packing of FA particles by PVA in the composites with a few interstitial voids. In general, at low temperature during the fabrication process, FA particles were finely dispersed and thoroughly encompassed by PVA coating. However, at higher temperature condition (such as at 105°), PVA coating was over extended and FA particles were randomly and largely dispersed in the in the matrix, thus the inter-connectivity of the composites was reduced, and possibility of crack extension was increased.

4.4.3 Pore size distribution of the polymer-treated FA composites

The effect of cellulose-PVA modification of FA on mechanical properties was investigated. The results were compared to the PVA-FA composites with/without cellulose modification in Figure 4-15. When the weight ratio of FA is the same, PVA-FA composites modified with cellulose showed relatively higher porosity than those without cellulose modification. In particular, cellulose addition increased the pore volume of inter-microspores that at the range from 1-10μm. The PVA addition made a complex effect on the particle size distribution, which made the particle size distribution curve extremely asymmetric. For example, as showed in Figure 4-16, when the proportion of PVA in the FA composites was increased to 40 wt%, the particle size distribution trended to increase at the size range that larger than 10μm. In general, the center pore diameter of the particle size distribution is trending from below 10μm to 100 μm. However, compared with the cellulose-modified PVA-FA composites, the center pore diameter of the particle size distribution remained almost the same. This result suggested that the cellulose could control the particle size distribution of the FA composites, and tend to adjust the particle size distribution in a suitable capillary size range.

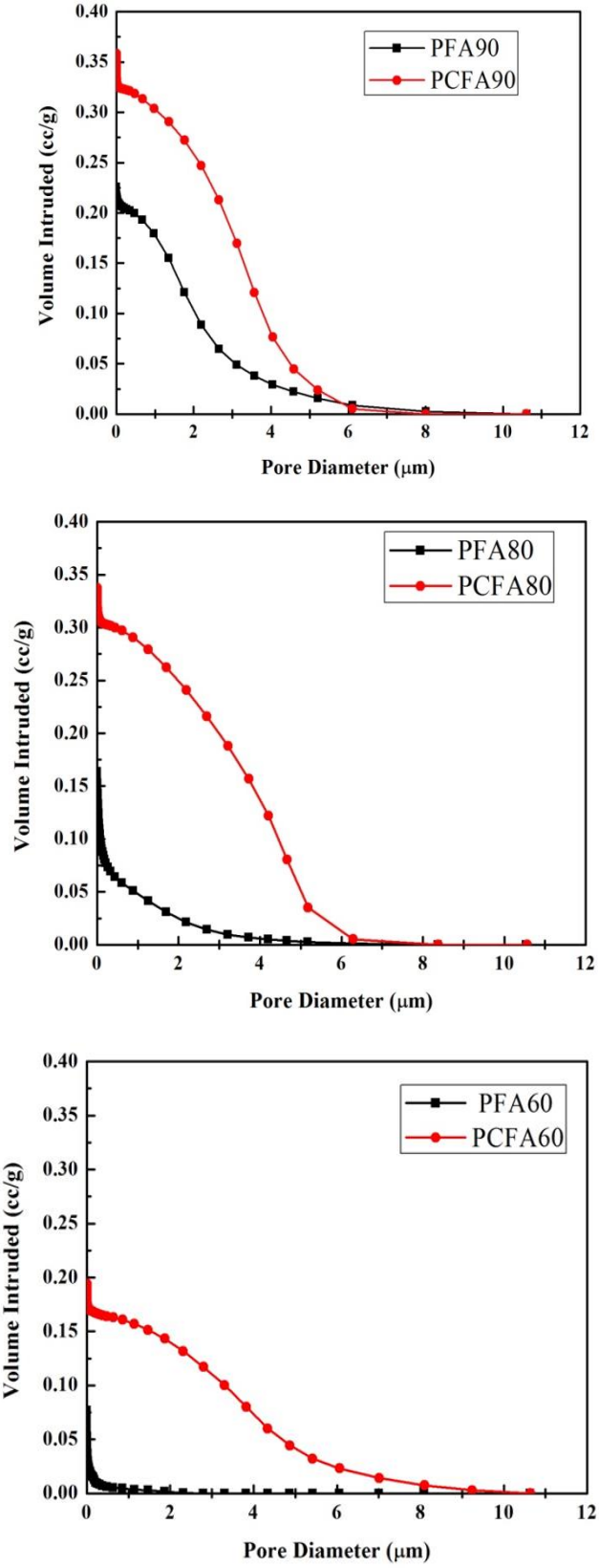

Figure 4-15. Pore volume of polymer-modified FA composites with the different mixing ratios

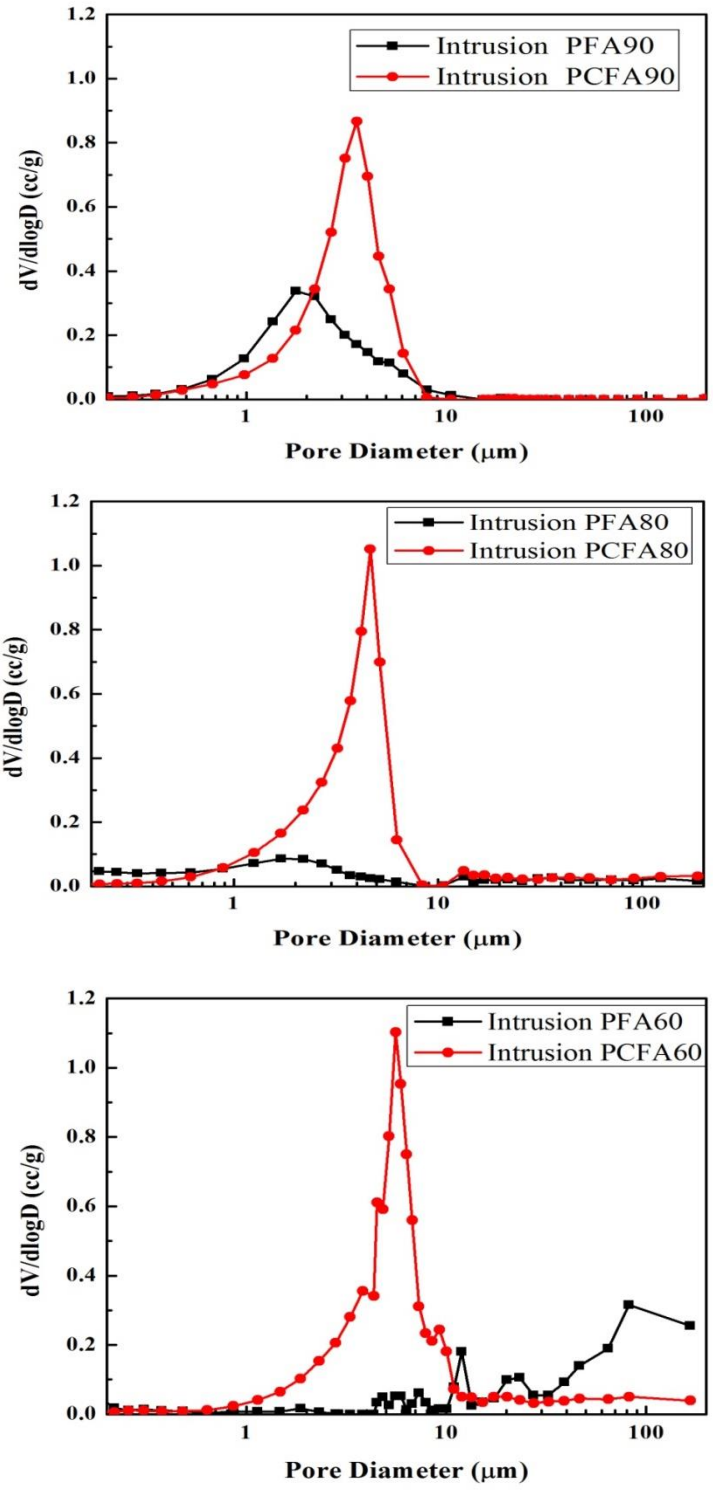

Figure 4-15. Pore size distribution of polymer-modified FA composites with the different mixing ratios

4.4.4 FTIR analysis of the chemical functional group of the FA- composites

According to FTIR spectra, the stretching vibrations of Si-O-Al bonds mainly appeared in the ranges of 1200-600 cm^{-1}. Hydrogen bonding between the Al-O/Si-O with long-chain chemical functional groups may exist in the PVA-cellulose-modified FA. In fly ash particles and polymer-modified FA composites, broad absorption bands are centered at 3400 cm^{-1}, which reflect the combination of –OH groups. In the polymer-modified FA composites, the well-known set of absorption bands at around 3340 cm^{-1} of –OH stretching, 2948/2902 cm^{-1} of C-H stretching, about 1093 cm^{-1} of C-OH stretching, which indicate the existence of possible intermolecular or intramolecular hydrogen bonding between FA and polymer chains. Chemical bridges on the surface of FA particles may improve the mechanical properties of the polymer modified-fly ash composites (Dilip, 2009). The chemical function groups such as O-H could increase the water retention ability of the material. In comparison the spectra of PVA and cellulose are in Figure 4-16 .According to the FTIR, there is a plausible bonding of PVA and fly ash which showed in Figure 4-18.

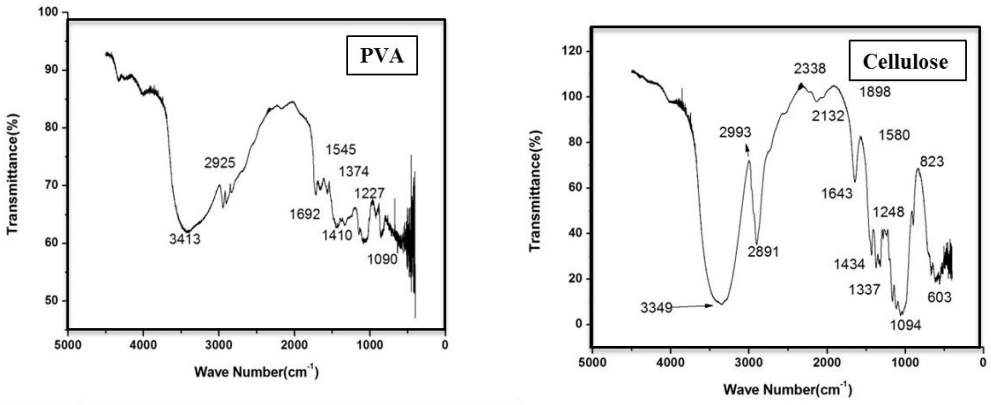

Figure 4-16 FTIR spectra of PVA and cellulose.

Table 4-2. The selected FTIR absorption peaks in PVA, cellulose

Peak position of structural groups in (cm^{-1})							
	OH str	C-H str	C=O str	O-H bend	C-H bend	C-O-C str	C-OH str
PVA	3413	2925/2875	1692	1410	1374	1227	1090
Cellulose	3349	2993/2891	1643	1434	1337	1248	1094

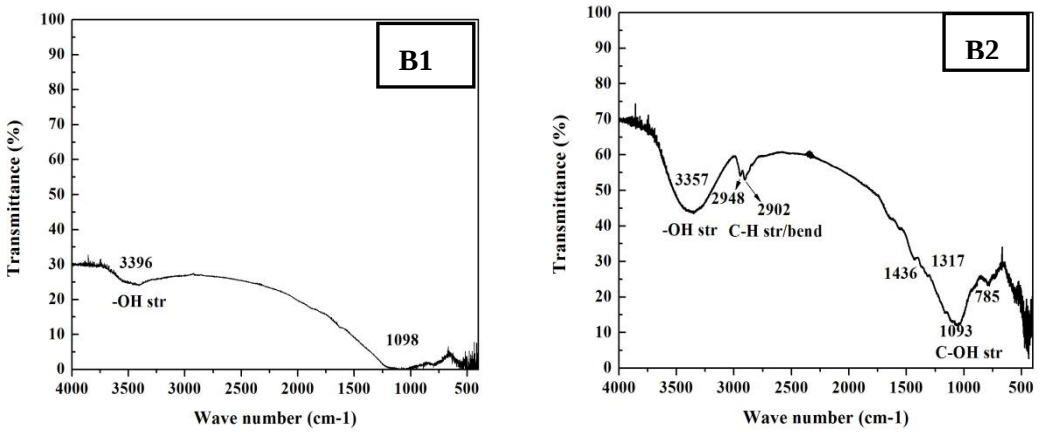

Figure 4-17. FTIR spectra of unmodified-FA [B1] and PVA-cellulose-FA composite [B2].

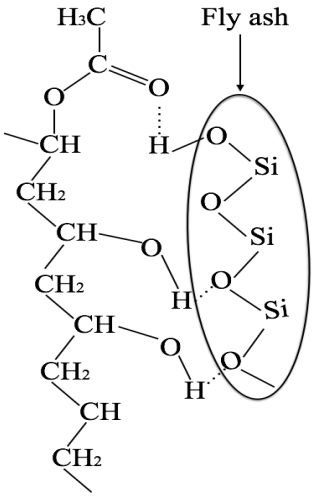

Figure 4-18. A plausible diagram of hydrogen bonding between PVA and FA

4.4.5 The water retention capacity of the polymer-fly ash composites measured as EMC

4.4.5.1The comparison of the EMC of polymer treated FA composites with pure soil/sand.

The EMC values of PVA-FA composites and PVA-cellulose FA composites were measured though the drying experiment for 12 hours. The EMC curves are shown in Figure 4-19, which are compared with the EMC value of the pure silica sand. In the first 2 hours, the EMC curves of polymer-FA composites and silica sand were almost the same. However, after about 3 hours, the water in the polymer treated FA composites evaporated slower than the pure silica sand. Water evaporation of the polymer treated FA composites is faster at the first drying stage, mainly because of the free water evaporation at the initial time period. The water evaporation rate of the polymer-treated FA composites was slower at the middle stage. Also, in the final stage, the residual water of polymer treated FA composites was more significant than the pure silica sand. This result showed that the evaporation of the water inside the polymer-FA composites was greatly inhibited. The EMC values were calculated according to the EMC curves. The result showed that the EMCs of polymer-FA composites were significantly increased.

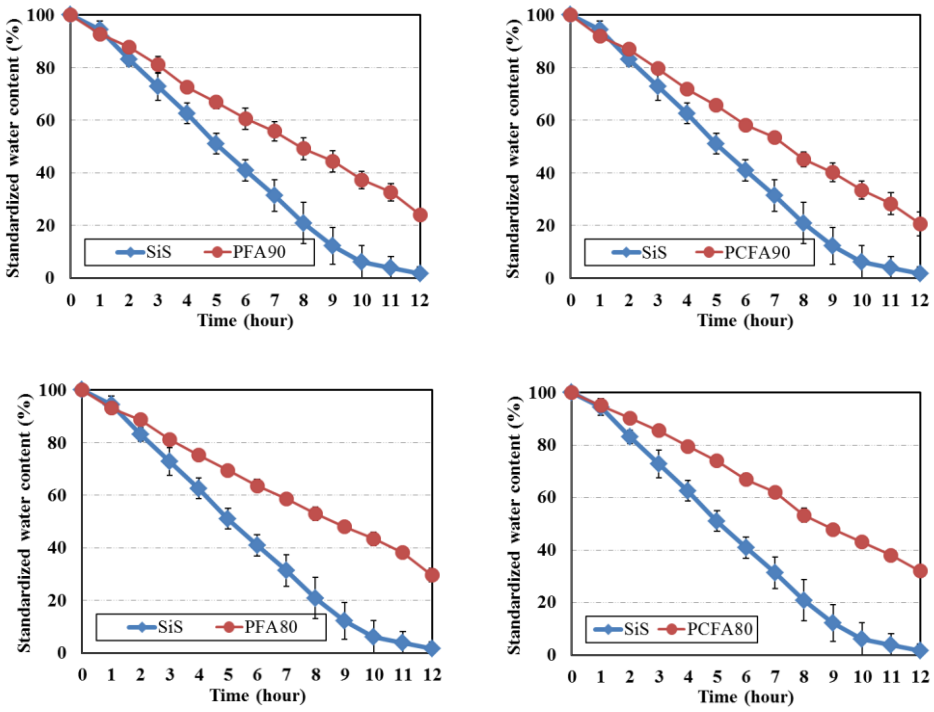

Figure 4-19. The EMC curves of polymer treated FA composites compared with silica sand.

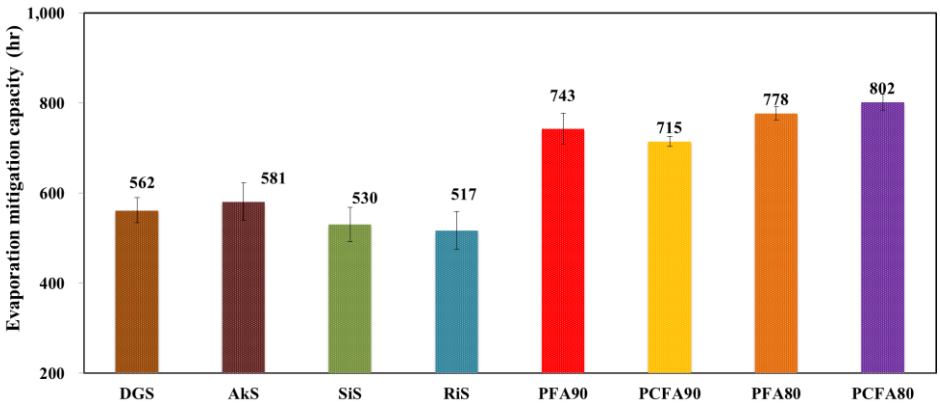

Figure 4-20. The EMC value of polymer treated FA composites compared with the pure soil/sand

4.4.5.2 The hydrophilic capillary zone theory

The effect of the polymer-FA composites on the EMC could be explained as “the hydrophilic capillary zone theory,” as showed in Figure 4-21. In soil and sand systems, water exists as gravitational water and capillary water. When the temperature increased, free water evaporates first, and becomes steam and diffuses. Capillary water evaporation is relatively slow. The capillary water evaporation can be influenced by physical and chemical properties like pore size distribution and hydraulic properties. Therefore, the EMC value of PCFA80 is highest, because it contained a relatively high weight ratio hydrophilic polymer and suitable pore size range. The modification of PVA and cellulose can improve hydrophilicity. Especially the number of chemical functional groups such as -OH was increased. As illustrated in Chapter 3, the hydrophilic groups are significant to increase the EMC, through forming hydrogen bonding and hydration water-shell around the material. PCFA80 also contained high pore volume, and the pore size range is in the range of capillary size, which is suitable for water retention. In addition, in the case of the PCFA90 compared with PFA 90, though PCFA90 contained a suitable pore size range and has high porosity, it has a little hydrophilic functional group inside the pore structure. Because of lacking hydrophilic chemical groups, the material surface of the capillary zone cannot seize the water molecule for long time under the high temperature condition. Thus, the EMC value of PCFA90 is lower than the PFA90. Therefore, the improvement of the hydrophilic groups is applicable to increase the water retention ability of the water retention material. Although porous structure at a suitable capillary pore size range is assumed to increase the EMC largely, the results of the drying experiment on the EMC values showed that the capillary size -pore structure didn’t make a significant difference on the EMC values. Pore size ranges smaller 1μm, or larger than 10μm, might have a non-negligible impact on the EMC.

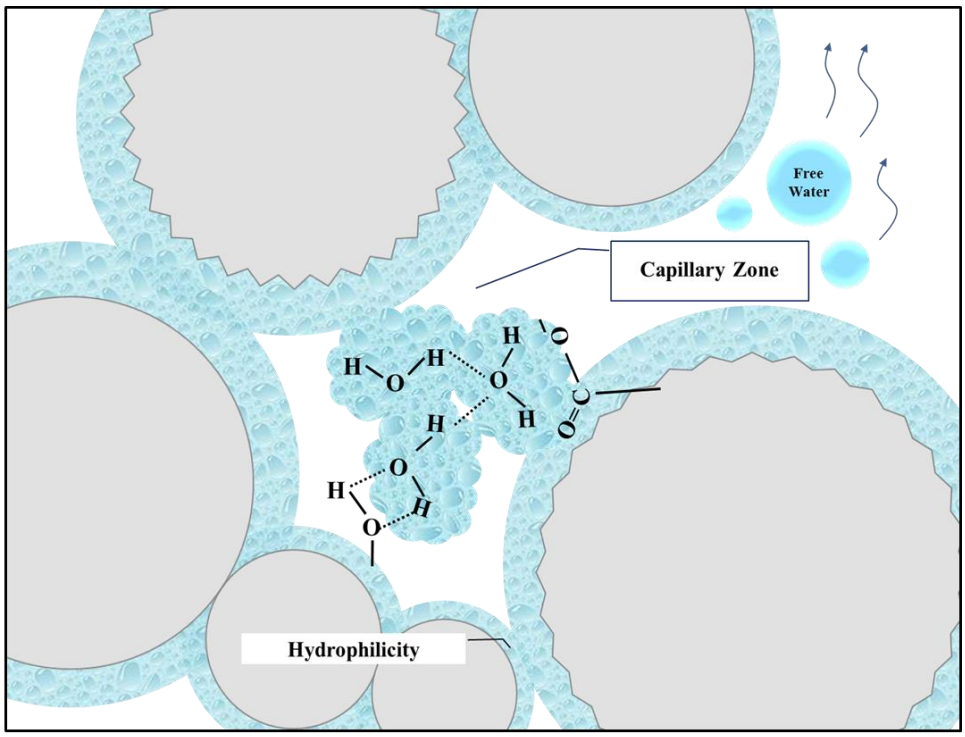

Figure 4-21. The hydrophilic capillary zone theory

4.4.6 The result of methylene blue absorption test

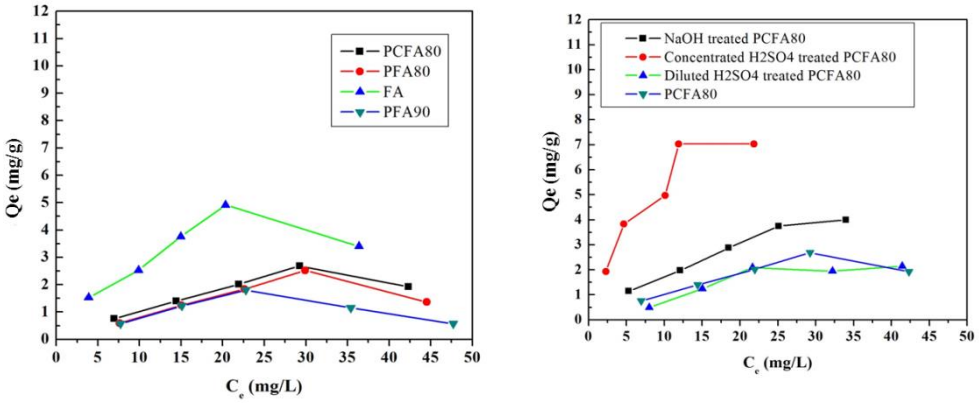

Figure 4-22 Comparison of Qe and Ce on the MB solution absorption by in different treatments of FA composites at room temperature.

Figure 4-22 showed the comparison of the absorption ability of the polymer treated FA and the raw fly ash. The results showed that the adsorption ability of polymer-FA was decreased; this could be explained from the physical factor that the surface area of the polymer-FA-composites was decreased. And also, according to the FTIR, the chemical functional groups on the FA are limited. Furthermore, in order to study the impact of the chemical functional groups, the polymer-FA composites were activated by different types of treatments. Adsorption isotherms studies were conducted to examine the distribution of MB molecules in solid/liquid interface. Figure 4-23 showed the results of fitting the linear Langmuir and Freundlich isotherm equations into the MB adsorption equilibrium data. Compared with the Longmuir model, the Freundlich isotherm model indicates better fitting results for the adsorption process of MB onto the NaOH treated polymer-FA composites, which suggested that the MB molecules adsorbed on the adsorbent surface is non-monolayer. Based on the Longmuir isotherm model, the maximum MB adsorption capacity values of high concentrated H_2SO_4 is 20.4mg/g, which is much higher than the other treatments. According to the FTIR, broad band between 3600 and 3200cm−1 was attributed to -OH. The band around 2974, was mostly recognized as stretching vibration of aliphatic carbon–(CH)n structure. At around 1645cm−1 which implies the stretching vibration of –C=O in the carboxylic. At 1421cm−1, which was represented the C=C stretching. At 1055cm−1, it might be corresponded to the C–O–R. This peak could also be ascribed to the –Si-O stretching. In particular, at around 563 cm-1, it is the C=O wag. The result of the XPS showed that the high concentrated H_2SO4 FA composites have a relatively higher element weight ratio of oxygen. Compared with the FRIR result, it can be concluded that the C=O is significant chemical group for the MB absorption.

The MB test suggested the single polymer treatment on the FA would not make sufficient chemical functional groups on the FA particle, and it might decrease the surface area

as the polymer-Fa composites. Therefore, to improve the polymer-FA as the absorbent material, further chemical activation such as the addition of the C=O functional group is necessary for increasing the absorption ability.

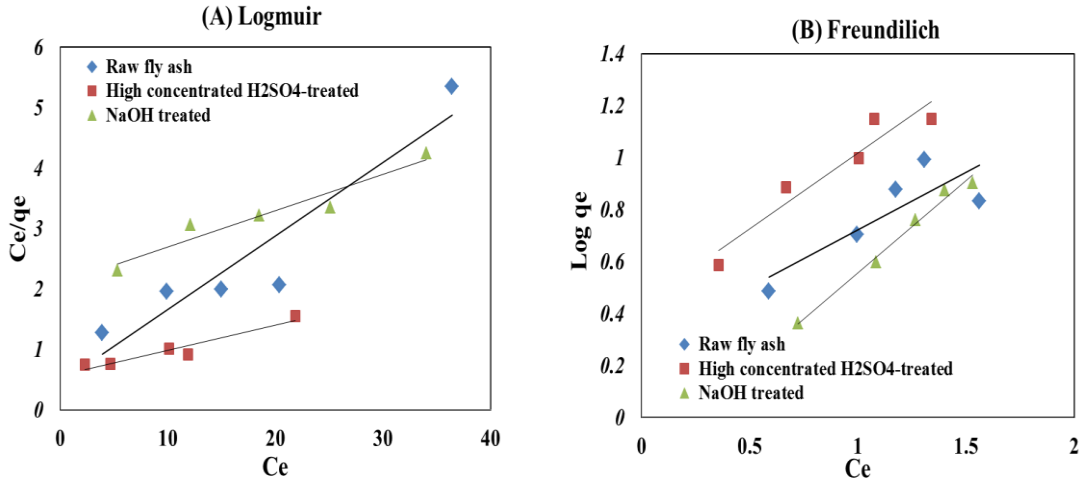

Figure 4- 23 The Langmuir and Freundlich isotherm equations on the MB adsorption equilibrium data.

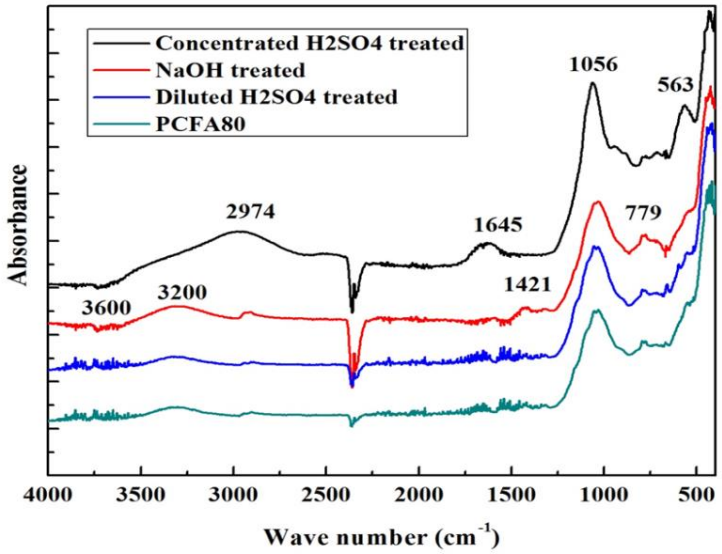

Figure 4-24 The FTIR of the chemical activated polymer-FA

Table 4-1 Element weight ratios of treated FA tested by FIIR.

	C1s	O1s	Al2p	Si2p	Fe2p3
Concentrated H2SO4 Treated FA	28.7	56.5	4.6	8.3	1.9
NaOH (0.5mol/L) Treated FA	39.5	45.5	4.2	8.8	1.9
H2SO4(0.25mol/L) Treated FA	39.0	44.6	2.2	12.2	2.1

Reference

1. Acharya, S. K., Mishra, S. C. (2007). Weathering behavior of fly-ash jute polymer composite. *Journal of Reinforced Plastics and Composites*. 26(12), 1201-1210.
2. Anovitz, M Lawrence., Cole R David. (2015). Characterization and Analysis of Porosity and Pore Structures. *Mineralogy and Geochemistry.* 80 (1), 61-164.
3. Dilip Nath et al. (2009) LAP LAMBERT Academic Publishing GmbH & Co.KG
4. Giesche, Herbert. (2006). Mercury porosimetry: a general (practical) overview. *Part. Part. Syst. Charact.* 23, 1-11
5. Griffiths PR. (1983). Fourier transform infrared spectrometry. *Science*. 222(4621):297-302.
6. International Union of Pure and Applied Chemistry (IUPAC). (1972). Manual of symbols and terminology for physicochemical quantities and units, Butterworths, London
7. Kai Hui Zuo et al. (2008). Applied Ceramic Technology, 5(2),198-203.
8. Kaneko, K. (1994). Determination of pore size and pore size distribution: 1. Adsorbents and catalysts. *J. Membrane Sci*. 96, 59–89.
9. Khoshbouy, Reza., et al. (2019). Preparation of high surface area sludge-based activated hydrochar viahydrothermal carbonization and application in the removal of basic dye. *Environmental Research.* 175, 457–467
10. Konno, Hidetaka, (2016). X-ray photoelectron spectroscopy. *Materials Science and Engineering of Carbon : Characterization.* 153 -171
11. Kumar, B., Garg, R., Singh, U. (2012). Utilization of fly ash as filler in Hdpe/fly ash polymer composites: A review. *International Journal of Applied Engineering Research.* 7, 1679-1682.
12. Leon, Y. Leon. A. Carlos. (1998). New perspectives in mercury porosimetry. *Advances in Colloid and Interface Science*. 76-77, 341-372

13. Mays, T.J. (2007). A new classification of pore sizes. *Studies in Surface Science and Catalysis*. 160, 57-62

14. Meroufel, B., et al. (2013). Adsorptive removal of anionic dye from aqueous solutions by Algerian kaolin: Characteristics, isotherm, kinetic and thermodynamic studies. *J. Mater. Environ. Sci*. 4 (3), 482-491

15. Sahai, RSN., Pawar, Neha. (2014). Studies on mechanical properties of fly ash filled PPO composite with coupling agent. *International Journal of Chemical, Environmental & Biological Sciences (IJCEBS)*. 2 (4), 187-192.

16. Satapathy, Sukanya., Nando, B.G et al. (2013). HDPE-fly ash/Nano fly ash composites. *J. Appl. Polym.* 130 (6), 4558-4567.

17. Sheriff, Z., Ilavarasi, M., Niranjana, K. (2017). Analysis and fabrication of polymer reinforced fly-ash composites engine. *First International Conference on Recent Advances in Aerospace Engineering (ICRAAE), Coimbatore*. Page 1-6.

18. Singla, Manoj., Chawla, Vikas. (2010). Mechanical properties of epoxy resin-fly ash composite. *Journal of Minerals & Materials Characterization & Engineering.* 9(3), 199-210.

19. Westermarck, Sari. (2000). Use of mercury porosimetry and nitrogen adsorption in characterisation of the pore structure of mannitol and microcrystalline cellulose powders, granules and tablets. *Academic Dissertation, Pharmaceutical Technology Division, Department of Pharmacy, University of Helsinki, Finland. ISBN 952-91-2536-4 (html)*

20. Zhang, Zhengyong., et al. (2009). Adsorption isotherms and kinetics of methylene blue on a low-cost adsorbent recovered from a spent catalyst of vinyl acetate synthesis. *Applied Surface Science.* 256 (8), 2569-2576.

21. Zdravkov, Borislav D, et al. (2007). Pore classification in the characterization of porous

materials: A perspective. *Central European Journal of Chemistry*. 5(2) 2007 385–395

Chapter 5 Conclusions

In Chapter 1, the background of this study is introduced. The purpose of this thesis is to find the appropriate utilization of raw FA. Global FA generation is estimated to be 800 million Mg/yr worldwide, and desertification all over the world has become more and more severe and threating agricultural productions nowadays in the arid and semi-arid area. If FA can be used as water retention material to ameliorate soil is attractive in the arid area, it would benefit the environment and economy. Besides, functional polymers are promising candidates in the fabrication of FA based composites because of their high chemical stability, good compressive strength, and high durability. If FA can be recycled as water retention and absorbent materials, it would not only solve the FA management problem and desertification problem at the same time but also provide potential applications of FA in the agriculture and industry field.

In Chapter 2, the difference between water holding capacity (WHC) and evaporation mitigation (EMC) are discussed. Water holding capacity (WHC) of soil shows the amount of water that remains at a certain gravity and pressure; however, in the arid area, water loss via evaporation is more realistic than pressure-driven water loss. In this research, evaporation mitigation (EMC) was identified to specify water evaporation resistance ability. The drying experiment was conducted to measure the EMC of soil/sand and FA mixed samples. The effect of the raw FA amendment on soil/sand moisture was investigated, focusing on soil/sand sieving size. Although the raw FA amendment increased WHC of soil/sand slightly, it is much lower than the sieving size effect. FA amendment also gave limited impacts on EMC. On the other hand, the EMC of tested soil/sand clearly showed sieving size dependency regardless of the FA

mixing ratio. The effects of the FA amendment on EMC are also much smaller than the sieving size effect. The sieving size effects on EMC are very complicated with depending on soil/sand type and drying temperature. This study found that the sieving size dependency of EMC could be explained partially by organic matter content in each soil/sand sieving size fraction. Correlations between organic matter contents and EMC are contrasted with depending on drying temperature. Temperature-dependent hydraulic properties of organic matter components in soil/sand might explain the temperature dependency. According to the results, it is concluded that organic matters play an important part in EMC, although physical sieving size is important for WHC. If FA is used in the arid/semi-arid areas to increase the EMC of sandy soil, proper modification of FA properties using organic compounds will be necessary to suppress water evaporation from the soil system.

In Chapter 3, polymer treatments on FA particles were investigated on the effect of EMC of soils/sands. Different kinds of polymers were used in this study. In general, polymer-treatments of FA increased EMC of soils/sands, though in some cases, the effects were limited. SEM observation was conducted to investigate the morphology changes of FA particles. According to SEM observation, small FA particles were bond together and form FA aggregates. Aggregates generated after polymer modification, it may partially explain the variation of EMCs. However, surface modification can't sufficiently explain EMC changes. It suggests a complex mechanism of EMC in soil/sand mixed with raw/treated FA. Further study showed that the hydrophilic groups such as –OH and –COO- on the polymer-modified FA play the important roles in the EMC value of soil/sand. Therefore, sufficient surface modification with hydrophilic groups could greatly increase the water retention ability of FA particles. On the other hand, the chemical modification by polymer on fly ash is limited. Therefore, if fly ash particles can be made into composites, multiple modifications could be conducted for increasing EMC. Apart

from increasing the hydrophilic functional groups on the surface of fly ash, the improvement of the porous structure could also contribute to the rise of the EMC.

In Chapter 4, biodegradable polymer polyvinyl alcohol (PVA) was used as the matrix; cellulose was used as the crosslinking holder to form supporting structures of the FA based porous composites. The scanning electron microscope observed the morphology of the composites. The three-dimensional structure of hexagon, which is a structure in a stable state with lower energy, was found inside the specimen. Cellulose combined FA-aggregates are formed, in which PVA chains facilitated the intimated contact. The compression strength of the FA composites increased as the percentage of PVA increased. The porosity and water permeability of the FA composites decreased as the percentage of PVA in the composites increased. PVA-FA composites modified with cellulose showed good porosity compared to those without cellulose modification. This indicated cellulose might improve structure by increasing inter-connectivity. The EMC value increased as the ratio of PVA and cellulose increased both with the weight ratio of 10 wt%. The effect of the polymer-FA composites on the EMC could be explained as “the hydrophilic capillary zone theory.” The capillary water evaporation can be influenced by chemical factors such as hydraulic properties and physical such as pore size distribution. The EMC value of the PCFA80 composite is highest because it contained a relatively high weight ratio hydrophilic polymer and suitable pore size range. The modification of PVA and cellulose can improve the hydrophilicity and the porosity, which are useful to increase the EMC. However, the results of the drying experiment of the FA composites showed that the capillary size-pore structure didn’t make a significant difference in the EMC values. Therefore, pore size range smaller 1μm, or larger than 10μm, might have a non-negligible impact on the EMC. Besides, to improve the polymer-FA composites as the adsorbent material, further chemical activation, such as the addition of the C=O functional

groups, can be useful to increase the adsorption ability.